

REMARKS

I. Status of the Claims

Claims 1-13 were canceled and new claims 19-23 were added in a preliminary Amendment submitted August 19, 2003. Claims 14-18 were canceled in a Response to Restriction Requirement submitted March 25, 2004. Claim 19 has been canceled, claims 20-23 have been amended and new claims 24-36 have been added in the Amendment submitted herewith. Claims 20-36 are therefore presently pending in the application.

II. Support for the Claims

Support for new claims 24-36 can be found at least in the specification and claims as originally filed. More specifically, support for new claims 24, 26 and 31 can be found at least in the specification at page 5, line 26 through page 6, line 2, Figures 1-3 of the specification and original claims 1-18. Support for the phrase "cross reactive" immune response can be found at least at page 6, lines 6-8.

III. Objections to the Specification

The Action states that the first paragraph of the specification does not reflect the issued status of Application No. 09/264,747. In the Amendment submitted herewith, Applicant has amended the first paragraph of the specification, inserting "now U.S. Patent 6,645,503", after "U.S. Application No. 09/264,747, filed March 09, 1999". Applicant therefore respectfully requests withdrawal of the objection.

The Action further states that the use of trademarks has been noted in the application and that the trademarks should be capitalized and accompanied by the generic terminology. Applicant has made the requested trademark changes in the Amendment submitted herewith, and therefore respectfully requests withdrawal of the objection.

IV. Claims Rejected Under Judicially Created Doctrine of Obviousness-Type Double Patenting

Claims 19-23 are rejected under the judicially created doctrine of obviousness-type double patenting as being unpatentable over claims 1-7 of Arumugham *et al.* (U.S. Patent 6,645,503). Submitted herewith is a terminal disclaimer to obviate the double patenting rejection of the presently pending application. Applicant therefore respectfully requests withdrawal of the rejection of claims 19-23 under the judicially created doctrine of obviousness-type double patenting.

V. Claims Rejected Under 35 U.S.C. § 101

Claims 19-23 are rejected under 35 U.S.C. § 101 as being directed to non-statutory subject matter, as the claims allegedly read on a product of nature. As suggested by the Examiner, new claims 24, 26 and 31 have been amended to recite an “isolated” LPS molecule. Applicant's amendment is believed to obviate the rejection, and therefore respectfully request withdrawal of the rejection of claims 19-23 under 35 U.S.C. § 101.

VI. Claims Rejected Under 35 U.S.C. § 112, First Paragraph (New Matter)

Claims 19-23 are rejected under 35 U.S.C. § 112, first paragraph, as allegedly containing subject matter which was not described in the specification in such a way as to reasonably convey to one of skill in the art that the inventor, at the time the application was filed, had possession of the claimed invention. The Action states that the specification does not provide descriptive support for a “conserved portion of the LPS” from *Neisseria gonorrhoeae*, *Haemophilus influenzae*, non-typable *Haemophilus influenzae*, *Haemophilus ducreyi*, *Helicobacter pylori*, *Escherichia coli*, *Chlamydia*, *Salmonella*, *Salmonella typhimurium*, *Salmonella Minnesota*, *Proteus mirabilis*, *Pseudomonas aeruginosa*, *Moraxella catarrhalis*, *Bordetella pertussis*, *Shigella*, *Klebsiella* or *Vibrio cholera*, and as such, the conserved portion of the LPS from these bacteria is new matter. Applicant respectfully traverses this rejection.

Independent claim 19 has been canceled and replaced by new independent claims 24, 26 and 31. Claim 24 is directed to an antigenic conjugate comprising an isolated LPS from *Neisseria meningitidis* or *Neisseria gonorrhoeae*, wherein the conjugate elicits a cross reactive immune response against heterologous strains of *Neisseria meningitidis* or *Neisseria gonorrhoeae*. Claim 26 is directed to an antigenic conjugate comprising an isolated LPS from *Haemophilus influenzae*, non-typable *Haemophilus influenzae* or *Haemophilus ducreyi*, wherein the conjugate elicits a cross reactive immune response against heterologous strains of *Haemophilus influenzae*, non-typable *Haemophilus influenzae* or *Haemophilus ducreyi*. Claim 31 is directed to an antigenic conjugate comprising a carrier protein covalently bonded to the conserved portion of an isolated LPS from *Salmonella*, *Salmonella typhimurium* and *Salmonella minnesota*, wherein the conjugate elicits a cross reactive immune response against heterologous strains of *Salmonella*, *Salmonella typhimurium* and *Salmonella minnesota*.

Applicant asserts that the presently claimed "conserved LPS" portion of the bacteria set forth above are fully described and supported in the specification as originally filed. For example, FIG. 1A shows the conserved LPS inner core portion of *Salmonella*, FIG. 2A (inset box) and FIG. 3B show the conserved LPS inner core portion of *Neisseria*, and FIG. 2B (inset box) and FIG. 3A show the conserved LPS inner core of *Haemophilus*. The specification further cites references describing the structural characterization of LPS from non-typable *Haemophilus influenzae* strain 2019 (page 2, lines 22-25; Phillips *et al.*, 1992; **Exhibit A**) and *Neisseria gonorrhoeae* strain 1291 (page 2, lines 25-28; John *et al.*, 1991; **Exhibit B**). Finally, the specification states at page 6, lines 19-21, that "in order to elicit a [immune] response to heterologous strains or genera of bacteria, the structure of the inner core and lipid A must be conserved and utilized in the present conjugates". "The portion of the pathogen contained in the 'conserved portion' (*i.e.*, the inner core) is highly conserved among bacterial strains and thus, broadly cross reactive antibodies arise from these structures" (page 6, lines 28-30).

Applicant therefore asserts that the specification fully describes and conveys to one of skill in the art, that Applicant had possession of the claimed invention (*i.e.*, the conserved LPS portion of *Neisseria meningitidis*, *Neisseria gonorrhoeae*, *Haemophilus influenzae*, non-typable

Haemophilus influenzae, *Haemophilus ducreyi*, *Salmonella*, *Salmonella typhimurium* and *Salmonella Minnesota*) at the time the application was filed. Applicant respectfully requests withdrawal of the new matter rejection of claims 19-23 under 35 U.S.C. § 112, first paragraph.

The Action further states that the limitation "cross protective" does not appear in the specification as originally filed, and as such, is considered new matter. Claims 24, 26 and 31 have been amended, deleting the word "protective" and inserting the word "reactive" therefore. Support for the phrase "cross reactive" can be found in original claims 1, 14, 17 and 18; and in the specification (e.g., page 5, line 2 and page 6, line 9). Applicant therefore respectfully requests withdrawal of the new matter rejection of claims 19-23 under 35 U.S.C. § 112, first paragraph.

VII. Claims Rejected Under 35 U.S.C. § 112, First Paragraph (Lack of Enablement)

Claims 19-23 are rejected under 35 U.S.C. § 112, first paragraph, as allegedly containing subject matter which was not described in the specification in such a way as to reasonably convey to one of skill in the art that the inventor, at the time the application was filed, had possession of the claimed invention. The Action states that the "claimed conjugate is required to comprise GlcNAc-Hep2-phosphoethanolamine-KDO₂-LipidA and is required to elicit a 'cross protective immune response' against heterologous strains of any Gram negative bacteria". The Action alleges that "there is absolutely no evidence that antigenic conjugates of the conserved structure of non-meningococcal origin, GlcNAc-Hep2-phosphoethanolamine-KDO₂-LipidA, were produced and evaluated for cross-protectivity against even a single heterologous strain of a single Gram negative bacteria". Applicant respectfully traverses the rejection.

New claims 24, 26 and 31 are directed to antigenic conjugates comprising isolated LPS from *Neisseria*, *Haemophilus* and *Salmonella*, respectively, wherein the conjugate elicits a cross reactive immune response against heterologous strains of *Neisseria*, *Haemophilus* and *Salmonella*, respectively. As set forth above in Section VI, Applicant

asserts that the “conserved LPS” portion of *Neisseria*, *Haemophilus* and *Salmonella* are fully described and supported in the specification as originally filed.

Applicant further asserts that the specification readily enables one of skill in the art to practice the claimed invention without undue experimentation. Applicant's specification demonstrates that anti-sera from a conjugate comprising the conserved LPS portion from *Neisseria meningitidis* is cross reactive (page 19, line 15 through 16, line 5) with LPS from heterologous strains of *Neisseria meningitidis* (e.g., *Neisseria meningitidis* strains A1, H44/76, 2996, Immunotypes L1-L12) and bactericidal (page 21, line 14 through page 22, line 15) against heterologous *Neisseria meningitidis* group A strains (e.g., strain A1) and Group B strains (e.g., strains H44/76 and 2996). Applicant's specification further demonstrates that anti-sera against the *Neisseria meningitidis* LPS conjugate is cross reactive with the LPS from various *genera* of Gram negative bacteria (page 20, line 8 through page 21, line 12). For example, the LPS of the bacteria tested (i.e., *Haemophilus influenza*, *Neisseria gonorrhoeae*, *Moraxella catarrhalis* and *Helicobacter pylori*) were all cross reactive with the anti-sera (FIG. 4).

Applicant reiterates that the specification teaches that the inner core structure of the LPS molecules from *Salmonella* (FIG. 1A), *Neisseria* (FIG. 2A (inset box), FIG. 3B) and *Haemophilus* (FIG. 2B (inset box), FIG. 3A) are conserved among these bacteria and states that in order to elicit a response against heterologous strains or genera of bacteria, the structure must be conserved and utilized in the LPS conjugates of the invention. Furthermore, the teachings and experimental data of the present invention clearly demonstrate that the conserved LPS portion (i.e., the inner core portion: GlcNAc-Hep2-phosphoethanolamine-KDO₂-LipidA) elicits a cross reactive immune response against (1) heterologous strains of *Neisseria meningitidis*, (2) different species of *Neisseria* (e.g., *Neisseria gonorrhoeae*) and (3) Gram negative bacteria (e.g., *Haemophilus*, *Moraxella*, *Salmonella* and *Helicobacter*). Applicant therefore asserts the specification enables one of skill in the art to make and use the claimed conjugates comprising isolated LPS from *Neisseria*, *Haemophilus* and *Salmonella* without undue experimentation, and as such, respectfully request withdrawal of the rejection of claims 19-23 under 35 U.S.C. § 112, first paragraph.

The Action states further, "with regard to the LPS of Gram negative bacterial species, *Neisseria*, or *N. gonorrhoeae* in particular, the state of the art documents structural heterogeneity or structural differences (see Lee *et al. Infect. Immun.* 63:2508-2515, 1995; and John *et al. J. Biol. Chem.* 266:19303-19311, 1991, both from Applicant's IDS). The states of the art further reflects the existence of intra- and inter-strain antigenic variations suggesting the gonococci's potential for reinfection and continued virulence (see lines 1-4 in column 2 of Rice *et al.*, US 6,099,839, published 8/8/2000)". The Action concludes that in light of the art-recognized unpredictability in obtaining a broadly protective immune response, the lack of adequate disclosure and guidance, the breadth of the claims, the unpredictability identified in the relevant art and the quantity of experimentation necessary, that "undue experimentation would have been required to reproducibly practice the invention, as claimed." Applicant respectfully traverses.

As set forth above, the claims of the present invention are directed to antigenic conjugates comprising the conserved portion of an isolated LPS from *Neisseria*, *Salmonella* or *Haemophilus*. The conserved portion of the LPS comprises GlcNAc-Hep2-phosphoethanolamine-KDO₂-LipidA. As the Examiner has pointed out in the paragraph above, the LPS of Gram negative bacterial species often exhibit structural heterogeneity or structural differences. Applicant asserts however, that the structural differences in the LPS molecules cited in the Action, and in Applicant's specification, occur in the outer core portion of the LPS, not in the conserved (inner core) LPS portion. For example, Plested *et al. (Infection and Immunity*, 67:5417-5426, 1999; **Exhibit C**) state at page 5417, second column, second paragraph, "It is known that, in addition to this inter-strain variation, individual *N. meningitidis* strains exhibit extensive phase variation of the outer core LPS structures". "Despite the extensive antigenic variation of LPS, the inner core of the LPS is relatively highly conserved" (emphasis added).

Applicant contends that the conserved portion of the LPS molecules (*i.e.*, the inner core portion: GlcNAc-Hep2-phosphoethanolamine-KDO₂-LipidA) claimed in the present invention does not exhibit the structural heterogeneity or variation observed in the LPS outer core

portion. Applicant therefore asserts that the specification enables one of skill in the art to make and use the presently claimed invention without undue experimentation, and as such, respectfully withdrawal of the rejection of claims 19-23 are under 35 U.S.C. § 112, first paragraph.

VIII. Claims Rejected Under 35 U.S.C. § 112, Second Paragraph

Claims 19-23 are rejected under 35 U.S.C. § 112, second paragraph, as allegedly being indefinite for failing to particularly point out and distinctly claim the subject matter which Applicants regard as the invention.

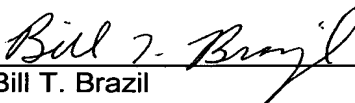
The Action states that claim 19 is incorrect in the recitation of "*Minnesota*" and "cholera" as opposed to "*minnesota*" and "*cholerae*". Claim 19 has been canceled. New claims 25, 27 and 31 recite the species *minnesota* with a lower case "m". Claim 21 has been amended and new claims 28 and 34 have been written to recite "*cholerae*" as suggested by the Examiner. Applicant's amendment and new claims are believed to obviate this rejection, and therefore respectfully request withdrawal of the rejection of claim 19 under 35 U.S.C. § 112, second paragraph.

Claim 21 is rejected as the recitation of FHA "fragments" is allegedly vague and indefinite. Claim 21 has been amended, deleting the word "fragments". New claims 28 and 34 recite "FHA of *Bordetella pertussis*". Applicant's amendment and new claims are believed to obviate this rejection, and therefore respectfully request withdrawal of the rejection of claim 19 under 35 U.S.C. § 112, second paragraph.

Claim 23 is rejected as the term "effective amount" is allegedly vague and indefinite. Claim 23 has been amended, deleting the phrase "an effective amount". The phrase "an effective amount" has been omitted from new claims 30 and 36. Applicant believes that the amendment and new claims obviate the this rejection and therefore respectfully request withdrawal of the rejection of claim 23 under 35 U.S.C. § 112, second paragraph.

The notice set a three-month period to comply, to and including September 24, 2004.
Thus, this response is believed to be timely filed. Should any fees be deemed necessary,
the Commissioner is authorized to deduct said fees from Deposit Account No. 01-1425.

Respectfully submitted,



Bill T. Brazil
Agent for Applicants
Reg. No. 50,733

Wyeth
Patent Law Department
Five Giralda Farms
Madison, NJ 07940
Tel. No. (732) 274-4843

Structural Characterization of the Cell Surface Lipooligosaccharides from a Nontypable Strain of *Haemophilus influenzae*[†]

Nancy J. Phillips,[‡] Michael A. Apicella,[§] J. McLeod Griffiss,^{||} and Bradford W. Gibson^{*,||}

Department of Pharmaceutical Chemistry, University of California, San Francisco, California 94143, Department of Medicine, State University of New York, Buffalo, New York 14215, and Centre for Immunochemistry, Department of Laboratory Medicine and Veterans Affairs Medical Center, University of California, San Francisco, California 94143

Received December 2, 1991; Revised Manuscript Received February 19, 1992

ABSTRACT: Oligosaccharides released from the lipooligosaccharides (LOS) of *Haemophilus influenzae* nontypable strain 2019 by mild acid hydrolysis were fractionated by size exclusion chromatography and analyzed by liquid secondary ion mass spectrometry. The major component of the heterogeneous mixture was found to be a hexasaccharide of *M*_r 1366, which lost two phosphoethanolamine groups upon treatment with 48% aqueous HF. The dephosphorylated hexasaccharide was purified and shown by tandem mass spectrometry, composition analysis, methylation analysis, and two-dimensional nuclear magnetic resonance studies to be Galβ1→4Glcβ1→(Hepα1→2Hepα1→3)4Hepα1→5anhydro-KDO, where Hep is *L*-glycero-*D*-manno-heptose and KDO is 3-deoxy-*D*-manno-octulosonic acid. An analogous structure containing authentic KDO was generated from LOS that had been HF-treated prior to acetic acid hydrolysis, suggesting that the reducing terminal anhydro-KDO moiety is produced as an artifact of the hydrolysis procedure by β-elimination of a phosphate substituent from C-4 of KDO. Mass spectral analyses of *O*-deacylated LOS and free lipid A confirmed that, in addition to the two phosphoethanolamines on the oligosaccharide and two phosphates on the lipid A, another phosphate group exists on the KDO. This KDO does not appear to be further substituted with additional KDO residues in intact *H. influenzae* 2019 LOS. The terminal disaccharide epitope, Galβ1→4Glcβ1→, of the hexasaccharide is also present on lactosylceramide, a precursor to human blood group antigens. It is postulated that the presence of this structure on *H. influenzae* LOS may represent a form of host mimicry by the pathogen.

Haemophilus influenzae is a Gram-negative pathogen which colonizes the human upper respiratory tract. The bacterium is found in both encapsulated and unencapsulated (nontypable) forms, which differ significantly in their ability to cause disease and evade the host's immune system (Mäkelä, 1988; Moxon, 1990). In developed countries, *H. influenzae* type b (Hib),¹ a capsular serotype, is the leading cause of bacterial meningitis in young children. The capsular polysaccharide of this organism plays a critical role in mediating the virulence of Hib (Moxon & Vaughn, 1981). Nontypable strains of *H. influenzae* (NTHI), which are commonly present in the nasopharynx of 50–80% of healthy carriers (Turk, 1982), have only recently been recognized to be important human pathogens. Both invasive diseases and localized infections of the respiratory tract are caused by NTHI (Murphy & Apicella, 1987). Since NTHI lacks a capsular polysaccharide, its pathogenicity is mediated more directly by surface components of the bacterial outer membrane, including proteins and lipooligosaccharides (LOS) (Campagnari et al., 1987; Patrick et al., 1987).

Like the LOS of *Neisseria gonorrhoeae*, *Neisseria meningitidis*, and *Bordetella pertussis*, the LOS of *H. influenzae* do not contain the repeating oligosaccharide units (O-antigens) characteristic of the lipopolysaccharides (LPS) made by enteric bacteria. Rather, the LOS of these mucosal pathogens contain short, multiantennary glycans similar to those found in rough mutants of enteric bacteria which lack O-antigens. A single strain of *H. influenzae* generally produces a heterogeneous mixture of LOS with oligosaccharides (OS) of different sizes (Campagnari et al., 1987; Patrick et al., 1987, 1989). An understanding of the precise structural features of the OS moieties of LOS is essential to identifying surface-exposed epitopes available for host/pathogen interactions.

A structural model for neisserial LOS has been constructed (Phillips et al., 1990) based on published oligosaccharide (Jennings et al., 1980, 1983; Gibson et al., 1989; Di Fabio et al., 1990; Yamasaki et al., 1991) and lipid A structures (Takayama et al., 1986). To date, much less is known about the LOS from *H. influenzae*. Various groups have studied the chemical composition of Hib LOS (Flesher & Insel, 1978;

[†] Financial support was provided by grants from the National Institute of Allergy and Infectious Diseases (AI21620 and AI24616). We also acknowledge support from the National Institutes of Health (RR01640), the National Science Foundation Instrumentation Program, and the Research Service of the Department of Veterans Affairs. This is Report No. 55 from the Centre for Immunochemistry of the University of California, San Francisco.

^{*} To whom correspondence should be addressed at the School of Pharmacy 926-S, 513 Parnassus Ave., University of California, San Francisco, CA 94143-0446.

[‡] Department of Pharmaceutical Chemistry, UCSF.

[§] SUNY at Buffalo.

^{||} Department of Laboratory Medicine and Veterans Affairs Medical Center, UCSF.

¹ Abbreviations: 1D, one dimensional; 2D, two dimensional; COSY, 2D *J*-correlated spectroscopy; DQF-COSY, double-quantum filtered COSY; Gal, galactose; GalNAc, *N*-acetylglucosamine; Glc, glucose; GlcNAc, *N*-acetylglucosamine; HBEE, ethyl 4-hydrazinobenzoate; Hep, *L*-glycero-*D*-manno-heptose; Hex, hexose; HexNAc, *N*-acetylhexosamine; Hib, *Haemophilus influenzae* type b; HOHAHA, 2D homonuclear Hartmann-Hahn spectroscopy; KDO, 3-deoxy-*D*-manno-octulosonic acid; LOS, lipooligosaccharide; LPS, lipopolysaccharide; LSIMS, liquid secondary ion mass spectrometry; (M-H)⁺, deprotonated molecular ion; MS/MS, tandem mass spectrometry; NMR, nuclear magnetic resonance; NOE, nuclear Overhauser effect; NOESY, 2D NOE spectroscopy; NTHI, nontypable *Haemophilus influenzae*; OS, oligosaccharide; PEA, phosphoethanolamine; PPEA, pyrophosphoethanolamine.

Parr & Bryan, 1984; Inzana et al., 1985; Zamze & Moxon, 1987; van Alphen et al., 1990) and the LOS from other serotype strains (Zamze & Moxon, 1987). Glucose, galactose, and L-glycero-D-manno-heptose have been consistently observed, along with glucosamine and/or galactosamine in some strains. Phosphate and phosphoethanolamine are also common constituents. 3-Deoxy-D-manno-octulosonic acid (KDO), a nearly universal component of bacterial LPS, could not be readily detected in *H. influenzae* LOS using the traditional thiobarbituric acid assay (Flesher & Insel, 1978; Zamze & Moxon, 1987). This suggested that KDO was either absent from *H. influenzae* LOS or modified. Using an alternate semicarbazide assay and gas chromatography-mass spectrometry (GC/MS), the presence of KDO in Hib strain Eagan was confirmed by Inzana et al. (1985). Subsequently, phosphorylated KDO was identified in the LOS from a deep-rough genetically engineered strain of *H. influenzae* (Rb⁺I69) (Zamze et al., 1987). The LOS from this strain was later shown to contain a truncated OS moiety containing only a single KDO, which was found to be phosphorylated on either C-4 or C-5 (Helander et al., 1988). We now report the structural characterization of the LOS from a wild-type NTHI strain (strain 2019) which contains a much larger oligosaccharide moiety, yet also possesses a "KDO-related" epitope associated with the LOS of two recombinant *H. influenzae* strains (Spinola et al., 1990; Campagnari et al., 1990).

EXPERIMENTAL PROCEDURES

Materials

LPS from *Salmonella typhimurium* TV119 Ra mutant, galactose, glucose, galactosamine, glucosamine, 3-deoxy-D-manno-octulosonic acid (KDO) and anhydrous hydrazine were all obtained from Sigma (St. Louis, MO). Aqueous HF (48%) was purchased from Mallinckrodt (Muskegon, MI), acetic anhydride from Supelco (Bellefonte, PA), and iodomethane from Fluka (Buchs, Switzerland). Sodium hydroxide pellets (99.9%) and sodium borodeuteride (98% D) were purchased from Aldrich (Milwaukee, WI). The standard mixture of partially methylated alditol acetates used for GC/MS analysis was obtained from Biocarb (Lund, Sweden). 18-M Ω water required for the Dionex chromatography was generated from deionized water using a Millipore milli-Q water purification system. Acetonitrile, water, methanol, and methylene chloride were obtained from Burdick and Jackson (Muskegon, MI). All other reagents and solvents used were of reagent grade.

Methods

Isolation and Purification of LOS. The LOS of *H. influenzae* nontypable strain 2019 (NTHI 2019) was prepared using the extraction procedure of Darveau and Hancock (1983). Briefly, this method uses sequential enzyme digestions to remove RNA, DNA, peptidoglycan, and bacterial proteins. The LOS is then extracted from the denatured proteins by SDS extraction, followed by extensive dialysis and precipitation with ethanol (Darveau & Hancock, 1983). The isolated LOS was analyzed by sodium dodecyl sulfate-polyacrylamide gel electrophoresis (SDS-PAGE) and found to consist of one major component and several minor species (Campagnari et al., 1990), with the major component appearing roughly comparable in size to the *Salmonella minnesota* Rb mutant.

Isolation of OS from LOS. The LOS from NTHI 2019 (32 mg) and commercially available *S. typhimurium* TV119 Ra mutant (20 mg) were hydrolyzed in 1% acetic acid (2 mg of LOS/mL) for 2 h at 100 °C with stirring. The hydrolysates were centrifuged at 5000g for 20 min at 4 °C, and the su-

pernatants were removed. Pellets were washed (one or two times) with 1–3 mL of H₂O and centrifuged again (5000g, 20 min, 4 °C). The supernatants and washings were pooled and lyophilized. The lyophilized OS fractions were redissolved in 0.5–1 mL of H₂O and centrifuge-filtered using Microfilter tubes with 0.45- μ m Nylon-66 membrane filters (Rainin). *H. influenzae* 2019 OS fractions often contained traces of SDS which could be removed by passing the OS (dissolved in 1 mL of H₂O) through a C₁₈ Sep-Pak (Waters Associates) and eluting with 3–4 mL of H₂O.

Gel Filtration Chromatography. The NTHI 2019 OS fraction (11.5 mg) was dissolved in 0.3 mL of 0.05 M pyridinium acetate buffer (pH 5.2), centrifuge-filtered, and applied to two Bio-Gel P-4 columns connected in series (1.6 \times 79 cm and 1.6 \times 76.5 cm, <400 mesh; Bio-Rad). The columns were equipped with water jackets maintained at 30 °C. Upward elution at a flow rate of \approx 10 mL/h was achieved with a P-1 peristaltic pump (Pharmacia), and fractions were collected at 10-min intervals and evaporated to dryness in a Speed-Vac concentrator. A refractive index detector (Knauer) was used to monitor column effluent, and chromatograms were recorded and stored with a Shimadzu C-R3A Chromatopac integrator. Selected OS fractions were pooled, dephosphorylated, and fractionated again on a Bio-Gel P-4 column (1.6 \times 84 cm) as described above.

OS samples weighing less than 1–2 mg were alternatively purified by a gel filtration HPLC system employing a Waters 6000A HPLC pump and two 600 \times 7.5 mm Bio-Sil TSK-125 columns (Bio-Rad) connected in series. Samples were eluted in 1% acetic acid or 0.05 M pyridinium acetate (pH 5.2) at a flow rate of 1 mL/min. Fractions were collected in 0.5–1-mL volumes, and detection was as described above.

High-Performance Anion Exchange Chromatography with Pulsed Amperometric Detection. Anion exchange chromatography was performed using a Dionex BioLC (Dionex, Sunnyvale, CA). The system was equipped with a gradient pump, pulsed amperometric detector, and CarboPak PA1 column (4 \times 250 mm). The following pulse potentials and durations were used for detection: $E_1 = 0.05$ V ($t_1 = 480$ ms); $E_2 = 0.60$ V ($t_2 = 120$ ms); $E_3 = -0.60$ V ($t_3 = 60$ ms). The response time of the PAD was set to 3 s, and an output range of 300 or 1000 nA was typically used. As previously described (Phillips et al., 1990), the four standard eluents used were H₂O, 1 M NaOH, 200 mM NaOH, and 1 M NaOAc. A Dionex anion micromembrane suppressor was used when collection of desalted samples was undertaken. The dephosphorylated NTHI 2019 hexasaccharide (\approx 2 μ g) was eluted using the following gradient: (1) 16 mM NaOH for 15 min, (2) linear to 100 mM NaOH in 10 min, (3) linear to 500 mM NaOAc in 30 min while holding 100 mM NaOH constant. The same separation was obtained when gradient steps 1 and 2 were decreased to 5 min each.

For composition analysis, \approx 15 nmol of the dephosphorylated NTHI 2019 hexasaccharide was dissolved in 200 μ L of H₂O, treated with 200 μ L of 4 M trifluoroacetic acid, and heated for 4.5 h at 100 °C. The hydrolysate was evaporated to dryness in a Speed-Vac concentrator, redissolved in 20 μ L H₂O, and dried again. For anion exchange chromatography, the sample was dissolved in 100 μ L of H₂O, and 20 μ L was injected. To elute all the monosaccharide components, the following gradient was used: (1) 16 mM NaOH for 20 min, (2) linear to 40 mM NaOH in 10 min, (3) linear to 100 mM NaOH and 100 mM NaOAc in 5 min, and (4) linear to 160 mM NaOAc in 15 min while holding 100 mM NaOH constant. Response factors for the various monosaccharides were

determined with a standard monosaccharide mixture containing GalNH₂, GlcNH₂, Gal, Glc, and KDO. Approximately 10 nmol of the dephosphorylated OS from *S. typhimurium* Ra mutant was hydrolyzed under the same conditions to provide authentic L-glycero-D-manno-heptose.

Derivatization of Oligosaccharides with Ethyl 4-Hydrazinobenzoate (HBEE) and HPLC Purification. Oligosaccharides (10–100 nmol) were dissolved in 10 μ L of H₂O and placed in 1-mL glass Reacti-Vials. Approximately 3 molar equiv of HBEE reagent in 40 μ L of methanol was added to each sample, followed by \approx 0.5 μ L of glacial acetic acid. The reaction mixtures were placed in a heating block at 80 °C for 30 min, cooled, and then dried under a stream of N₂. The derivatized OS samples were redissolved in H₂O and separated using a Rainin HPLC system with a reverse-phase C₁₈ column (Vydac, 25 cm \times 4.6 mm i.d.). The HBEE-OS were eluted with a linear gradient of H₂O to 50% CH₃CN in 50 min at a flow rate of 1 mL/min and detected at 320 nm with a Kratos 783 variable wavelength detector. Both HPLC solvents contained 0.05% trifluoroacetic acid (John & Gibson, 1990).

O-Deacylation of LOS. The NTHI 2019 LOS sample was O-deacylated following the procedure of Helander et al. (1988). Approximately 11 mg of LOS was placed in a 25-mL glass centrifuge tube and treated with 1.1 mL of anhydrous hydrazine. The sample was shaken at 37 °C in a water bath for 20 min with occasional sonication and then cooled to –20 °C and diluted with 5.5 mL of chilled acetone (–20 °C), added dropwise. The precipitated O-deacylated LOS was centrifuged at 12000g for 20 min, and the supernatant was removed. The pellet was washed with cold acetone and centrifuged a second time. Finally, the precipitated O-deacylated LOS was dissolved in 500 μ L of H₂O, frozen, and lyophilized.

HF-Treatment of Oligosaccharides, O-Deacylated LOS, and LOS. LOS, O-deacylated LOS, or OS (0.1–1 mg) were placed in 1.5-mL polypropylene tubes. In an ice bath, samples were treated with cold 48% aqueous HF to make 5–10 μ g/ μ L solutions. OS and O-deacylated LOS were then kept for 16–24 h at 4 °C; intact LOS were HF-treated for up to 48 h at 4 °C. Aqueous HF was evaporated under a stream of N₂ in a polypropylene desiccator containing NaOH pellets. The desiccator was connected to a water aspirator with an in-line NaOH trap.

Methylation Analysis. Linkage analysis was performed on purified OS using the microscale method of Lavery and Hakomori (1987) modified for use with powdered NaOH (Larson et al., 1987). Given the resistance of Hep–Hep bonds to acid hydrolysis, the longer hydrolysis times (21 h) and slightly greater acidic conditions of the older Hakomori procedure (Stellner et al., 1973) were used. As described in detail elsewhere (Phillips et al., 1990), the OS were dissolved in DMSO and treated with powdered NaOH and CH₃I. After being stirred at room temperature for 45 min, the solutions were extracted with CH₂Cl₂/H₂O. The permethylated samples were hydrolyzed in 0.5 N sulfuric acid in 95% acetic acid for 16 h at 80 °C, diluted with an equal volume of H₂O, and heated for 5 h at 80 °C. The hydrolysates were partially neutralized using a NaOH solution (2.6 molar equiv relative to H₂SO₄), dried, and then reduced with NaBD₄ in 0.01 N NaOH at 4 °C overnight. The dried samples were then converted to their partially methylated alditol acetates by treatment with 300 μ L of acetic anhydride at 100 °C for 2 h and analyzed by GC/MS on a VG70SE mass spectrometer. To determine the linkage position of the reducing terminal KDO moiety, two additional reduction steps were added to the methylation analysis procedure (York et al., 1985). As

described elsewhere (John et al., 1991), the ketone of the KDO moiety was first reduced to a secondary alcohol with NaBD₄ prior to methylation. After methylation and before the hydrolysis step, the methyl ester of the permethylated KDO moiety was converted to a primary alcohol by reduction with NaBD₄.

Preparation of Alditol Acetates. OS from NTHI 2019 (36 μ g) and *S. typhimurium* TV119 Ra mutant (50 μ g) were hydrolyzed under the conditions used for composition analysis by anion exchange chromatography (described above). The monosaccharides were then reduced by treatment with 150 μ L of 10 mg/mL NaBD₄ in 1 M NH₄OH for 2.3 h at room temperature. The reactions were quenched and worked up as in the methylation analysis procedure. Samples were then dried in vacuo over P₂O₅ for 2 h and peracetylated using the method described above. GC/MS analysis was performed using the conditions for partially methylated alditol acetates.

Nuclear Magnetic Resonance Spectroscopy. All 1D and 2D ¹H NMR spectra were recorded on a GE GN-500 spectrometer at 25 °C. The dephosphorylated NTHI 2019 hexasaccharide (1.5 mg) was lyophilized 3–4 times from 99.96% D₂O (Aldrich) and then dissolved in 0.3 mL of 99.996% D₂O (Merck Sharp & Dohme). A trace of acetone was added to the sample as an internal reference (δ 2.225). The phase-sensitive double-quantum filtered COSY (DQF-COSY) spectrum (Rance et al., 1983) was acquired with time-proportional phase incrementation of the first pulse (Redfield & Kuntz, 1975; Marion & Wüthrich, 1983). The data matrix consisted of 800 \times 1024 data points, acquired with 16 scans per t_1 value and a spectral width of \pm 1506 Hz. The matrix was apodized with a 45°-shifted sine-bell window function in both dimensions and zero-filled to produce a 2K \times 4K real data matrix. The 2D homonuclear Hartmann–Hahn (HOHAHA) spectrum was obtained using the MLEV-17 sequence (Bax & Davis, 1985) and quadrature detection method of States et al. (1982). A spectral width of \pm 1000 Hz was used, with a 90-ms relay mixing time. A data matrix of 456 \times 2048 data points was acquired with 12 scans per t_1 increment. The matrix was zero-filled in the t_1 dimension and apodized with Gaussian window functions in both dimensions to give 1K \times 2K real points. The phase-sensitive 2D nuclear Overhauser effect (NOESY) spectrum was acquired following the method of States et al. (1982), using a 400-ms mixing time and 2.8-s interscan delay. The spectral width was \pm 2000 Hz, and the data matrix contained 400 \times 1024 data points, with 16 scans per t_1 value. Zero-filling and Gaussian apodization functions were used in both dimensions to give a final 2K \times 2K matrix. All data processing was done on a VAX computer with a Unix operating system using programs developed and modified at the UCSF NMR facility as previously described by Basus et al. (1988), including some recent improvements (M. Day, unpublished data).

Liquid Secondary Ion Mass Spectrometry (LSIMS). LSIMS was performed using a Kratos MS50S mass spectrometer with a cesium ion source (Falick et al., 1986). To prepare samples for LSIMS analysis, ca. 1 μ L of glycerol/thioglycerol (1:1) was applied to the stainless steel probe tip and aliquots of the sample solution (dissolved in H₂O) were added with intermittent drying. (To suppress undesired adduct ions, \approx 0.5 μ L of 0.1 N HCl was sometimes added to the matrix.) A Cs⁺ ion primary beam energy of 10 keV was used, and the secondary sample ions were accelerated to 8 keV. Scans were taken in the negative-ion mode at 300 s/decade and recorded with a Gould ES-1000 electrostatic recorder. The spectra were mass calibrated manually with Ultramark

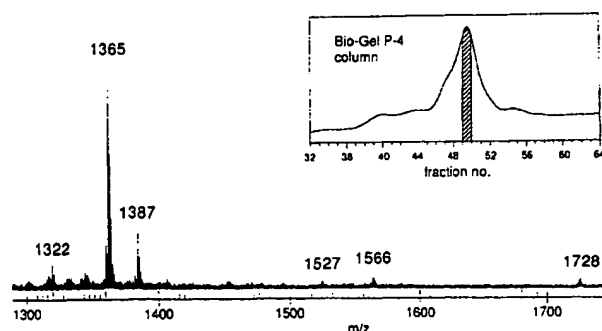


FIGURE 1: Partial negative-ion LSIMS spectrum of Bio-Gel P-4 column fraction number 49. (Inset) Oligosaccharide region of the Bio-Gel P-4 column elution profile. The elution volume of the major peak was 150 mL, and V_0 and V_i for the column were ≈ 80 and 280 mL, respectively.

1621 to an accuracy of better than ± 0.2 Da.

Tandem Mass Spectrometry (MS/MS). A four-sector mass spectrometer (Kratos Concept II HH, Kratos Analytical, Manchester, England) equipped with a 4% diode array detector on MS-II was used for all analyses as previously described (Walls et al., 1990). All samples were prepared as described above for the two-sector experiments. Spectra were taken in the negative-ion mode using a Cs^+ beam energy of 18 keV to produce abundant deprotonated molecular ions in MS-I. The isotopically pure ^{12}C component of the parent deprotonated molecular ion was then collisionally activated in the collision cell between MS-I and MS-II. The helium collision gas was used at a pressure sufficient to attenuate the parent ion beam to one-third of its initial value. The collision cell was floated at a potential of 2 kV, resulting in a collision energy of 6 keV. The fragment ions (or "daughter ions") resulting from decomposition of the collisionally activated parent ions were then mass analyzed and detected in MS-II. The magnet and electric sector of MS-II were stepped to produce a series of contiguous 4% mass frames. The mass scales on MS-I and MS-II were both calibrated with CsI using a Kratos Mach 3 data system as previously described (Walls et al., 1990).

Electrospray Mass Spectrometry. Samples were analyzed on a Bio-Q mass spectrometer (VG Instruments, Manchester, England) with an electrospray ion source. *O*-Deacylated LOS were first dissolved in H_2O and then diluted 1:1 with electrospray solvent (50:50 $\text{CH}_3\text{CN}/\text{H}_2\text{O}$ with 1% HOAc). Five microliters was injected with a Rheodyne 8125 injector located downstream from a syringe pump set at 2.0 $\mu\text{L}/\text{min}$. The electrospray tip voltage was typically 4.0 kV. The mass spectrometer was scanned from m/z 400 to 2000 with a scan time of 10 s. Data were collected in multichannel analysis mode, and data processing was handled by the VG data system.

RESULTS

Oligosaccharides Released from the LOS of NTHI Strain 2019. Mild acid hydrolysis of the LOS generated a water-soluble OS fraction that produced a major peak with small shoulders when separated by Bio-Gel P-4 chromatography (Figure 1, inset). Fractions were dried and analyzed by liquid secondary ion mass spectrometry (LSIMS) in the negative-ion mode. Figure 1 shows the LSIMS spectrum of fraction 49, which represents the center of the OS peak. The major molecular ions observed in all of the oligosaccharide-containing column fractions are listed in Table I. As indicated, the principal component of the major peak (fractions 46–51) was an OS of M_r 1366.² Earlier eluting fractions contained higher

Table I: Molecular Ions Detected in the Bio-Gel P-4 Column Fractions of the *H. influenzae* 2019 Oligosaccharide Mixture^{a,b}

fraction no.	deprotonated molecular ions; $(M-H)^-$
37	2077, ^c 1407, 1245
38	2077, ^c 1730, 1530, ^d 1407, 1245
39	2093, 1915, ^c 1730, 1530, ^d 1407, 1245
40	2093, 1915, ^c 1591, ^c 1530, ^d 1322, 1245
41	1591, ^c 1530, ^d 1322
42	1851, 1591, ^c 1322
43	1851, 1591, ^c 1365, 1322
44	1851, 1689, 1591, ^c 1365
45	1851, 1689, 1407, 1365
46	1689, 1407, 1365
47	1728, 1689, 1407, 1365
48	1728, 1566, 1527, 1365, 1322
49	1728, 1566, 1365, 1322
50	1728, 1566, 1365, 1322, 1203
51	1774, ^d 1566, 1365, 1203
52	1774, ^d 1566, 1404, 1365, 1242, 1203
53	1612, ^d 1566, 1404, 1242, 1203
54	1612, ^d 1566, 1404, 1242
55	1612, ^d 1404, 1242
56	1404, 1242

^a Masses are listed as the nominal mass values of the ^{12}C -containing isotope. Major components are listed in boldface type. ^b Most major species also gave sodiated molecular ions, $(M+\text{Na}-2\text{H})^-$. Additionally, several species were detected as +226 Da^c and +208 Da^d adduct ions, whose ionization could be suppressed by acidification of the LSIMS matrix and whose mass increments are consistent with free fatty acids known to be present in the LOS preparation.

Table II: Molecular Weights and Proposed Compositions of the Major Oligosaccharides Present in the *H. influenzae* 2019 Sample^a

$(M-H)^-$	M_r	proposed compositions
1203	1204	KDO*, Hep ₃ , Hex, PEA ₂
1242	1243	KDO*, Hep ₃ , Hex ₂ , PEA
1245	1246	KDO*, Hep ₃ , Hex, PEA ₂ , Ac
1322	1323	KDO*, Hep ₃ , Hex ₂ , (P + PEA, or HexNAc) ^b
1365	1366	KDO*, Hep ₃ , Hex ₂ , PEA ₂
1404	1405	KDO*, Hep ₃ , Hex ₃ , PEA
1407	1408	KDO*, Hep ₃ , Hex ₂ , PEA ₂ , Ac
1527	1528	KDO*, Hep ₃ , Hex ₃ , PEA ₂
1566	1567	KDO*, Hep ₃ , Hex ₄ , PEA
1689	1690	KDO*, Hep ₃ , Hex ₄ , PEA ₂
1728	1729	KDO*, Hep ₃ , Hex ₅ , PEA
1730	1731	KDO*, Hep ₃ , Hex ₃ , PEA ₂ , (P + PEA, or HexNAc) ^b
1851	1852	KDO*, Hep ₃ , Hex ₅ , PEA ₂
2093	2094	KDO*, Hep ₃ , Hex ₆ , PEA, (P + PEA, or HexNAc) ^b

^a KDO* refers to anhydro-KDO and P stands for phosphate. ^b (P + PEA) and HexNAc have the same nominal mass increment of 203 Da.

molecular weight oligosaccharides representing minor components of the mixture.

Oligosaccharides derived from the LOS of human mucosal pathogens generally consist of a limited number of common sugars, including hexose (Hex), *N*-acetylhexosamine (HexNAc), heptose (Hep), and 3-deoxy-*D*-manno-octulosonic acid (KDO), phosphate, phosphoethanolamine (PEA), and pyrophosphoethanolamine (PPEA) (Gibson et al., 1989; Phillips et al., 1990). *O*-Linked acetate groups are occasionally found on core HexNAc residues (John et al., 1991). A preliminary composition can often be assigned to an unknown OS by simple combination of these components.^{3,4} In the present case,

² All masses are reported as the nominal mass of the ^{12}C -containing isotope unless otherwise noted.

³ The residue masses for the ^{12}C -containing components of common LOS monosaccharides and other structural moieties are 162.05 (Hex), 203.08 (HexNAc), 192.06 (Hep), 220.06 (KDO), 291.10 (NeuAc), 42.01 (Ac), 123.01 (PEA), 79.97 (phosphate), and 202.98 Da (PPEA).

⁴ A computer program was used (W. Hines, UCSF) that permits the determination of all possible compositions for an OS of specified molecular weight containing up to nine different structural moieties.

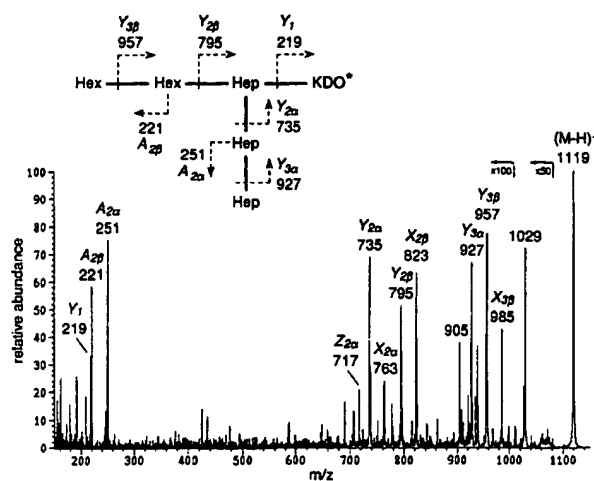


FIGURE 2: MS/MS spectrum of the major dephosphorylated hexasaccharide at $(M-H)^- = 1119$. Fragments are labeled according to the nomenclature proposed by Domon and Costello (1988). X, Y, and Z fragments arise from glycosidic bond or ring cleavages with charge retention at the reducing terminus; A, B, and C ions are nonreducing terminal fragments. The α and β subscripts distinguish the major and minor branches, respectively. Other sequence ions present but not labeled on the spectrum include m/z 955 (X_{3a}), 939 (Z_{3a}), 909 (Z_{3a}), 777 (Z_{2a}), and 247 (X_1). KDO* refers to anhydro-KDO. The large fragment ion at m/z 1029, $(M-H-90)^-$, is believed to result from ring cleavage of the reducing-terminal anhydro-KDO moiety.

however, it was not possible to assign preliminary compositions to the NTHI oligosaccharides observed using only these residues. Additional experimental evidence (discussed below) led to the proposal that a KDO-like moiety, anhydro-KDO, exists on the reducing terminus of the NTHI 2019 oligosaccharides. With the incorporation of this residue, it was possible to generate proposed compositions for the majority of the OS molecular ions (Table II). All of the proposed structures possess a common core consisting of three heptoses and an anhydro-KDO moiety. Structural heterogeneity would appear to be confined to the phosphate substituents and branch saccharides.

Partial Structure of the Major Hexasaccharide Component. The major component of the NTHI 2019 oligosaccharides was a hexasaccharide (M_r 1366) with a proposed composition of two hexoses, three heptoses, two PEAs, and an anhydro-KDO (Table II). Dephosphorylation of this component with aqueous HF produced a new species of M_r 1120, indicating the removal of two PEA groups. To prepare a sufficient quantity of the dephosphorylated major component for structural studies, several fractions from the center and later-eluting side of the initial Bio-Gel P-4 column peak were pooled and HF-treated. The dephosphorylated material was then rechromatographed on a Bio-Gel P-4 column, and fractions were analyzed by LSIMS. Again, fractions were pooled across the center and later-eluting side of the Bio-Gel P-4 column peak in order to absolutely minimize contamination of the M_r 1120 component with higher molecular weight materials.

Negative ion tandem mass spectrometry was used to determine the sequence and partial structure of the major OS at M_r 1120 (m/z 1119). When selected for collision-induced dissociation, the parent $(M-H)^-$ ion at m/z 1119 produced the fragment ion spectrum shown in Figure 2. Fragment ions are identified following the nomenclature proposed by Domon and Costello (1988). Reducing terminal Y-type sequence ions resulting from glycosidic bond cleavages indicate that the molecular ion can lose either a nonreducing terminal Hex-Hex (m/z 957 and 795) or Hep-Hep (m/z 927 and 735) di-

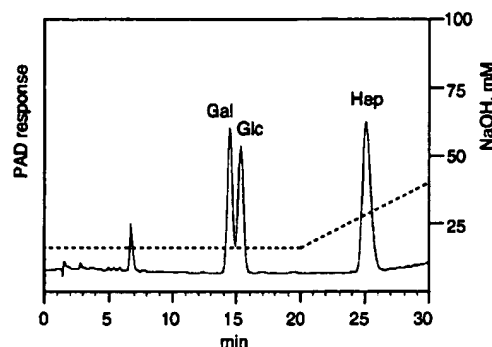
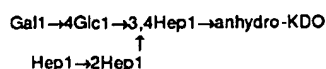


FIGURE 3: Monosaccharide components of the dephosphorylated NTHI 2019 hexasaccharide observed by high-performance anion exchange chromatography with pulsed amperometric detection. From comparison with monosaccharides obtained from hydrolyzed *S. typhimurium* Ra OS, a Gal:Glc:Hep ratio of 1.0:1.1:2.7 was measured for the NTHI 2019 OS. Conditions are as stated under Methods.

saccharide. The Y_1 ion at m/z 219 arises from loss of the entire Hex_2Hep_3 moiety. This fragmentation pattern is consistent with a biantennary structure containing two nonreducing terminal disaccharide branches attached to a disubstituted heptose which is glycosidically linked to the reducing terminal anhydro-KDO moiety (Figure 2). These fragments, which account for the two hexoses and three heptoses in the proposed composition, support the assignment of an anhydro-KDO reducing terminal moiety with a residue mass of 202 Da. Additionally, the Hep-Hep branch establishes that the geometry of the Hep_3 core is different from the Hep_3 core found in *Salmonella* and *Escherichia coli* LPS. In these latter LPS (Galanos et al., 1977; Prehm et al., 1975), branching occurs from the penultimate heptose in a heptose trisaccharide structural moiety, rather than from the first heptose linked to the reducing terminal KDO. MS/MS analysis of the intact hexasaccharide (M_r 1366) indicated that the two PEA groups in the structure are present on the core. Fragments resulting from the loss of nonreducing terminal $Hep(PEA)$ (m/z 1050) and a $Hep(PEA)$ - $Hep(PEA)$ branch (m/z 735) located one PEA group on each of the branch heptoses (data not shown).

To determine the precise monosaccharide composition of the major hexasaccharide, ≈ 15 nmol of the dephosphorylated sample were hydrolyzed and analyzed using high-performance anion exchange chromatography (Hardy et al., 1988) as shown in Figure 3. The NTHI 2019 sample was found to contain galactose and glucose in virtually equimolar quantities, as determined by comparison with a standard monosaccharide mixture containing $GalNH_2$, $GlcNH_2$, Gal, Glc, and KDO. *L-Glycero-D-manno*-heptose was identified in the sample by comparison (and co-injection) with the authentic monosaccharide liberated from the OS of *S. typhimurium* Ra. By comparing the areas of the three NTHI 2019 components with the corresponding monosaccharides present in the *S. typhimurium* sample, roughly 3 molar equiv of *L-glycero-D-manno*-heptose relative to 1 equiv of Gal and 1 equiv of Glc were contained in the NTHI 2019 OS (see the legend to Figure 3). Authentic KDO, which elutes at 43.2 min, was not detected in the hydrolyzed NTHI 2019 OS, although minor unidentified components which may be anhydro-KDOs eluted during the NaOAc gradient portion of the program (35–50 min). To further support the identification of *L-glycero-D-manno*-heptose, alditol acetates were also prepared. GC/MS analysis confirmed that only a single heptose-derived alditol acetate with retention time corresponding to the authentic hepta-*O*-acetyl-*L-glycero-D-manno*-heptitol was present in the NTHI 2019 OS sample.

Methylation analysis of the dephosphorylated major component was performed to determine monosaccharide linkage assignments. Again, the dephosphorylated OS from *S. typhimurium* Ra mutant was used as a standard. The partially methylated alditol acetate derivatives were analyzed by GC/MS using both EI and CI techniques. The NTHI hexasaccharide sample was found to consist of terminal galactose (1,5-di-*O*-acetyl-2,3,4,6-tetra-*O*-methylgalactitol), 1,4-linked glucose (1,4,5-tri-*O*-acetyl-2,3,6-tri-*O*-methylglucitol), terminal heptose (1,5-di-*O*-acetyl-2,3,4,6,7-penta-*O*-methylheptitol), 1,2-linked heptose (1,2,5-tri-*O*-acetyl-3,4,6,7-tetra-*O*-methylheptitol), and 1,3,4-linked heptose (1,3,4,5-tetra-*O*-acetyl-2,6,7-tri-*O*-methylheptitol). GC/MS peaks for the terminal galactose and 1,4-linked glucose derivatives were of nearly equal intensity, consistent with the 1:1 molar ratio determined from monosaccharide composition analysis. A terminal galactose to terminal heptose ratio of ≈ 1.0 to 0.8 was measured relative to the normalized values obtained for the partially methylated alditol acetates from the *S. typhimurium* Ra mutant. GC/MS peaks for the 1,2-linked and 1,3,4-linked heptoses were comparable in size to the terminal heptose peak, but standards required to accurately quantify those components were unavailable. In addition to the terminal galactose, a small amount (<0.1 molar equiv) of terminal glucose was also detected in the NTHI sample. While this may arise from traces of the minor pentasaccharide (M_r 958) present in the NTHI 2019 OS mixture, a small amount of contaminating terminal glucose was also present in the partially methylated alditol acetate mixture derived from the *S. typhimurium* Ra. Taken together with the MS/MS data, these results are consistent with the following partial structure:



Origin of the Reducing Terminal Anhydro-KDO Moiety.

Whereas gonococcal LOS (Gibson et al., 1989), meningococcal LOS (Michon et al., 1990), and the LOS from *S. typhimurium* Ra mutant (John & Gibson, 1990) have been shown to yield "intact" oligosaccharides when subjected to mild acid hydrolysis, the NTHI 2019 LOS produced exclusively OS species which appeared to lack authentic KDO. Furthermore, these oligosaccharides were less stable than the corresponding gonococcal OS. Size exclusion chromatography of the sample in ammonium acetate, followed by evaporation of the solvent in vacuo, led to partial conversion of the oligosaccharides to species 28 Da lower in mass. This degradation reaction (apparent loss of CO from anhydro-KDO) was observed to go to completion when the sample was allowed to stand at 4 °C overnight in 1 M NH_4OH (pH 12), suggesting a base-catalyzed mechanism. Gonococcal OS, which are routinely chromatographed in 100 mM ammonium acetate (pH 7), do not undergo this degradation reaction.

Evidence that the NTHI 2019 OS did not contain authentic KDO was initially provided by composition and MS/MS analyses as discussed above. When the dephosphorylated major component from NTHI 2019 was derivatized with ethyl 4-hydrazinobenzoate (HBEE) and separated on reverse-phase HPLC as the corresponding hydrazone (John & Gibson, 1990), three major peaks and a few minor peaks were obtained (Figure 4A). Oddly, the major peaks all gave virtually the same LSIMS spectrum, with m/z 1281 as the most abundant molecular ion. From our previous experience, diastereomeric forms at the reducing terminus may be responsible for these multiple hydrazone-OS forms. Separation of the underivatized M_r 1120 OS using high-performance anion exchange chro-

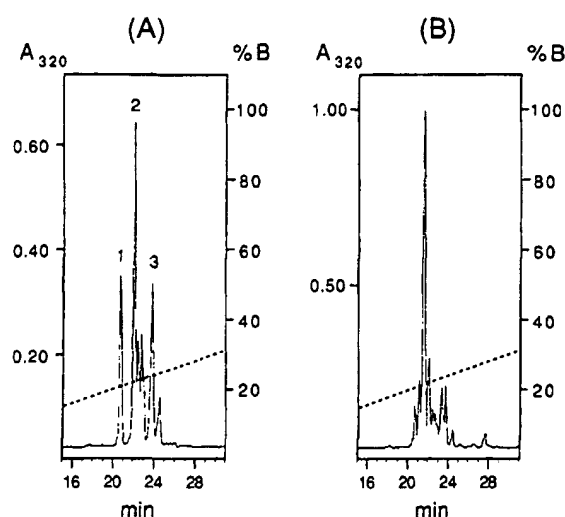


FIGURE 4: Reverse-phase HPLC chromatograms of NTHI 2019 OS derivatized with HBEE. (A) OS prepared by acid hydrolysis of LOS, followed by Bio-Gel P-4 purification and subsequent dephosphorylation. (B) OS prepared by dephosphorylation of LOS, followed by acid hydrolysis and Bio-Sil TSK purification. B is percent CH_3CN .

matography produced a similar result of three closely eluting components (data not shown). When these peaks were collected and analyzed by negative-ion LSIMS, they all gave m/z 1119 as the major molecular ion. These results were consistent with microheterogeneity at the reducing terminal anhydro-KDO moiety.

To rationalize the formation of diastereomeric anhydro-KDO structures in the NTHI 2019 hexasaccharide, a mechanism for their generation was sought. Elimination of a phosphate moiety from C-4 of KDO has been reported to occur during mild acid hydrolysis of intact LOS (Danan et al., 1982; Caroff et al., 1987). Loss of phosphate from the 4-position of KDO proceeds readily under these conditions because the C-4 substituent is β to the C-2 (anomeric) carbonyl carbon and can therefore undergo β -elimination. The reaction is believed to give rise to olefinic KDO derivatives, which can rearrange to form anhydro ring structures (Auzanneau et al., 1991). To ascertain whether elimination of a C-4 phosphate moiety from KDO might account for our results, OS was prepared from NTHI 2019 LOS using a modified method. Prior to acetic acid hydrolysis, the intact NTHI 2019 LOS was treated with aqueous HF to remove the phosphate esters. (Alternatively, the LOS was *O*-deacylated with hydrazine prior to HF treatment in order to increase its solubility in the aqueous solution.) Following removal of the aqueous HF, the dephosphorylated LOS was subjected to the standard mild acid hydrolysis conditions (1% acetic acid, 100 °C, 2 h), and the released oligosaccharides were fractionated on Bio-Sil TSK. LSIMS analysis of OS fractions revealed the presence of a new major component of M_r 1138 (m/z 1137). This OS was 18 Da larger than the previously obtained M_r 1120 OS generated from HF-treatment of the M_r 1366 OS and corresponded to a hexasaccharide composed of two Hex, three Hep, and one KDO. Clearly, the formation of this species using the modified method suggests that removal of an HF-labile moiety from the LOS prior to hydrolysis prevents formation of anhydro-KDO. In addition to the $(\text{M}-\text{H})^-$ ion at m/z 1137, small amounts of the m/z 1119 species were also present in these fractions, which most likely arise from nonquantitative removal of the HF-labile moiety from KDO in the LOS.

A TSK-purified OS fraction containing the M_r 1138 species was derivatized with HBEE and chromatographed on re-

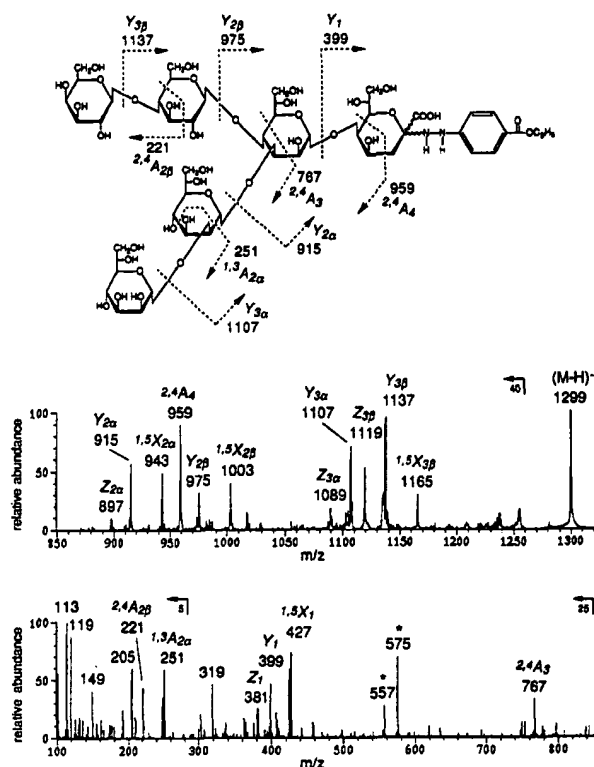


FIGURE 5: MS/MS spectrum of the major OS-HBEE component in Figure 4B at $(M-H)^- = 1299$. Other sequence ions present but not labeled on the spectrum include m/z 1135 (X_{3a}) and 957 (Z_{2b}). The ions labeled with asterisks appear to be Hep_3 fragments arising from cleavage of two glycosidic bonds. Linkage assignments and anomeric configurations indicated were derived from methylation analysis and NMR studies as discussed in the text.

verse-phase HPLC (Figure 4B). LSIMS analysis confirmed that the major component was an OS-HBEE derivative of M_r 1300, with the minor components corresponding to the previously obtained anhydro structures (M_r 1282). The MS/MS spectrum of the major component (Figure 5) supported the branching pattern deduced from MS/MS analysis of the underivatized, dephosphorylated anhydro structure (Figure 2). In this case, the derivatized sample exhibited more extensive fragmentation, including a complete series of nonreducing terminal A-type sequence ions. Furthermore, the MS/MS fragmentation pattern of the M_r 1300 OS-HBEE clearly defined a derivatized reducing terminal saccharide whose residue mass corresponds to authentic KDO.

Additional evidence for the presence of authentic KDO was provided by monosaccharide composition and methylation analyses of the M_r 1138 OS. Following hydrolysis, the sample was analyzed using anion exchange chromatography and found to contain authentic KDO. In order to determine the position of oligosaccharide linkage to KDO in the intact structure, the M_r 1138 OS sample was subjected to a modified methylation analysis reaction scheme designed to yield a partially methylated alditol acetate for reducing terminal KDO (York et al., 1985; John et al., 1991). When the M_r 1138 OS sample was treated in this fashion, a derivative resulting from 5-linked reducing terminal KDO (1,5-*O*-acetyl-2,4,6,7,8-*O*-methyl-3-deoxyoctitol) was obtained. The EI mass spectrum of this partially methylated alditol acetate was identical to the published spectrum of the 5-linked KDO derivative obtained from the OS of *N. gonorrhoeae* strain 1291_a (John et al., 1991). This result indicated that the 1,3,4-linked heptose residue in the NTHI 2019 OS is glycosidically linked to the C-5 of KDO

and supports the hypothesis that an HF-labile moiety exists on the C-4 of KDO in the intact LOS.

Assignment of Anomeric Configurations and Branch Regiochemistry in the Hexasaccharide. The 1H NMR spectrum of the major dephosphorylated hexasaccharide (M_r 1120; Hex_2 , Hep_3 , anhydro-KDO) reflected the sample microheterogeneity observed by chromatographic methods. Figure 6 shows the 500-MHz 1D 1H NMR and DQF-COSY spectra. Although the structure should contain only five monosaccharide residues with anomeric protons, more than five resonances are visible in the anomeric region of the spectrum, consistent with several diastereomeric forms. Furthermore, the C-3 deoxy protons, which occur at high field (δ 1.9 and 2.2) and serve as markers for KDO (Caroff et al., 1987), were conspicuously absent, suggesting that the KDO moiety was altered such that the environment of the C-3 protons was significantly changed. With linkage data and MS/MS results available to define the partial structure of the NTHI 2019 hexasaccharide, it was possible to attribute complexities in the 1H NMR spectrum to reducing terminal microheterogeneity (Auzanneau et al., 1991). Integration of the anomeric resonances suggested that the multiple signals could arise from a total of five protons existing in different subpopulations. On the basis of integrated areas (and coupling connectivities), the anomeric resonances were assigned to five spin systems (designated I, II, III, IV, and V) of three coexisting forms of the hexasaccharide structure as described below.

The anomeric resonances of spin systems III (δ 5.165, $J_{1,2} < 3$ Hz) and V (δ 4.456, $J_{1,2} = 7.5$ Hz) accounted for two anomeric protons which were not noticeably affected by the reducing terminal microheterogeneity. The most lowfield-shifted anomeric proton signal (II) consisted of three closely occurring broad peaks (δ 5.705, $J_{1,2} < 3$ Hz; δ 5.682, $J_{1,2} < 3$ Hz; δ 5.669, $J_{1,2} < 3$ Hz) which together integrated for one proton. A set of three overlapping doublets (δ 4.556, $J_{1,2} = 7.5$ Hz; δ 4.554, $J_{1,2} = 7.5$ Hz; δ 4.546, $J_{1,2} = 7.5$ Hz) integrated for another single anomeric proton (IV), and a group of three resolved broad peaks (δ 5.098, $J_{1,2} < 3$ Hz; δ 5.080, $J_{1,2} < 3$ Hz; δ 5.031, $J_{1,2} < 3$ Hz) accounted for the final anomeric proton (I). The additional resonances present in the highfield end of the anomeric region (δ 4.611, $J = 4.0$ Hz; δ 4.476, $J = 4.5$ Hz; δ 4.404, $J \approx 2.5$ Hz) were attributed to the anhydro-KDO moiety.⁵

On the basis of their chemical shifts and large coupling constants, the anomeric resonances of spin systems V (δ 4.456) and IV (δ 4.556, 4.554, and 4.546) were assigned to two β -linked saccharides. Given the composition of the OS, these resonances were readily attributed to the galactose and glucose residues, the only monosaccharides present with axial H-2 protons. The remaining lowfield-shifted broad peaks suggested α -linked *manno*-heptose residues. To distinguish these resonances, partial assignments of the galactose, glucose, and three *manno*-heptose spin systems present in the oligosaccharide were determined by application of DQF-COSY and 2D HOHAHA spectroscopy.

The anomeric proton at δ 4.456 was assigned to the galactose spin system (V) on the basis of the vicinal coupling constants measured for the H-1, H-2, H-3, and H-4 ring protons from cross-peaks in the DQF-COSY spectrum (Table III). The small $J_{3,4}$ coupling observed defines a sugar with the *galacto* configuration. The glucose spin system (IV) could

⁵ When the OS was first dissolved in D_2O , these signals showed additional splitting and were coupled to resonances at δ 3.1–3.25. Prolonged sitting in D_2O fully exchanged the resonances at δ 3.1–3.25 and altered the splitting pattern of the coupled protons.

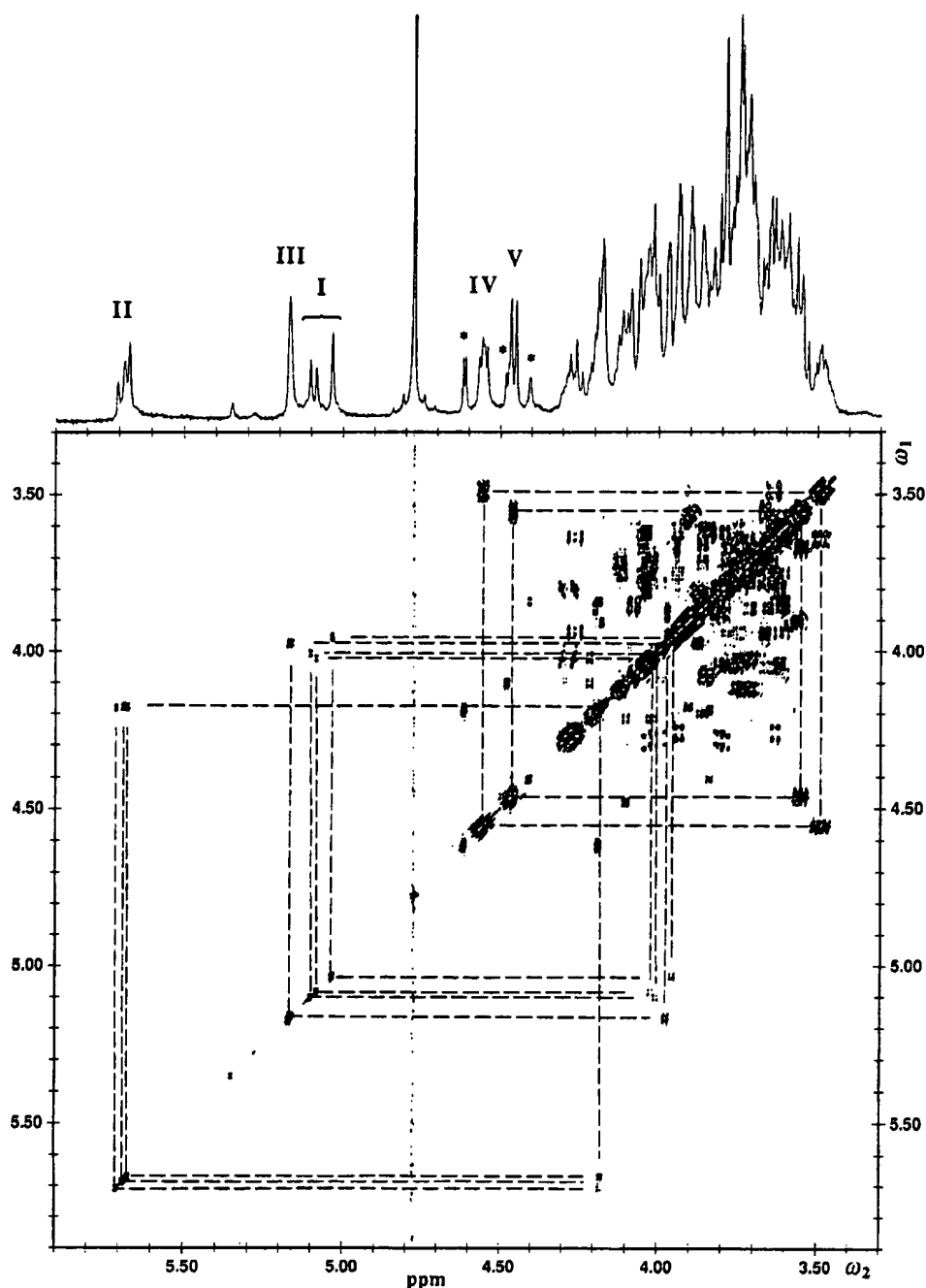


FIGURE 6: Section of the 500-MHz phase-sensitive DQF-COSY spectrum of 1.5 mg of the dephosphorylated hexasaccharide (M_r 1120) in 0.3 mL of D_2O at 25 °C. Negative contour levels are shaded. The 1D 1H NMR spectrum is shown above the 2D data set, with anomeric protons labeled as shown in Table III and explained in the text. Cross-peaks correlating anomeric (H-1) and H-2 resonances are connected with dashed lines. Resonances in the anomeric region labeled with asterisks are believed to represent C-4 protons of 4,7- and/or 4,8-anhydro-KDO moieties (Auzanneau et al., 1991; Pozsgay et al., 1987). The peak at δ 4.78 is HOD.

only be mapped from H-1 (δ 4.556, 4.554, 4.546) to H-3 in the DQF-COSY spectrum. 2D HOHAHA spectroscopy was needed to reveal that the resonances for H-3, H-4, and H-5 are strongly coupled in this 1,4-linked β -glucose residue, as has been observed in related oligosaccharides (Michon et al., 1990; Inagaki et al., 1987). Figure 7A shows selected regions taken from below the diagonal in the 2D HOHAHA spectrum at the ω_1 frequencies of the anomeric resonances. Cross-peaks to the glucose anomeric proton show that magnetization transfer occurred throughout the entire spin system. The chemical shift of H-5 was measured from the H-5/H-6 cross-peak in the DQF-COSY spectrum, leaving the H-4

proton to be associated with the HOHAHA cross-peak at $\approx \delta$ 3.59.

All of the downfield-shifted anomeric resonances exhibited small $J_{1,2}$ couplings, consistent with α -linked saccharides. Protons H-1 (δ 5.165) to H-5 of III were assigned from the DQF-COSY and HOHAHA data (Figure 7A). The small $J_{2,3}$ coupling constant measured from the H-2/H-3 DQF-COSY cross-peak confirmed the *manno* configuration for this residue. The three signals assigned to the downfield-shifted anomeric proton of II (δ 5.705, 5.682, 5.669) all gave cross-peaks to about the same frequency in the DQF-COSY spectrum, consistent with their being assigned to the same mo-

Table III: Partial Proton NMR Assignment of the NTHI 2019 Hexasaccharide (D₂O, 25 °C)^a

proton	V Galβ1		IV 4Glcβ1		I 4Hepa1	
			Hepa1→2Hepa1→3			
			III	II		
H-1	4.456	4.556	5.165	5.705	5.098	
		4.554		5.682	5.080	
		4.546		5.669	5.031	
H-2	3.55	3.49	3.97	4.18	4.01	
				4.18	4.02	
				4.18	3.95	
H-3	3.67	3.64	3.88	3.91	4.02	
				3.90	4.03	
				3.90	3.94	
H-4	3.94	≈3.59	3.80	3.59	4.28	
				3.57	4.29	
				3.56	4.26	
H-5	3.71 ^c	≈3.62	4.03 ^b	4.05 ^b	3.80	
				4.05 ^b	3.79	
				4.04 ^b	3.63	
H-6		3.85			≈4.12 ^{b,c}	
					≈4.13 ^{b,c}	
					≈4.12 ^{b,c}	
H-6'		4.08				
J _{1,2}	7.5 ^d	7.5 ^d	3	3	3	
J _{2,3}	10	9–10	4	sm ^e	3–4	
J _{3,4}	4		8	≈6	9–10	
J _{4,5}	sm ^e				10	

^aChemical shifts are reported in ppm. *J* values are apparent coupling constants (Hz) measured from DQF-COSY cross-peaks unless otherwise noted. The anhydro-KDO spin system (*) was not assigned, although downfield-shifted resonances appearing at δ 4.611, 4.476, and 4.404 were attributed to it (see Figure 6). ^bTentative assignment from HOHAHA data. ^cTentative assignment from NOESY data. ^dCoupling constants measured from the 1D spectrum. ^eSmall coupling (unresolved in the DQF-COSY spectrum).

nosaccharide. Protons H-1, H-2, H-3, and H-4 of this spin system were mapped following COSY connectivities, with HOHAHA cross-peaks to the closely occurring anomeric signals providing a more reliable means of determining precise chemical shifts (Figure 7A). In this case, microheterogeneity caused overlap of DQF-COSY cross-peaks, permitting only approximate measurements of coupling constants for ring protons. The anomeric resonances assigned to I exhibited the greatest degree of chemical shift variation, suggesting that this residue was closest to the heterogeneous anhydro-KDO moiety. The H-1/H-2 cross-peaks in the DQF-COSY spectrum located the H-2 protons, but coupling connectivities could not be readily followed to H-3. Cross-peaks to the anomeric protons in the HOHAHA spectrum, however, suggested that the H-3 protons were strongly coupled to the H-2 protons in each case. With the H-3 protons revealed, connectivity to H-4 and H-5 could be followed in the DQF-COSY spectrum.

2D NOESY spectroscopy was used to determine the identities of the heptose residues and establish the location of branches on the trinked heptose. Sections of the NOESY spectrum showing cross-peaks to anomeric protons are presented in Figure 7B. The anomeric resonances of *manno*-heptose residues I, II, and III all showed intraresidue NOE cross-peaks to their respective H-2 protons, consistent with the *manno* configuration. In addition to this coupling, H-1 of terminal heptose residue III showed interresidue NOEs to H-2 and H-1 of residue II. Interresidue NOEs between two anomeric protons are characteristic of 1,2-linkages in the α-configuration (Romanowska et al., 1988). H-1 of residue II showed an interresidue NOE to H-3 (and possibly H-2) of

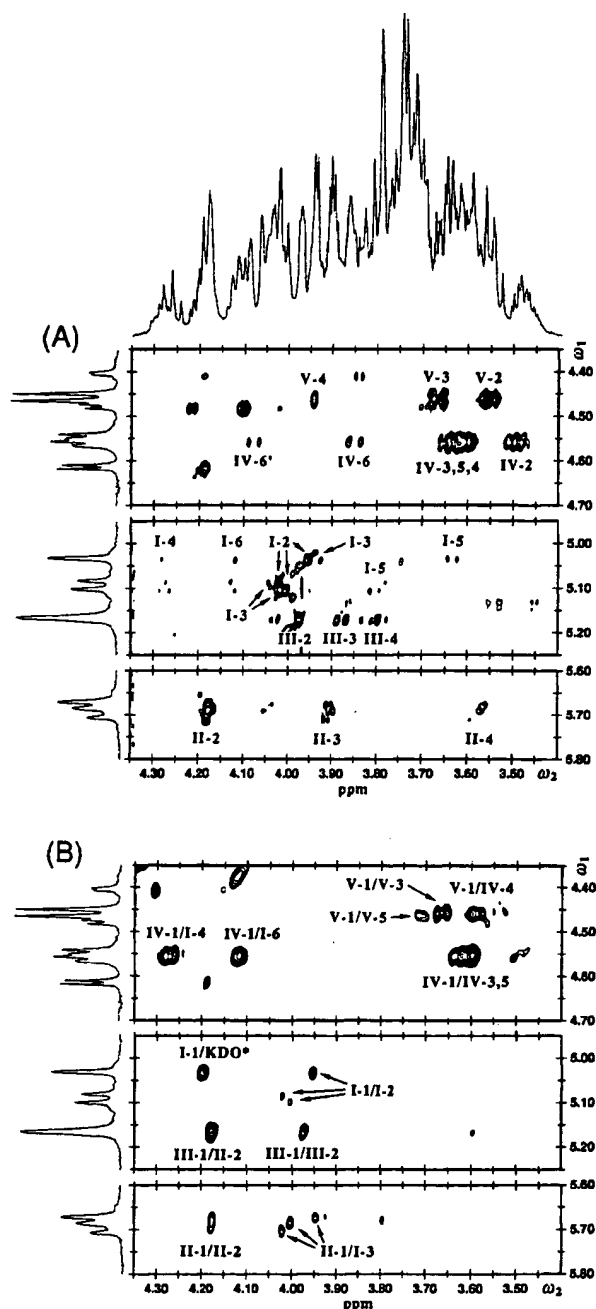


FIGURE 7: (A) Selected regions of the 2D HOHAHA spectrum of the dephosphorylated hexasaccharide in 0.3 mL of D₂O at 25 °C, acquired with a 90-ms mixing time. The middle and lower sections were plotted at lower contour levels than the upper section. Regions of the 1D spectrum are shown above and beside the 2D plots and cross-peaks to anomeric protons are labeled. Roman numerals represent sugar residues and numbers refer to proton assignments. (B) Corresponding regions of the 2D NOESY spectrum acquired with a 400-ms mixing time. All sections were plotted at the same contour levels. A NOE cross-peak between III-1 and II-1 is present in the full spectrum. Assignments of I-6 and V-5 are tentative.

residue I, establishing that II is linked to the 3-position of I. The anomeric proton of terminal β-galactose residue V showed an intraresidue NOE cross-peak to H-3 and interresidue coupling to the H-4 proton of IV. An additional NOE cross-peak to the anomeric proton of V was tentatively assigned to H-5 of V, a proton which could not be assigned from the DQF-COSY and HOHAHA data. The anomeric proton of

β -glucose residue IV showed intraresidue NOE cross-peaks to H-3 and H-5 and interresidue couplings to H-4 of residue I and a resonance tentatively assigned to H-6 of I. This supported placing the Gal β 1 \rightarrow 4Glc β 1 \rightarrow branch on the 4-position of I. One of the anomeric resonances assigned to residue I (δ 5.031) showed a NOE cross-peak to a signal tentatively assigned to the anhydro-KDO spin system (Figure 7B). However, the specific assignment of this heptose linkage to C-5 of authentic KDO was made on the basis of methylation analysis data (discussed above). With respect to the 1,3,4-linked heptose I, this branching pattern is clearly related to that observed in oligosaccharides from meningococcal and gonococcal LOS.

Analysis of *O*-Deacylated NTHI 2019 LOS. In order to confirm the existence of phosphorylated KDO in the LOS, mass spectrometric experiments were performed on modified LOS species. Crude NTHI 2019 LOS was *O*-deacylated by treatment with hydrazine and subsequently dephosphorylated. Without further purification, the *O*-deacylated, dephosphorylated LOS was analyzed directly by negative-ion LSIMS (spectrum not shown). A major molecular ion was seen at m/z 1911, with minor components at m/z 1991, 2073, and 2235. The predicted molecular weight for a molecule consisting of the dephosphorylated M_r 1138 hexasaccharide and an *O*-deacylated, dephosphorylated lipid A moiety bearing two *N*-linked 3-hydroxytetradecanoic acid residues is M_r 1912. The ion at m/z 1991 corresponds to the m/z 1911 component bearing a residual phosphate group (+80 Da), and the higher mass ions (m/z 2073 and 2235) represent species bearing additional hexose residues (+162 Da/Hex). Independent LSIMS analysis of the free NTHI 2019 lipid A (obtained by mild acid hydrolysis of intact LOS) produced a major molecular ion at m/z 1823, consistent with a lipid A structure consisting of a glucosamine disaccharide bearing four 3-hydroxytetradecanoic acid residues, two tetradecanoic acids, and two phosphates (spectrum not shown). Glucosamine, tetradecanoic acid, and 3-hydroxytetradecanoic acid were detected in compositional analyses of the NTHI 2019 lipid A (W. Melaugh, unpublished results), suggesting that the molecular weight and composition of this lipid A are consistent with the *H. influenzae* lipid A structure reported by Helander et al. (1988). Taken together, these LSIMS results suggested that only a single KDO links the OS to the lipid A moiety in NTHI 2019 LOS. In the LSIMS spectrum of the *O*-deacylated, dephosphorylated LOS, there was no evidence of species containing additional KDOs.

Attempts to analyze the intact *O*-deacylated NTHI 2019 LOS (with phosphate groups still present) using negative-ion LSIMS were not successful. Since two PEA groups are present on the OS structure, electrospray MS (Smith et al., 1990) in the positive-ion mode was attempted as an alternative means of producing stable molecular ions. The resulting spectrum contained a mixture of protonated and sodiated doubly and triply charged ions (spectrum not shown), consistent with an *O*-deacylated LOS bearing two PEA groups and three phosphate moieties (measured average mass, 2399.9 \pm 0.6). Having demonstrated the existence of two PEAs on the OS moiety and two phosphates on the lipid A structure, we conclude from this electrospray MS data that a third phosphate group exists on the KDO moiety linking the lipid A to the OS (Figure 8). Again, no evidence was seen for additional KDOs in the LOS structure.

DISCUSSION

SDS-PAGE indicated that the NTHI 2019 LOS consisted of one major component and several minor species. Mass

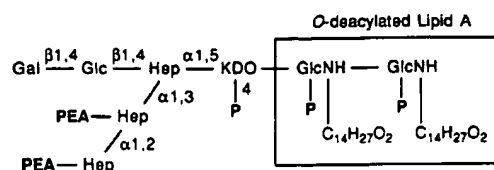
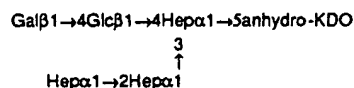


FIGURE 8: Proposed structure of the *O*-deacylated NTHI 2019 LOS derived from electrospray MS data and LSIMS analysis of the dephosphorylated species as discussed in the text. Phosphate (P) and phosphoethanolamine (PEA) substituents are shown in boldface type.

spectral studies of chemically modified LOS revealed that the major structure was a hexasaccharide ketosidically linked via a single bridging KDO to a lipid A moiety. In the native LOS, the bridging KDO is apparently phosphorylated on C-4. As a result of this substitution, acid hydrolysis of the intact LOS yields oligosaccharides with anhydro-KDO on the reducing terminus rather than intact KDO (Auzanneau et al., 1991). The demonstration that a species with intact KDO could be obtained from LOS that had been HF-treated prior to acetic acid hydrolysis confirmed that anhydro-KDO was generated as an artifact of the hydrolysis procedure. While the microheterogeneity associated with the anhydro-KDO moiety could have in principle been avoided by initial dephosphorylation of the LOS, efforts to produce a preparation completely free of the anhydro forms were unsuccessful.

The major dephosphorylated hexasaccharide was shown by tandem mass spectrometry, methylation analysis, and NMR studies to have the following structure:



In the unmodified OS, both the terminal and dilinked heptose moieties are substituted with PEA. In addition to this species, we also observed higher molecular weight components in the NTHI 2019 OS mixture which most certainly contain different terminal epitopes. Methylation analysis of Bio-Gel P-4 fractions containing oligosaccharides larger than the major hexasaccharide component revealed additional sugars, including terminal glucose, 1,3-linked galactose, 1,2,3-linked heptose, terminal *N*-acetylglucosamine, and 1,4-linked *N*-acetylglucosamine. The presence of a second trlinked heptose moiety suggests that extension of the basal hexasaccharide structure may occur by elaboration of a new oligosaccharide branch from the 3-position of the penultimate heptose. Given the propensity of Hib LOS to undergo rapid phase variation (Kimura & Hansen, 1986; Kimura et al., 1987), it is possible that larger oligosaccharide structures may be more abundant in vivo. In a study of the LOS from Hib strain Eagan, Inzana et al. (1985) observed a major OS species of 1768 Da which was found to contain β -D-galactose and nonreducing terminal β -D-galactose linked to *N*-acetyl-D-galactosamine.

With the complete characterization of the dephosphorylated NTHI 2019 hexasaccharide and partial structural elucidation of the total LOS, we can begin to construct a structural model for *H. influenzae* LOS. Unlike the inner core structure of neisserial LOS, we have found a Hep₂-KDO core in the NTHI 2019 OS. The KDO is phosphorylated on C-4 and does not appear to be substituted with additional KDOs. This observation is interesting in connection with an earlier structural study conducted on the LPS of a deep-rough mutant strain of *H. influenzae* (strain I-69 Rd⁻/b⁺) whose oligosaccharide moiety was found to consist of only a single KDO, phosphorylated on either C-4 or C-5 (Helander et al., 1988). At the time, it was postulated that the phosphate substituents might

act as signals for (or blockers of) KDO-transferases and heptosyltransferases, which were reported to be lacking or inactive in the mutant strain (Helander et al., 1988). Our results are consistent with the hypothesis that phosphorylation on the 4-position of KDO prevents the addition of further KDOs to the core region of *H. influenzae* LOS. Alternatively, it is possible that species with additional KDOs would be too labile to give molecular ions under LSIMS or electrospray MS conditions, although we have previously observed intact LOS structures with two KDOs in *O*-deacylated, dephosphorylated gonococcal LOS (John et al., 1991; Phillips et al., 1990). Interestingly, phosphorylated KDO has also been observed in the LOS of *Bordetella pertussis*, the respiratory tract pathogen which causes whooping cough (Caroff et al., 1987, 1990).

Various Gram-negative pathogens share common epitopes (Campagnari et al., 1990; Virji et al., 1990). Recent studies have suggested that mucosal pathogens mimic host oligosaccharide structures in their LOS as a means of evading host defenses (Mandrell et al., 1988; Campagnari et al., 1990; John et al., 1991). The terminal lactose moiety (Gal β 1 \rightarrow 4Glc β 1 \rightarrow) present in the NTHI 2019 hexasaccharide is an epitope also present on lactosylceramide, a human glycosphingolipid and a precursor to human blood group antigens. Recently, a digalactoside moiety (Gal α 1 \rightarrow 4Gal β 1 \rightarrow) also found in mammalian glycolipid structures was detected on *H. influenzae* LOS using a monoclonal antibody specific for that epitope (Virji et al., 1990). Distinct from these terminal epitopes, a "KDO-related" epitope has been associated with NTHI 2019, as well as several recombinant *H. influenzae* strains (Campagnari et al., 1990; Spinola et al., 1990). While the genes coding for the expression of this epitope have been cloned (Spinola et al., 1990), the precise chemical structure of the epitope is not known. Further detailed studies of the LOS from additional strains *H. influenzae* will be needed to establish whether phosphorylated KDO may be a feature of this "KDO-related" epitope and identify other important epitopes involved in host/pathogen interactions.

ACKNOWLEDGMENTS

We gratefully acknowledge the invaluable technical assistance of L. Reinders and thank members of the UCSF Mass Spectrometry (F. Walls and D. Maltby) and NMR Facilities (Drs. V. Basus, D. Banville, D. Kerwood, and S. Farr-Jones) for much help and guidance.

Registry No. Gal β 1 \rightarrow 4Glc β 1 \rightarrow (Hep α 1 \rightarrow 2Hep α 1 \rightarrow 3)4Hep α 1 \rightarrow 5-KDO, 140148-99-8.

REFERENCES

- Auzanneau, F.-I., Charon, D., & Szabó, L. (1991) *J. Chem. Soc., Perkin Trans. 1*, 509.
- Bax, A., & Davis, D. G. (1985) *J. Magn. Reson.* 65, 355.
- Basus, V. J., Billeter, M., Love, R. A., Stroud, R. M., & Kuntz, I. D. (1988) *Biochemistry* 27, 2763.
- Campagnari, A. A., Gupta, M. R., Dudas, K. C., Murphy, T. F., & Apicella, M. A. (1987) *Infect. Immun.* 55, 882.
- Campagnari, A. A., Spinola, S. M., Lesse, A. J., Abu Kwaik, Y., Mandrell, R. E., & Apicella, M. A. (1990) *Microb. Pathog.* 8, 353.
- Caroff, M., Lebbar, S., & Szabó, L. (1987) *Carbohydr. Res.* 161, c4.
- Caroff, M., Chaby, R., Karibian, D., Perry, J., Deprun, C., & Szabó, L. (1990) *J. Bacteriol.* 172, 1121.
- Danan, A., Mondange, M., Sarfati, S. R., & Szabó, P. (1982) *J. Chem. Soc., Perkin Trans. 1*, 1275.
- Darveau, R. P., & Hancock, R. E. W. (1983) *J. Bacteriol.* 155, 831.
- Di Fabio, J. L., Michon, F., Brisson, J.-R., & Jennings, H. J. (1990) *Can. J. Chem.* 68, 1029.
- Domon, B., & Costello, C. E. (1988) *Glycoconjugate J.* 5, 397.
- Falick, A. M., Wang, G. H., & Walls, F. C. (1986) *Anal. Chem.* 58, 1308.
- Fletcher, A. R., & Insel, R. A. (1978) *J. Infect. Dis.* 138, 719.
- Galanos, C., Lüderitz, O., Rietschel, E. T., & Westphal, O. (1977) *Int. Rev. Biochem.* 14, 197.
- Gibson, B. W., Webb, J. W., Yamasaki, R., Fisher, S. J., Burlingame, A. L., Mandrell, R. E., Schneider, H., & Griffiss, J. M. (1989) *Proc. Natl. Acad. Sci. U.S.A.* 86, 17.
- Hardy, M. R., Townsend, R. R., & Lee, Y. C. (1988) *Anal. Biochem.* 170, 54.
- Helander, I. M., Lindner, B., Brade, H., Altmann, K., Lindberg, A. A., Rietschel, E. T., & Zähringer, U. (1988) *Eur. J. Biochem.* 177, 483.
- Inagaki, F., Kohda, D., Kodama, C., & Suzuki, A. (1987) *FEBS Lett.* 212, 91.
- Inzana, T. J., Seifert, W. E., Jr., & Williams, R. P. (1985) *Infect. Immun.* 48, 324.
- Jennings, H. J., Bhattacharjee, A. K., Kenne, L., Kenny, C. P., & Calver, G. (1980) *Can. J. Biochem.* 58, 128.
- Jennings, H. J., Johnson, K. G., & Kenne, L. (1983) *Carbohydr. Res.* 121, 233.
- John, C. M., & Gibson, B. W. (1990) *Anal. Biochem.* 187, 281.
- John, C. M., Griffiss, J. M., Apicella, M. A., Mandrell, R. E., & Gibson, B. W. (1991) *J. Biol. Chem.* 266, 19303.
- Kimura, A., & Hansen, E. J. (1986) *Infect. Immun.* 51, 69.
- Kimura, A., Patrick, C. C., Miller, E. E., Cope, L. D., McCracken, G. H., Jr., & Hansen, E. J. (1987) *Infect. Immun.* 55, 1979.
- Larson, G., Karlsson, H., Hansson, G. C., & Pimlott, W. (1987) *Carbohydr. Res.* 161, 281.
- Lever, S. B., & Hakomori, S. (1987) *Methods Enzymol.* 138, 13.
- Mäkelä, P. H. (1988) *Eur. J. Clin. Microbiol. Infect. Dis.* 7, 606.
- Mandrell, R. E., Griffiss, J. M., & Macher, B. A. (1988) *J. Exp. Med.* 168, 107.
- Marion, D., & Wüthrich, K. (1983) *Biochem. Biophys. Res. Commun.* 113, 967.
- Michon, F., Beurret, M., Gamian, A., Brisson, J.-R., & Jennings, H. J. (1990) *J. Biol. Chem.* 265, 7243.
- Moxon, E. R. (1990) in *Principles and Practice of Infectious Diseases* (Mandell, G. L., Douglas, R. G., Jr., & Bennett, J. E., Eds.) p 1722, Churchill Livingstone Inc., New York.
- Moxon, E. R., & Vaughn, K. A. (1981) *J. Infect. Dis.* 143, 517.
- Murphy, T. F., & Apicella, M. A. (1987) *Rev. Infect. Dis.* 9, 1.
- Parr, T. R., Jr., & Bryan, L. E. (1984) *Can. J. Microbiol.* 30, 1184.
- Patrick, C. C., Kimura, A., Jackson, M. A., Hermanstorfer, L., Hood, A., McCracken, G. H., Jr., & Hansen, E. J. (1987) *Infect. Immun.* 55, 2902.
- Patrick, C. C., Pelzel, S. E., Miller, E. E., Haanes-Fritz, E., Radolf, J. D., Gulig, P. A., McCracken, G. H., Jr., & Hansen, E. J. (1989) *Infect. Immun.* 57, 1971.
- Phillips, N. J., John, C. M., Reinders, L. G., Gibson, B. W., Apicella, M. A., & Griffiss, J. M. (1990) *Biomed. Environ. Mass Spectrom.* 19, 731.
- Pozsgay, V., Jennings, H., & Kasper, D. L. (1987) *Eur. J. Biochem.* 162, 445.

- Prehm, P., Strim, S., Jann, B., & Jann, K. (1975) *Eur. J. Biochem.* 56, 41.
- Rance, M., Sorensen, O. W., Bodenhausen, G., Wagner, G., Ernst, R. R., & Wüthrich, K. (1983) *Biochem. Biophys. Res. Commun.* 117, 479.
- Redfield, A. G., & Kuntz, S. D. (1975) *J. Magn. Reson.* 19, 250.
- Romanowska, E., Gamian, A., Lugowski, C., Romanowska, A., Dabrowski, J., Hauck, M., Opferkuch, H. J., & von der Lieth, C.-W. (1988) *Biochemistry* 27, 4153.
- Smith, R. D., Loo, J. A., Edmonds, C. G., Barinaga, C. J., & Udseth, H. R. (1990) *Anal. Chem.* 62, 882.
- Spinola, S. M., Abu Kwaik, Y., Lesse, A. J., Campagnari, A. A., & Apicella, M. A. (1990) *Infect. Immun.* 58, 1558.
- States, D. J., Harberkorn, R. A., & Ruben, D. J. (1982) *J. Magn. Reson.* 48, 286.
- Stellner, K., Saito, H., & Hakomori, S. (1973) *Arch. Biochem. Biophys.* 155, 464.
- Takayama, K., Qureshi, N., Hyver, K., Honovich, J., Cotter, R. J., Mascagni, P., & Schneider, H. (1986) *J. Biol. Chem.* 261, 10624.
- Turk, D. C. (1982) in *Haemophilus influenzae, epidemiology, immunology, and prevention of disease* (Sell, S. H., & Wright, P. F., Eds.) p 1, Elsevier, Amsterdam.
- van Alphen, L., Klein, M., Geelen-van den Broek, L., Riemens, T., Eijk, P., & Kamerling, J. P. (1990) *J. Infect. Dis.* 162, 659.
- Virji, M., Weiser, J. N., Lindberg, A. A., & Moxon, E. R. (1990) *Microb. Pathog.* 9, 441.
- Walls, F. C., Baldwin, M. A., Falick, A. M., Gibson, B. W., Kaur, S., Maltby, D. A., Gillece-Castro, B. L., Medzihradzky, K. F., Evans, S., & Burlingame, A. L. (1990) in *Biological Mass Spectrometry* (Burlingame, A. L., & McCloskey, J. A., Eds.) p 197, Elsevier, Amsterdam.
- Yamasaki, R., Bacon, B. E., Nasholds, W., Schneider, H., & Griffiss, J. M. (1991) *Biochemistry* 30, 10566.
- York, W. S., Darvill, A. G., McNeil, M., & Albersheim, P. (1985) *Carbohydr. Res.* 138, 109.
- Zamze, S. E., & Moxon, E. R. (1987) *J. Gen. Microbiol.* 133, 1443.
- Zamze, S. E., Ferguson, M. A. J., Moxon, E. R., Dwek, R. A., & Rademacher, T. W. (1987) *Biochem. J.* 245, 583.

The Structural Basis for Pyocin Resistance in *Neisseria gonorrhoeae* Lipooligosaccharides*

(Received for publication, February 22, 1991)

Constance M. John†, J. McLeod Griffiss‡, Michael A. Apicella¶, Robert E. Mandrell§, and
Bradford W. Gibson† ||

From the †Department of Pharmaceutical Chemistry and §Centre for Immunochemistry, Department of Laboratory Medicine and Veterans Affairs Medical Center, University of California, San Francisco, California 94143 and the ¶Department of Medicine, State University of New York, Buffalo, New York 14215

Pyocin resistance in a strain of *Neisseria gonorrhoeae* has been found to be associated with structural differences in the oligosaccharide moieties of the gonococcal outer membrane lipooligosaccharides (LOS). *N. gonorrhoeae* strain 1291 had been treated with several pyocins, usually lethal bacteriocins produced by *Pseudomonas aeruginosa*, and a series of surviving mutants were selected. The LOS of these pyocin-resistant mutants had altered electrophoretic mobilities in sodium dodecyl sulfate-polyacrylamide gels (Dudas, K. C., and Apicella, M. A. (1988) *Infect. Immun.* 56, 499-504). Structural analyses of the oligosaccharide portions of the wild-type (1291wt) and five pyocin-resistant strains (1291_{mut}) by liquid secondary ion mass spectrometry, tandem mass spectrometry, and methylation analysis revealed that four of the mutant strains make oligosaccharides that differ from the wild-type LOS by successive saccharide deletions (1291_{mut}) and, in the oligosaccharide of 1291_{wt}, by the addition of a terminal Gal to the 1291_{wt} structure. The composition, sequence, and linkages of the terminal tetrasaccharide of the wild-type LOS are the same as the lacto-*N*-neotetraose terminus of the human paragloboside (Galβ1→4GlcNAcβ1→3Galβ1→4Glc-ceramide), and both glycolipids bound the same monoclonal antibodies O6B4/3F11 that recognize this terminal epitope. None of the pyocin-resistant mutants bound this antibody. The 1291_{wt} LOS bound a monoclonal antibody that is specific for Galα1→4Galβ1→4Glc-ceramide (P^h glycosphingolipid) and shared a common composition, sequence, and linkages with this latter glycosphingolipid. Organisms that bound the anti-P^h monoclonal occurred at the rate of ~1/750 among the wild-type parent strain. This structural information supports the conclusion that treatment with pyocin selects for mutants with truncated LOS structures and suggests that

the oligosaccharides contained in the LOS of the wild-type strain and 1291_{wt} mimic those of human glycosphingolipids.

Neisseria gonorrhoeae is a Gram-negative bacteria that colonizes human mucosal surfaces producing an array of pathological responses and disease. In order to develop successful strategies that can interfere with the virulence, growth, and/or dissemination of this organism, it is important to understand the factors that enable the gonococci to colonize the genital mucosa and evade the host defense system (1). It is almost certainly significant then that *N. gonorrhoeae* and the other mucosal pathogens such as *Neisseria meningitidis* and *Haemophilus influenzae* produce highly branched and relatively short lipopolysaccharides (LPS).¹ These LPS lack the repeating and variable *O*-antigens that are characteristic of the LPS of the enteric Gram-negative bacteria. To reflect these structural differences, it has been suggested that *N. gonorrhoeae* LPS and other bacterial LPS that share similar features are more accurately referred to as lipooligosaccharides (LOS).

As a principal surface component, gonococcal LOS interacts directly with host cell membranes and circulating glycoproteins and stimulates an immune response during infection (2-4). Certain LOS can also activate the complement system, and some strains with antigenically distinct LOS are able to evade complement-mediated cell lysis (3, 5-9). Gonococcal LOS share structures and epitopes with human glycosphingolipids that are precursors to blood group antigens (10). These LOS oligosaccharides are sialylated *in vivo* by host cytidine monophospho-*N*-acetylneuraminic acid in a manner similar to that of host glycosphingolipids (GSL) (11, 12).

Understanding how LOS functions in the pathogenesis of gonococcal diseases and, in particular, the role of molecular mimicry of host cell GSLs in this pathogenesis requires that the structures of these LOS be determined. Gonococcal LOS are, however, considerably heterogeneous and difficult to characterize. Each gonococcal strain expresses from two to six different LOS of *M*, 3150-7100, as determined by sodium dodecyl sulfate-polyacrylamide gel electrophoresis (13). The structure of the highly conserved gonococcal lipid A moiety

* This work was supported by grants from the National Science Foundation (Biological Instrumentation Program Grant DIR8700766), the National Institutes of Health (Grants AI21620, AI24616, AI8384, and RR01614), and the Veterans Administration. This is Report 33 from the Centre for Immunochemistry of the University of California, San Francisco and was presented in part at the 89th meeting of the American Society for Microbiology, New Orleans, May 14-18, 1989 and at the 1st Congress of the International Endotoxin Society, San Diego, May 10-12, 1990. The costs of publication of this article were defrayed in part by the payment of page charges. This article must therefore be hereby marked "advertisement" in accordance with 18 U.S.C. Section 1734 solely to indicate this fact.

|| To whom correspondence and reprint requests should be addressed: School of Pharmacy 926-S, 513 Parnassus Ave., University of California, San Francisco, CA 94143-0446. Tel.: 415-476-5320; Fax: 415-476-0688.

¹ The abbreviations used are: LPS, lipopolysaccharide; CID, collision-induced dissociation; GSL, glycosphingolipid; HBEE, ethyl-4-hydrazinobenzoate; Hep, heptose; Hex, hexose; KDO, 2-keto-3-deoxy-manno-octulosonic acid; LOS, lipooligosaccharide; LSIMS, liquid secondary ion mass spectrometry; (M-H)⁺, deprotonated molecular ion; mAb, monoclonal antibody; MS/MS, tandem mass spectrometry; PEA, phosphoethanolamine; PMAA, partially methylated alditol acetate.

has been determined by ^1H NMR and laser desorption mass spectrometry (14) and is unlikely to account for these differences. Considerable variation in the oligosaccharide components has been found in these LOS, and their corresponding oligosaccharides differ in size, sugar composition, and antigenic expression (9). We have determined the first oligosaccharide structures for a set of LOS of a single pyocin-resistant gonococcal strain, JW31R (15). Even for this comparatively simple mutant, over five major and seven minor oligosaccharide components were found.

In the enteric bacteria *Salmonella* and *Escherichia*, a series of core-defective rough mutants, or R-type mutants, were used to elucidate the structures of their LPS and biosynthetic pathways. These mutants were produced by exposing the bacteria to the lethal action of bacteriophages. The survivors were found to have truncated LPS lacking the O-antigen polysaccharide (R_0) and successive saccharide deletions in the outer and inner core regions (R_0 – R_4). Their structures provided critical information about LPS biosynthesis and were used in determining the structures of the inner and outer core LPS regions (2, 16).

In an analogous manner, pyocin, a bacteriocin isolated from *Pseudomonas aeruginosa* has been found to select for *N. gonorrhoeae* that express variant LOS (17–23). These surviving strains are now resistant to pyocin binding and pyocin-mediated cell lysis (24). The exact mechanism for the development of resistance and the nature of the alteration in the LOS has not been established. Petricoin and Stein (25) have defined two genetic loci responsible for pyocin transformation of *N. gonorrhoeae* that results in alteration of the expression of LOS antigens. In this current study, we have described the compositions, saccharide orders, and linkages of the oligosaccharides isolated from the LOS made by an isogenic series of pyocin-resistant mutants of a single strain, 1291, that differ in their LOS electrophoretic mobility and antigenic determinants (23).

EXPERIMENTAL PROCEDURES²

RESULTS AND DISCUSSION

Molecular Weights and Compositions—The oligosaccharides from the wild-type (1291wt) and mutant gonococcal strains (1291_a) eluted from the TSK or Bio-Gel P-4 size exclusion columns as broad peaks. Based on retention times, these oligosaccharides would be expected to have masses between 1000–2000 Da. As shown in Fig. 1 (Miniprint), LSIMS spectra of the underivatized oligosaccharides yielded deprotonated molecular ions, $(M - H)^-$, ranging from m/z 947³ (for 1291_a) to m/z 1678 (for 1291wt).

In most cases, monosaccharide compositions (i.e. Hex, HexNAc, Hep, and KDO) could be readily assigned to these oligosaccharides based on the known composition of neisserial LOS and their corresponding molecular weights. Table 1 (Miniprint) lists the $(M - H)^-$ ions, their corresponding molecular weights, and the proposed compositions for the major oligosaccharide species from the wild-type and mutant strains. Only two lower mass species (m/z 943 and 901) from the LOS of pyocin-resistant strains 1291_a and 1291_b could not

be assigned compositions. A comparison of masses before and after aqueous HF treatment allowed us to assign a single PEA group to each oligosaccharide by distinguishing between the isobaric moieties HexNAc and phosphorylphosphoethanolamine, both of which have a nominal residue mass of 203 Da.

LSIMS Analysis of Oligosaccharide-hydrazones—In order to confirm the preliminary compositions and assign partial structures for these oligosaccharide species, the hydrazone benzoate ethyl ester (HBEE) derivatives were prepared for each oligosaccharide after aqueous HF treatment and purified by high pressure liquid chromatography (29). LSIMS analysis of the major high pressure liquid chromatography peaks gave abundant molecular ions corresponding to the oligosaccharide-HBEE derivatives, as well as some limited fragment ions. In general, cleavage at either side of the glycosidic bond with charge retention at the reducing terminal KDO-HBEE moiety produced ions of the Y and Z types, according to the nomenclature recommendations of Domon and Costello (38) (see Fig. 2, Miniprint). For example, the major oligosaccharide-HBEE species from 1291wt LOS produced an abundant molecular ion at m/z 1675 (see Fig. 3, Miniprint). This $(M - H)^-$ ion is consistent with the expected mass for an oligosaccharide containing Hex₃HexNAc₂Hep₂KDO plus the ethyl 4-hydrazinobenzoate. Abundant Y type fragments were also observed at m/z 1513, 1310, 1148, and to a lesser extent, 986 that help define the major nonreducing branch as Hex→HexNAc→Hex→Hex→. A smaller ion is also observed at m/z 1472 that is consistent with the loss of a terminal HexNAc from a second nonreducing branch. Unfortunately, due to the high matrix background at the lower masses, no other fragments are seen that might otherwise define the connectivity of these two nonreducing branches to the core Hep₂KDO region. In Fig. 3B, the negative ion LSIMS spectra of the 1291_b oligosaccharide-HBEE shows an abundant $(M - H)^-$ ion at m/z 1472. Fragment ions (Y type) at m/z 1310, 1148, and 986 define a Hex→Hex→Hex nonreducing branch, and m/z 1269 identifies a nonreducing terminal HexNAc. For both the 1291wt and 1291_b oligosaccharide-HBEEs, smaller Z (Y – H₂O) and X (Y + CO) fragments also accompanied most of the more abundant Y fragments, except at lower masses where they tend to be of equal abundance.

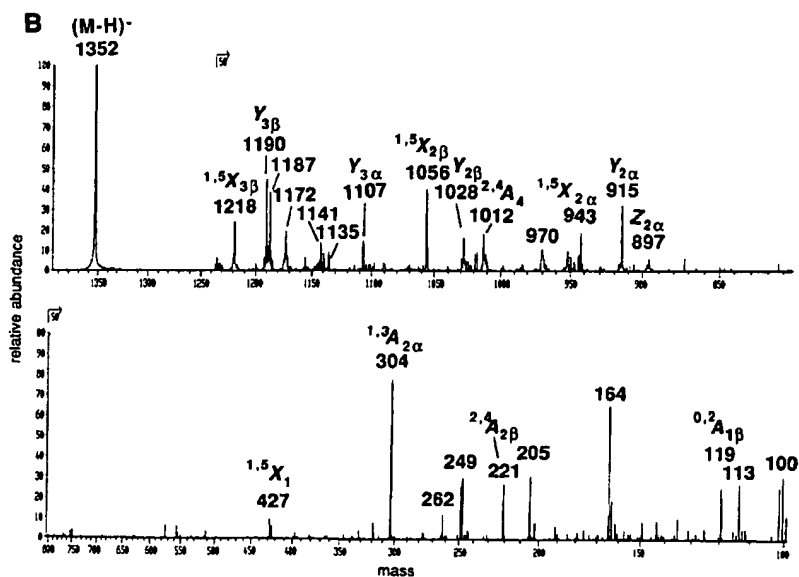
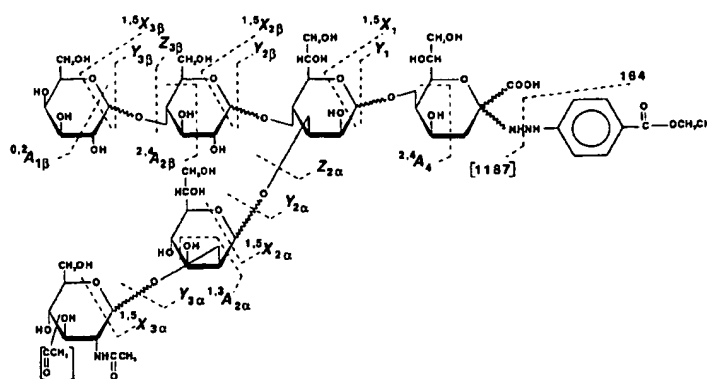
Tandem Mass Spectrometry—A set of partial structures were constructed from the LSIMS spectra of the free oligosaccharides and their HBEE derivatives that defined the nonreducing branches attached to the core region. Tandem spectra were then obtained to substantiate the correctness of these preliminary structures and to define the structure and substitutions of the core Hep₂KDO region. The more extensive array of ion fragments observed under tandem CID conditions provided structural information on less labile linkages, such as those between heptose moieties and ions that might otherwise be lost in the high background in the corresponding LSIMS spectra (29).

Fig. 4A shows the MS/MS CID daughter ion spectrum of the 1291c HBEE-oligosaccharide. Abundant ions are present at m/z 1148, 986, and 1107 that support both a Hex-Hex and HexNAc nonreducing branch. In addition, fragments that arise from cleavage between the Hep-Hep and Hep-KDO glycosidic linkages (see m/z 915 and 399, for example) allow us to assign the two nonreducing branches to the Hep attached to the reducing terminal KDO (i.e. Hex→Hex→Hep→KDO) and to the second heptose (i.e. HexNAc→Hep→Hep→KDO).

As mentioned earlier, many of these oligosaccharides also contained a single O-acetyl group (30). Previous analyses of meningococcal oligosaccharides suggested that the O-acetyl group is attached to the nonreducing terminal HexNAc (39).

² Portions of this paper (including "Experimental Procedures," Figs. 1–3, and Tables 1, 3, and 4) are presented in miniprint at the end of this paper. Miniprint is easily read with the aid of a standard magnifying glass. Full size photocopies are included in the microfilm edition of the Journal that is available from Waverly Press.

³ Nominal masses are given throughout the text for both ions and molecular weights unless otherwise noted. Both values are based on the isotopically pure ^{12}C component of the natural isotopic distribution.



Tandem CID analysis of these gonococcal 1291 oligosaccharides that also contain an *O*-acetyl group have identified a similar substitution at the terminal HexNAc. For example, in the spectrum shown in Fig. 4B, the $^{13}A_2$ fragment ion for the nonreducing terminal HexNAc is only weakly present at m/z 262. However, a much larger peak is found 42 Da higher at m/z 304, corresponding to a $^{13}A_2$ fragment for terminal *O*-acetyl-HexNAc. Several other larger reducing terminal fragments containing *O*-acetyl HexNAc are also seen in this spectra that clearly identify the *O*-acetyl group attached to the terminal HexNAc on the second core heptose.

The tandem mass spectrometric analysis of the non-HF-treated oligosaccharides made it possible to identify the second heptose as the site of attachment of PEA, as fragment ions containing this heptose were shifted by 123 Da relative to those observed in the HF-treated tandem CID spectrum. Recent work with oligosaccharide from meningococcal LOS had established the analogous second heptose as the site of attachment of a PEA moiety (40). In addition, the fragments observed in the MS/MS analyses of derivatized 1291_a oligosaccharides suggested that the PEA moiety is attached to the C-3 of the second heptose. Nonreducing terminal fragments of the same $^{13}A_2$ type as shown in Fig. 4 were observed containing PEA that then had to be on either the nonreducing terminal HexNAc or on C-2 or C-3 of the adjacent Hep. However, fragment ions for loss of HexNAc alone from the reducing terminus were found in the same spectrum. Methylation analysis had already identified a glycosidic linkage at the C-2 position of the second heptose. Therefore, the only possible attachment site for PEA was the C-3 of the second heptose.

Based on the LSIMS and MS/MS data alone, several partial structures consisting of phosphorylated, *O*-acetylated biantennary oligosaccharides could be proposed for the wild-type and pyocin-resistant LOS. The proposed wild-type oligosaccharide was Hex→HexNAc→Hex→Hex→(HexNAc(OAc))→Hep(PEA)→Hep→KDO. The oligosaccharides from the pyocin mutants 1291_a through 1291_e, with the exception of 1291_b, were truncated versions of this wild-type structure and are listed in Table 2. The 1291_b LOS-oligosaccharide was different and has a hexose triose attached to the first core heptose, i.e. Hex→Hex→Hex→(HexNAc(OAc))→Hep(PEA)→Hep→KDO, a structure not seen in the major wild-type oligosaccharide but that could be present in low abundance.

Methylation Analysis—Linkages and monosaccharide identities were determined by methylation analysis of the total oligosaccharide fractions of the wild-type and five pyocin-resistant gonococcal mutants (see Table 3, Miniprint). For the more heterogeneous 1291_a, only one of the earlier eluting components of the TSK oligosaccharide fraction was analyzed. In all cases, the partially permethylated alditol acetates (PMAAs) that were identified by gas chromatography/mass spectrometry analysis were consistent with the mass spectrometric structures that had already been determined.

The 1291_a oligosaccharide fraction contained 2,3,6-tri-*O*-methylglucitol and 2,4,6-tri-*O*-methylgalactitol arising from two internal hexoses (1,4-Glc and 1,3-Gal) in approximately equal molar ratios and a PMAA arising from a terminal GlcNAc (2-acetamido-2-deoxy-3,4,6-tri-*O*-methylglucitol) in a 2 M excess. Two substituted heptoses (3,4,6,7-tetra-*O*-methylheptitol and 2,6,7-tri-*O*-methylheptitol) arising from 1,2-Hep and 1,3,4-Hep were also identified but could not be accurately quantitated due to a lack of standards and the apparent resistance of Hep-Hep glycosidic bonds to hydrolysis (30). In the 1291wt oligosaccharide fraction, a pattern almost

identical with the major one seen in the 1291_a oligosaccharide was observed. One exception, however, was that instead of the two terminal GlcNAcs, an internal 1,4-GlcNAc (2-acetamido-2-deoxy-3,6-di-*O*-methylglucitol) and a terminal Gal (2,3,4,6-tetra-*O*-methylgalactitol) were present. The PMAAs found in 1291_c through 1291_e (like 1291_a) were consistent with sugars arising from a common oligosaccharide structure that contained sequential saccharide deletions of the Gal1→4GlcNAc1→3Gal1→4Glc1→4Hep1→oligosaccharide branch. Based on this assumption, we assigned the two monosubstituted hexoses (i.e. 1,3-Gal and 1,4-Glc) identified in the methylation analysis of the 1291wt to the internal Hex-Hex disaccharide defined by the mass spectral data and in the same order, i.e. →3Gal1→4Glc1→. The 1291_b oligosaccharide contained 2,3,6-tri-*O*-methylgalactitol (1,4-Gal) and 2,3,4,6-tetra-*O*-methylgalactitol (terminal Gal) and supported an alternative structure Gal1→4Gal1→4Glc1→4Hep1. This 1291_b structure is based on the assumption that it was built up from the 1291_c with the single addition of a terminal Gal. A smaller amount of 1,3-Gal was also present in the 1291_b oligosaccharide that likely originated from wild-type LOS contamination. As will be discussed later, the assignments for 1291wt and 1291_a are also supported by their binding to the MAbs O6B4/3F11 and anti-P^k, respectively.

PMAAs originating from a 1,2-Hep, terminal GlcNAc, and 1,3,4-Hep were present in all oligosaccharide fractions, with the exception of 1291_a and 1291_e, which had mainly 2,4,6,7-tetra-*O*-methylheptitol (1,3-Hep) and only a small amount of 2,6,7-tri-*O*-methylheptitol (1,3,4-Hep). The smaller amount of 2,6,7-tri-*O*-methylheptitol (1,3,4-Hep) in 1291_a and 1291_e is clearly linked to the partial substitution at C-4 of the core 1,3-Hep by Glc. Therefore, one could now define a common core structure of GlcNAc1→2Hep1→3Hep1→ that must be linked to KDO. We then established the linkage of this core 1,3,4-Hep to KDO by the method of York *et al.* (37). Following the reduction of the 2-keto moiety of KDO and esterification of the carboxylate, a PMAA resulting from reducing terminal 5-linked KDO (1,5-*O*-acetyl-2,4,6,7,8-*O*-methyl-3-deoxyoctitol) was identified in the 1291_a oligosaccharide fraction as shown in Fig. 5 (Miniprint). It was assumed that this linkage is conserved among all the 1291 LOS, as has been the case so far for *N. meningitidis* LOS (39, 41, 42).

Structures of 1291wt and 1291_{a-e} Oligosaccharides—By combining the mass spectrometric, composition, and methylation data, structures containing the complete branching pattern (but without anomeric assignments) could be proposed for the oligosaccharides derived from the wild-type and each of the five pyocin mutants. The structures were built up from core oligosaccharides present in both 1291_a and 1291_e LOS by adding sequential sugars as indicated by mass spectra and methylation analyses. For example, the addition of Glc to the fourth position of 1,3-linked Hep was deduced by the presence of both 1,3,4-Hep and 1,3-Hep and a terminal Glc in the methylation analysis of 1291_a oligosaccharides. LSIMS spectra of the intact oligosaccharides had already determined the HexNAc→Hep→Hep→KDO and Hex→(HexNAc→Hep→)Hep→KDO structures, and therefore, these linkages must be present as Glc1→(HexNAc1→3Hep1→3)4Hep1→5KDO. The Hep and terminal HexNAc had been identified previously in all 1291 oligosaccharides as 1,2-Hep and terminal GlcNAc, and can be assigned as GlcNAc1→2Hep, yielding the core structure shown in Table 2 for 1291_a and 1291_e. Methylation analysis for 1291_c oligosaccharide found an internal 1,4-Glc (as opposed to a terminal Glc), along with a terminal Gal, i.e. Gal1→4Glc1→. This is consistent with the LSIMS spectrum that had previously defined a Hex₂ branch on the disubsti-

TABLE 2
Structures of 1291 wild-type and pyocin mutant LOS oligosaccharides

	Proposed composite structures	LSIMS-derived structures
1291 wt	Gal β 1—4GlcNAc β 1—3Gal β 1—4Glc1—4Hep1—5KDO <div style="text-align: center;"> 3 1 PEA—3Hep 2 1 GlcNAc(OAc) </div>	Hex—HexNAc—Hex—Hex—Hep—KDO <div style="text-align: center;"> PEA—Hep HexNAc(OAc) </div>
1291 _a	GlcNAc β 1—3Gal β 1—4Glc1—4Hep1—5KDO <div style="text-align: center;"> 3 1 PEA—3Hep 2 1 GlcNAc(OAc) </div>	HexNAc—Hex—Hex—Hep—KDO <div style="text-align: center;"> PEA—Hep HexNAc(OAc) </div>
1291 _c	Gal β 1—4Glc1—4Hep1—5KDO <div style="text-align: center;"> 3 1 PEA—3Hep 2 1 GlcNAc(OAc) </div>	Hex—Hex—Hep—KDO <div style="text-align: center;"> PEA—Hep HexNAc(OAc) </div>
1291 _{da}	Glc1—4Hep1—5KDO <div style="text-align: center;"> 3 1 PEA—3Hep 2 1 GlcNAc(OAc) </div>	Hex—Hep—KDO <div style="text-align: center;"> PEA—Hep HexNAc(OAc) </div>
1291 _{da}	Hep1—5KDO <div style="text-align: center;"> 3 1 PEA—3Hep 2 1 GlcNAc(OAc) </div>	Hep—KDO <div style="text-align: center;"> PEA—Hep HexNAc(OAc) </div>
1291 _b	Gal α 1—4Gal β 1—4Glc1—4Hep1—5KDO <div style="text-align: center;"> 3 1 PEA—3Hep 2 1 GlcNAc(OAc) </div>	Hex—Hex—Hex—Hep—KDO <div style="text-align: center;"> PEA—Hep HexNAc(OAc) </div>

tuted Hep. In an analogous manner, the oligosaccharides of 1291_a and 1291wt LOS contained extensions of this branch by the additions of GlcNAc at C-3 of Gal (1291_a) and an additional terminal Gal at C-4 of GlcNAc (1291wt). In 1291_b, the terminal Gal found in the 1291_c oligosaccharide is extended primarily at the fourth position (as opposed to C-3) with a terminal Gal instead of a GlcNAc. Otherwise, 1291_b

shares the same core structure found in all the other 1291 strains.

The oligosaccharide structures listed in Table 2 clearly (with the exception of 1291_b) are consistent with being biosynthetic intermediates of the major 1291 wild-type oligosaccharide by virtue of successive saccharide deletion. Indeed, the 1291_{a,c-e} mutants are analogous to the R_a-R_e mutants

constructed for *Salmonella typhimurium* and *Escherichia coli*. Previously published MAb binding studies found high level binding of 1291wt LOS and the MABs 3F11 and O6B4 that recognize the lacto-*N*-neotetraose containing paragloboside GSL, Gal β 1 \rightarrow 4GlcNAc β 1 \rightarrow 3Gal β 1 \rightarrow 4Glc-ceramide (10). It is not too surprising then to see this same structural moiety present in the 1291wt oligosaccharides but absent in the five pyocin mutants that did not bind these two MABs. This data suggests also that the anomeric configurations may be identical between this blood group antigen and that contained in the 1291wt LOS and are likely to be conserved in truncated parts of this structure present in the pyocin mutants 1291_{a,c-e}.

From the preliminary structure of the 1291_b oligosaccharide, it is clear that this species is not a biosynthetic precursor of the major 1291wt LOS structure as shown in Table 2. Strain 1291_b was selected by treatment of mutant strain 1291_c with pyocin, whereas the other mutant strains were pyocin-resistant after only one treatment (23). Although this strain has been classified a "second generation mutant," the significance of this distinction is not known. However, the oligosaccharides it produces clearly diverges from the major 1291wt oligosaccharide in at least two ways; the terminal position of the 1291_b oligosaccharide branch (i.e. Gal1 \rightarrow 4Gal1 \rightarrow 4Glc \rightarrow) has a Gal in place of the GlcNAc in the corresponding penultimate position of the wild-type structure, and this sugar is now linked to the fourth position instead of the third position of the neighboring Gal (see Table 2).

The similarity of the 1291_b oligosaccharide to the GSL Gal α 1 \rightarrow 4Gal β 1 \rightarrow 4Glc-ceramide (or P^k) prompted us to determine whether the 1291 mutant LOS could bind an anti-P^k MAB. The high affinity with which the MAB bound it clearly showed that the 1291_b LOS contained the P^k antigen (see Table 4, Miniprint). Since the 1291_b LOS contains a terminal trisaccharide of the same sequence and linkages as that present in this GSL, we concluded it must have the same anomeric configurations as well or it would not bind with such high affinity; Gal α 1 \rightarrow 4Gal β 1 \rightarrow 4Glc \rightarrow . 1291wt LOS also bound the anti-P^k MAB but with much less affinity (Table 4). This low affinity binding of the MAB to the 1291wt LOS could represent high affinity binding to a 1291_b alternative LOS structure present at low levels (<2%). This possibility was supported by the presence in the methylation analyses of 1291wt of a small amount of PMAA originating from 1,4-Gal (see Table 3, Miniprint) and confirmed by the presence of 9 P^k MAB-binding organisms among 6,500 progeny of strain 1291 (\approx 1 in 750 or 0.1–0.2%). Furthermore, we found that 36 of 70 different gonococcal strains bound the anti-P^k MAB with \geq 25% of its binding affinity for 1291_b. Virji *et al.* (43) also recently reported MAB binding studies that showed that Gal α 1 \rightarrow 4Gal, a digalactoside epitope common to *H. influenzae* LOS, is also present on 14 of 59 *N. gonorrhoeae* strains. Taken together, these observations suggest that *N. gonorrhoeae* 1291_b originates from the common 1291_c precursor in the LOS biosynthetic pathway and is expressed at only low levels (<1%). The LOS made by gonococcal strains are a mixture of structures that are made by different LOS phase variants (26). 1291_b would appear to be one such LOS variant that spontaneously arises at modest frequency and that was selected for by double pyocin treatment (23). Regulation of LOS variance is not well understood, but the relative LOS variants may be considerably different *in vivo* than when the organism is grown on artificial media.

Intact LOS Structure—To determine the mass for the intact LOS, O-deacylated and O-deacylated and HF-treated LOS were analyzed directly by negative ion LSIMS. For 1291wt LOS, a mass of *m/z* 2507 was observed for the O-deacylated

and HF-treated LOS and is precisely the mass expected for the intact LOS after removal of the PEAs, the O-acetate(s), and the two to three O-acyl fatty acids linked at the C-3 ring position of each of the two glucosamines of lipid A (14). O-Deacylated and HF-treated LOS from strain 1291_d gave an (M – H)[–] ion at *m/z* 1818, the expected mass for the modified LOS. The mass difference between 1291wt and the 1291_d LOS is 689 Da, which corresponds to one HexNAc and three Hex moieties (see Table 2) and supports our conclusion that the primary heterogeneity in these different LOS resides in the oligosaccharide portions.

CONCLUSIONS

Our efforts to understand the structural basis for the antigenic diversity and biosynthesis of gonococcal LOS have included strategies to decrease the inherent heterogeneity of the LOS that are produced by wild-type strains. To this end, a series of LOS variants of the wild-type strain 1291 with altered LOS have been isolated by treatment with pyocin, a bacteriocin isolated from *P. aeruginosa*. These bacteriocins bind to gonococcal LOS receptors and initiate lysis of the bacterium. Using a combination of advanced mass spectrometric and chromatographic techniques that require considerably less material than conventional structural studies, we have been able to structurally characterize the oligosaccharides from a set of pyocin-resistant gonococcal strains (1291_{a-c}). From these studies, it was found that four of the pyocin-resistant strains (1291_{a,c-e}) made LOS that had sequential saccharide deletions from the wild-type structure (1291wt). The selection of this set of biosynthetic precursors should allow us to probe into biosynthetic mechanisms and to establish the presence of important epitopes in this LOS. It is our plan now to isolate larger amounts of purified oligosaccharides from the LOS of 1291wt and one or two of the pyocin mutants to conduct the necessary NMR experiments to define their complete structures.

Previous data indicated that the lacto-*N*-neotetraose epitope recognized by the MABs 3F11 and O6B4 was present in a majority of gonococcal strains. In fact, 3F11 bound to the LOS isolated from 87 of 90 gonococcal strains (10) but significantly fewer of the related meningococcal LOS. Nonetheless, the entire lacto-*N*-neotetraose moiety has been identified in the structures of the oligosaccharide portions of the meningococcal LOS of L3, L7, and L9 serotypes (42). It is also interesting that O-acetate groups have been identified on the terminal GlcNAc of the meningococcal LOS glycans (39, 40) at similar levels (40–50%) to those we have observed on the gonococcal 1291 LOS.

Surprisingly, less similarity was found between these 1291 oligosaccharide structures present in the wild-type strain (or pyocin mutants) and those we previously reported for the gonococcal pyocin-mutant JW31R (15). In JW31R LOS, it was the second heptose that contained the larger oligosaccharide branch, GalNAc \rightarrow Hex \rightarrow Hex \rightarrow Hex \rightarrow (GlcNAc1 \rightarrow)Hep \rightarrow (Gal \rightarrow Glc \rightarrow)Hep \rightarrow KDO, rather than the first heptose in 1291wt, Gal1 \rightarrow 4GlcNAc1 \rightarrow 3Gal1 \rightarrow 4Glc1 \rightarrow (GlcNAc1 \rightarrow 3Hep1 \rightarrow 3)4Hep1 \rightarrow 5KDO. Furthermore, the presence of a GalNAc was not seen in the 1291 oligosaccharides, nor was the internal GlcNAc seen in JW31R LOS. In both cases, however, the inner core heptose region was similar, if not identical, and a single PEA and GlcNAc moiety is attached to the second Hep. The total absence of O-acetate on this terminal GlcNAc represents the only significant departure from this shared core structure. The significance of these conserved and differing structural features between the LOS of these two strains are as yet unclear, although the parent

structure to JW31R (or JW31) appears to be more similar to the wild-type 1291 strain and may also contain the lacto-*N*-neotetraose structure.⁴

More recently, the MAb 3F11 has also been found to bind to the LOS of *Haemophilus ducreyi*, another Gram-negative pathogen that colonizes genital mucosa (44). The MAb 3F11 bound to 16 of 17 *H. ducreyi* strains tested, suggesting that this epitope may be conserved to a similar extent as that in the LOS of *N. gonorrhoeae*. The biological significance of this conserved epitope is not known, but it may represent a critical component in the ability of these mucosal pathogens to attach themselves to the mucosal surface and/or evade the immune system.

The expression of the P^k antigen by the 1291_b that arises from the wild-type strain at a rate of $\approx 10^{-3}$ is also intriguing. This structure, like the lacto-*N*-neotetraose structure of paragloboside, is present in glycosphingolipids and is a precursor of the globoside blood group antigens. Tissue distribution studies have shown that P^k-antigens are present in the urogenital tract (45). It may be that the expression of both the P^k and the lacto-*N*-neotetraose oligosaccharide antigens are involved in host mimicry mechanisms that allow the gonococci to establish itself by evading the immune system. Gonococcal LOS almost certainly have other roles, such as in the adhesion to host cell surfaces (10), but the similarity to blood group antigens and to other antigens present normally in the host tissues colonized by gonococci provide a rationale for understanding the presence of these diverse oligosaccharide structures in the LOS molecule.

REFERENCES

- Gotschlich, E. C. (1984) in *Bacterial Vaccines* (Germanier, R., ed) pp. 353-371, Academic Press, New York
- Galanos, C., Luderitz, O., Rietschel, E. T., and Westphal, O. (1977) *Int. Rev. Biochem.* **14**, 239-335
- Ward, M. E., Lambden, P. R., Heckels, J. E., and Watt, P. J. (1978) *J. Gen. Microbiol.* **108**, 205-212
- Cooper, M. D., McGraw, P. A., and Melly, M. A. (1986) *Infect. Immun.* **51**, 425-430
- Tramont, E. C., Sadoff, J. C., and Wilson, C. (1977) *J. Immunol.* **118**, 1843-1851
- Ingwer, I., Petersen, B. H., and Brooks, G. (1978) *J. Lab. Clin. Med.* **92**, 211-220
- Schneider, H., Griffiss, J. M., Mandrell, R. E., Jarvis, G. A. (1985) *Infect. Immun.* **50**, 672-677
- Apicella, M. A., Westerink, M. A. J., Morse, S. A., Schneider, H., Rice, P. A., and Griffiss, J. M. (1986) *J. Infect. Dis.* **153**, 520-526
- Griffiss, J. M., O'Brien, J. P., Yamasaki, R., Williams, G. D., Rice, P. A., and Schneider, H. (1987) *Infect. Immun.* **55**, 1792-1800
- Mandrell, R. E., Griffiss, J. M., and Macher, B. (1988) *J. Exp. Med.* **168**, 107-126
- Mandrell, R. E., Lesse, A. J., Sugai, J. V., Shero, M., Griffiss, J. M., Cole, J. A., Parsons, N. J., Smith, H., Morse, S. A., and Apicella, M. A. (1990) *J. Exp. Med.* **171**, 1649-1664
- Apicella, M. A., Mandrell, R. E., Shero, M., Wilson, M. E., Griffiss, J. M., Brooks, G. F., Lammel, C., Breen, J. F., and Rice, P. A. (1990) *J. Infect. Dis.* **162**, 506-512
- Schneider, H., Hale, T. L., Zollinger, W. D., Seid, Jr., R. C., Hammack, C. A., and Griffiss, J. M. (1984) *Infect. Immun.* **45**, 544-549
- Takayama, K., Qureshi, N., Hyver, K., Honovich, J., Cotter, R. J., Mascagni, P., and Schneider, H. (1986) *J. Biol. Chem.* **261**, 10624-10631
- Gibson, B. W., Webb, J. W., Yamasaki, R., Fisher, S. J., Burlingame, A. L., Mandrell, R. E., Schneider, H., and Griffiss, J. M. (1989) *Proc. Natl. Acad. Sci. U. S. A.* **86**, 17-21
- Luderitz, O., and Westphal, O. (1966) *Angew. Chem. Int. Ed. Engl.* **5**, 198-210
- Blackwell, C. C., and Law, J. A. (1981) *J. Infect.* **3**, 370-378
- Connelly, M. C., Stein, D. C., Young, F. E., Morse, S. A., and Allen, P. Z. (1981) *J. Bacteriol.* **148**, 796-803
- Guymon, L. F., Esser, M., and Shafer, W. M. (1982) *Infect. Immun.* **36**, 541-547
- Morse, S. A., and Apicella, M. A. (1982) *J. Infect. Dis.* **145**, 206-216
- Stein, D., Clark, V., and Young, F. (1983) *Sex. Transm. Dis.* **10**, 7-13
- Winstanley, F. P., Blackwell, C. C., Tan, E. C., Patel, P. V., Parsons, N. J., Martin, P. M., and Smith, H. (1984) *J. Gen. Microbiol.* **130**, 1303-1306
- Dudas, K. C., and Apicella, M. A. (1988) *Infect. Immun.* **56**, 499-504
- Morse, S. A., Vaughan, P., Johnson, D., and Iglewski, B. H. (1976) *Antimicrob. Agents Chemother.* **10**, 354-362
- Petricoin, E. F., III, and Stein, D. C. (1989) *Infect. Immun.* **57**, 2847-2852
- Mandrell, R., Schneider, H., Apicella, M., Zollinger, W., Rice, P. A., and Griffiss, J. M. (1986) *Infect. Immun.* **54**, 63-69
- Zollinger, W. D., and Mandrell, R. E. (1977) *Infect. Immun.* **18**, 424-433
- Brodin, N. T., Dahmen, J., Nilsson, B., Messeter, L., Martensson, S., Heldrup, J., Sjogren, H. O., and Lundblad, A. (1988) *Int. J. Cancer* **42**, 185-194
- John, C. M., and Gibson, B. W. (1990) *Anal. Biochem.* **187**, 281-291
- Phillips, N. J., John, C. M., Reinders, L. G., Griffiss, J. M., Apicella, M. A., and Gibson, B. W. (1990) *Biomed. Environ. Mass Spectrom.* **19**, 731-745
- Helander, I. M., Lindner, B., Brade, H., Altmann, K., Lindberg, A. A., Rietschel, E. T., and Zahring, U. (1988) *Eur. J. Biochem.* **177**, 483-492
- Falick, A. M., Wang, G. H., and Walls, F. C. (1986) *Anal. Chem.* **58**, 1308-1311
- Walls, F. C., Baldwin, M. A., Falick, M. A., Gibson, B. W., Gillece-Castro, B. L., Kaur, S., Maltby, D. A., Medzhradsky, K. F., Evans, S., and Burlingame, A. L. (1990) in *Biological Mass Spectrometry* (McCloskey, J. A., and Burlingame, A. L., ed) pp. 197-216, Elsevier, Amsterdam
- Lavery, S. B., and Hakomori, S.-I. (1987) *Methods Enzymol.* **138**, 13-25
- Larson, G., Karlsson, H., Hansson, G. C., and Pimlott, W. (1987) *Carbohydr. Res.* **161**, 281-290
- Stellner, K., Saito, H., and Hakomori, S.-I. (1973) *Arch. Biochem. Biophys.* **155**, 464-472
- York, W. S., Darvill, A. G., McNeil, M., and Albersheim, P. (1985) *Carbohydr. Res.* **138**, 109-126
- Domon, B., and Costello, C. E. (1988) *Glycoconjugate J.* **5**, 397-409
- Michon, F., Beurret, M., Gamian, A., Brisson, J.-R., and Jennings, H. J. (1990) *J. Biol. Chem.* **265**, 7243-7247
- Dell, A., Azadi, P., Tiller, P., Thomas-Oates, J., Jennings, H. J., Beurret, M., and Michon, F. (1990) *Carbohydr. Res.* **200**, 59-76
- Jennings, H. J., Bhattacharjee, A. K., Kenne, L., Kenny, C. P., and Calver, G. (1980) *Can. J. Biochem.* **58**, 128-136
- Jennings, H. J., Johnson, K. G., and Keene, L. (1983) *Carbohydr. Res.* **121**, 233-241
- Virji, M., Weiser, J. N., Lindberg, A. A., and Moxon, E. R. (1990) *Microb. Pathog.* **9**, 441-450
- Campagnari, A. A., Spinola, S. M., Lesse, A. J., Kwaik, Y. A., Mandrell, R. E., and Apicella, M. A. (1990) *Microb. Pathog.* **8**, 353-362
- Kasai, K., Galton, J., Terasaki, P. I., Wakisaka, A., Kawahara, M., Root, T., and Hakomori, S.-I. (1985) *J. Immunogenet. (Oxf.)* **12**, 213-220

⁴B. W. Gibson and C. M. John, unpublished data.

Supplemental Material to The Structural Basis for Pyocin-Resistance in *Neisseria gonorrhoeae* Lipooligosaccharides*

by

Constance M. John, J. McLeod Griffiss, Michael A. Apicella, Robert E. Mandrell and
Bradford W. Gibson

EXPERIMENTAL

Isolation and purification of LOS and oligosaccharides. LOS from *N. gonorrhoeae* wild-type strain 1291 (1291wt) and five pyocin-resistant mutants (1291a-e) were isolated and purified from acetone dried organisms as previously described (23). Approximately 10-25 mg of crude LOS was hydrolyzed in 1% acetic acid (2 mg/ml) for 2 h at 100°C. The resulting mixture containing lipid A and oligosaccharide was then centrifuged (for 20 min at 5000 x g) and the water-soluble oligosaccharides removed. The precipitate was washed with 5 ml of H₂O, centrifuged, and combined with the first soluble fraction and lyophilized. For the 1291_a LOS, 0.1% SDS (wt/wt) was added to the acetic acid to increase solubility and removed after hydrolysis by a single pass through a C₁₈ Sep-Pak (Waters Assoc.).

About 5-10 mg of crude lyophilized oligosaccharide was then dissolved in 250 µl of 1% acetic acid and filtered through a 0.45 µm nylon filter. These oligosaccharides were applied to two TSK-125 Bio-Sil gel filtration HPLC columns (600 x 7.5 mm) linked in series. The oligosaccharides were eluted isocratically with 1% acetic acid at 1 ml/min and monitored by refractive index detection (Knauer RI detector). Fractions of 1 ml each were collected and those containing oligosaccharide were pooled and dried on a Savant liquid concentrator. Alternatively, the oligosaccharide fraction was taken up in 0.047 M pyridinium acetate (pH 5.2) and separated on a Bio-Gel P-4 column (80 x 2.5 cm, 37°C) equilibrated with the same buffer.

Solid Phase Radioimmunoassay of Gonococcal LOS. Outer membrane complexes containing LOS from *N. gonorrhoeae* 1291wt and 1291a-e were screened for binding to a commercial monoclonal antibody (MAB) that is specific for the P₁ blood group antigen by solid phase radioimmunoassay (SPRIA) as previously described (28,27). Anti-P₁ MAB was obtained from MonoCarb (Accurate Chemicals, Westbury, NY); it binds the glycosphingolipid antigen Gal α 1 \rightarrow 4Gal β 1 \rightarrow 4Glc \rightarrow Ceramide (28).

HF-treatment of oligosaccharides. To remove phosphoserine moieties, 0.1-1 mg of oligosaccharide(s) was placed in a 1.5 ml polypropylene tube and cold 48% aqueous HF was added to obtain a 0.1 µg/µl solution. HF-hydrolysis proceeded at 4°C for 18-24 h and excess HF was removed by vacuum in a polypropylene desiccator with a solid NaOH in-line trap. HF is extremely toxic and should only be used in a well-ventilated hood.

Derivatization of oligosaccharides with ethyl 4-hydrazinobenzoate. To prepare oligosaccharide hydrazones, approximately 20-200 µg of oligosaccharides, some of which had been previously HF-treated, were placed in 1 ml glass reaction vials and ~3 equivalents of ethyl 4-hydrazinobenzoate (HBEE) were added (29). We then added 10 µl of H₂O, 40 µl of MeOH, and between 0.25-0.5 µl of acetic acid. The reaction mixture was heated at 80°C for 30 minutes and dried at 30°C under a stream of N₂.

HPLC separation of oligosaccharide-hydrazones. The oligosaccharide-hydrazones were dissolved in 0.05% TFA and separated on a C₁₈ reverse phase HPLC column (Vydac, 25 cm x 4.8 mm i.d.). The column was equilibrated with H₂O/0.05% trifluoroacetic acid (solvent A), and the oligosaccharides were eluted with a linear gradient of 0 to 50% acetonitrile/0.05% trifluoroacetic acid (solvent B) at a flow rate of 1 ml/min. The column eluant was monitored at 335 nm with a Kratos 783 variable UV detector and selected peaks were dried prior to analysis by LSIMS.

Preparation of soluble LOS. To prepare soluble intact LOS derivatives (O-deacylated and dephosphorylated) for mass spectrometric analyses, several LOS were treated with hydrazine and aqueous-HF as previously described (30). Briefly, LOS samples were first O-deacylated following the procedure of Helander et al. (31) by incubating crude LOS (0.1-1 mg) in 200 µl of anhydrous hydrazine for 30 min at 37°C, followed by cooling to -20°C and adding cold acetone to precipitate the resulting O-deacylated LOS. The precipitated LOS was then centrifuged (12,000 x g for 20 min), the acetone and hydrazine removed and the precipitate again washed with cold acetone and centrifuged. The precipitated LOS was resuspended in 0.5 ml of water and lyophilized. To remove phosphate and PEA, O-deacylated LOS (10 µg/µl) was treated with aqueous HF as described above.

Mass Spectrometry. Both derivatized and underivatized oligosaccharides were dissolved in H₂O and aliquots transferred to a stainless steel probe tip, to which had been added approximately 1 µl of a glycerol/thioglycerol matrix (1:1). The O-deacylated HF-treated LOS were first dissolved in H₂O/methanol (1:1). All samples were analyzed using a Kratos MS-50 double focusing mass spectrometer operating at a mass resolution of 1500 to 2500 (m/z, 10% valley). A Ca⁺ ion primary beam of 10 keV was used to sputter and ionize the samples with secondary ions accelerated at 6-8 kV. Scans were acquired at 300 e/decade and recorded on a Gould electrostatic recorder as previously described (32). Ultramark 1621 was used to manually calibrate spectra to an accuracy of better than ± 0.3 Da.

Tandem (MS/MS) Analysis. Oligosaccharides derivatized with HBEE were dissolved in H₂O and transferred to a stainless steel probe previously loaded with 1 µl glycerol/thioglycerol matrix (1:1). All MS/MS spectra were obtained on a four-sector Kratos Concept II HPL mass spectrometer with an optically-coupled diode array detector on MS-2, as described in detail elsewhere (33). The spectra were acquired in the negative mode and a Ca⁺ primary beam energy of 18 keV was used to sputter and ionize the oligosaccharides. The deprotonated molecular ions, [M-H]⁻, were selected in MS-1 and passed through to the helium collision cell floated at 2 keV and pressure adjusted to attenuate the parent molecular ion by approximately 65%. The daughter ions were separated in MS-2 using a magnet jump with successive 4% mass windows and a constant B/E ratio. Daughter ions were detected on a one-inch optically coupled diode array detector and masses were assigned automatically by a Kratos Mach 3 data system that used Cal as an external reference for both MS-1 and MS-2.

Methylation analysis. Linkage analysis was performed using the microscale method of Levery and Hakamori (34), modified by replacing sodium hydride with NaOH for the formation of the dimethylsulfinyl carbanion (35). To partially compensate for low recoveries of heptose, hydrolysis times were increased and more acidic conditions were used (36). Details of this modified procedure have been described elsewhere (30).

To determine the linkage of the reducing terminal KDO, the ketone moiety was first reduced to a secondary alcohol prior to methylation and the methyl ester was reduced to a primary alcohol after methylation (37). This procedure was carried out by first placing 5-50 µg of oligosaccharide into 1 ml Reaction vials with Mininert valves (Pierce, Rockford, Illinois) and drying overnight in vacuo over P₂O₅. Reduction proceeded at room temperature for 1 h with the addition of 150 µl of a 10 mg/ml solution of NaBH₄ in 1 M NH₄OH. After reduction, the remaining NaBH₄ was destroyed by adding 50 µl of acetic acid. Following evaporation under a stream of N₂ (35°C), borate was removed as the methyl ester by alternately adding and evaporating 500 µl methanol with 1-2% acetic acid, repeated 7-8 times. To reduce the methyl ester of the terminal KDO moiety in the permethylated oligosaccharides, 250 µl of ethanol and 125 µl of a 10 mg/ml solution of NaBD₄/H₂O was added, and the solution incubated for 2 h at room temperature. Excess

NaBH₄ was destroyed by adding two drops of acetic acid. Evaporation and removal of borate was as above. The samples were then dried overnight in vacuo over P₂O₅.

Analysis of the partially methylated aldol acetates was performed on a VG70SE mass spectrometer equipped with a Hewlett Packard 5890 gas chromatograph and an on-column injector (J&W Scientific). Samples were chromatographed on a 30 m DB-1 column with a 1-µm film thickness (J&W Scientific) using a temperature program of 140°C to 280°C at 4°C/min. Electron impact ionization was carried out with a source temperature of 250°C using 70 eV, a trap current of 200 µA and an emission current of 1 mA. The scan conditions were 0.8 sec/decade with an interscan delay of 0.15 sec. Masses were assigned automatically using an VG Opus data system calibrated with an external PFK reference.

Anomeric assignments. The anomeric configurations of the major oligosaccharide branch in 1291wt and 1291_a LOS were assigned by reference to human OSLs. These OSLs have known structures that are immunologically identical to those found in the *Neisseria* LOS on the basis of MAb binding studies (10).

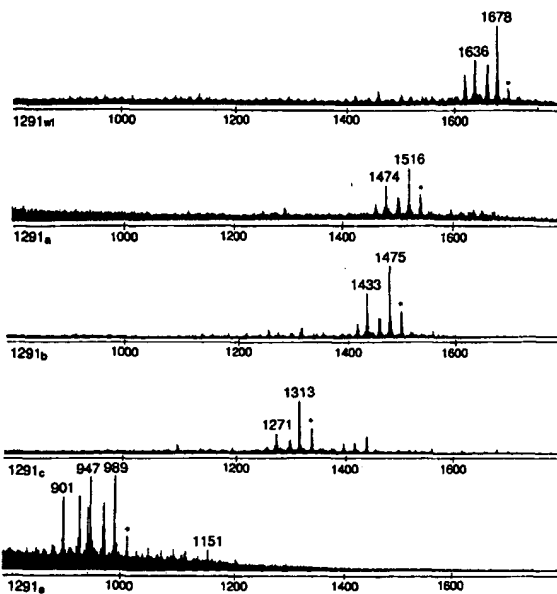


Figure 1. Negative-ion LSIMS spectra of the molecular ion regions of the oligosaccharides released after acetic acid hydrolysis of LOS from 1291wt and pyocin-resistant mutants 1291a,b,c and 1291_d. In each case only the major [M-H]⁻ species are labeled. The peaks 22 Da above and 18 Da below the major [M-H]⁻ ions correspond to sodiated species [M-2H+Na]⁻ and anhydrous species [M-H-H₂O]⁻. The spectrum of the 1291_d oligosaccharide fraction was essentially identical to that shown for 1291_a above, with the exception of a decreased ion abundance for [M-H]⁻ 1151.

Table 1. Compositions of Gonococcal 1291 LOS oligosaccharides

Strain	[M-H] ⁻	M _r	Proposed Composition ^a
1291wt	1678	1679	KDO, Hep ₂ , HexNAc ₂ , Hex ₃ , PEA, OAc
	1636	1637	KDO, Hep ₂ , HexNAc ₂ , Hex ₃ , PEA
	1555	1556	KDO, Hep ₂ , HexNAc ₂ , Hex ₃ , OAc
	1513	1514	KDO, Hep ₂ , HexNAc ₂ , Hex ₃
1291 _a	1516	1517	KDO, Hep ₂ , HexNAc ₂ , Hex ₃ , PEA, OAc
	1474	1475	KDO, Hep ₂ , HexNAc ₂ , Hex ₃ , PEA
1291 _b	1475	1476	KDO, Hep ₂ , HexNAc ₂ , Hex ₃ , PEA, OAc
	1433	1434	KDO, Hep ₂ , HexNAc ₂ , Hex ₃ , PEA
1291 _c	1313	1314	KDO, Hep ₂ , HexNAc ₂ , Hex ₃ , PEA, OAc
	1271	1272	KDO, Hep ₂ , HexNAc ₂ , Hex ₃ , PEA
1291 _d	1151	1152	KDO, Hep ₂ , HexNAc ₂ , Hex ₃ , PEA, OAc
	989	990	KDO, Hep ₂ , HexNAc ₂ , PEA, OAc
	947	948	KDO, Hep ₂ , HexNAc ₂ , PEA
	943	944	?
	901	902	?
1291 _e	1151	1152	KDO, Hep ₂ , HexNAc ₂ , Hex ₃ , PEA, OAc
	989	990	KDO, Hep ₂ , HexNAc ₂ , PEA, OAc
	947	948	KDO, Hep ₂ , HexNAc ₂ , PEA
	901	902	?

^a Other species observed but not reported in this list are sodiated [M+Na-2H]⁻, anhydrous [M-H₂O]⁻ and an artifact series [M-H+C₂H₄O₃]⁻ that has been reported earlier (19). Also, 1291_d LOS had additional minor heterogeneity in the oligosaccharide fraction that was also apparent from the methylation analysis data in Table 3.

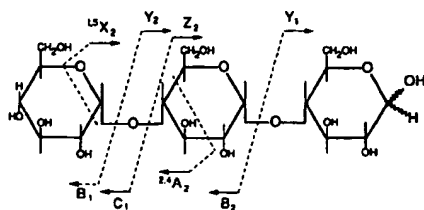


Figure 2. Carbohydrate fragmentation nomenclature based on that proposed by Domon and Costello (38). The mass differences between fragments of the same type, such as Y_1 and Y_2 above, define the residue weight, identity and sequence position. The nominal mass residue weights for the isotopically pure ^{12}C -component of common LOS monosaccharides and other moieties are 162 Da (Hex), 203 Da (HexNAc), 192 Da (Hep), and 220 Da (KDO), 123 Da (phosphoethanolamine, PEA) and 42 Da (acetate, Ac). In the case of branched structures, one defines the main branch as α and other branches as β , γ etc.

Table 3. Linkage Analysis of Gonococcal LOS Oligosaccharides

Strain	Linkage:	1-Glc	1-Gal	1,4-Gal	1,4-Glc	1,3-Gal	1,2-Hep	1,3-Hep	1,3,4-Hep	1-GlcNAc	1,4-GlcNAc
1291wt		-	0.7	<0.1	1.3	0.7	+	-	+	1.0	1.0
1291a*		0.1	0.2	-	0.9	0.7	+	-	+	2.0	0.3
1291b		-	1.1	0.6	1.5	0.2	+	-	+	1.2	-
1291c		-	1.2	-	0.9	-	+	-	+	0.4	-
1291d		0.2	-	-	-	-	+	+	(+)	1.0	-
1291e		0.5	-	-	-	-	+	+	(+)	1.0	-

* The oligosaccharides from 1291a also contained PMAAs resulting from reducing terminal 5-linked KDO and a number of additional heptose moieties in very low abundances such as 1,2,3-Hep, 1,2,7-Hep and 1,3,6-Hep.

Table 4. Binding of F^{ab}-antigen MAb to Outer Membrane Complexes* of *N. gonorrhoeae* 1291 and Pyocin-Resistant Mutants 1291a-g.

Strain	Counts
1291wt	283
1291a	73
1291b	15,443
1291c	97
1291d	67
1291e	67

* The outer membrane complexes were extracted from gonococcal colonies grown on at least 2-3 agar plates.

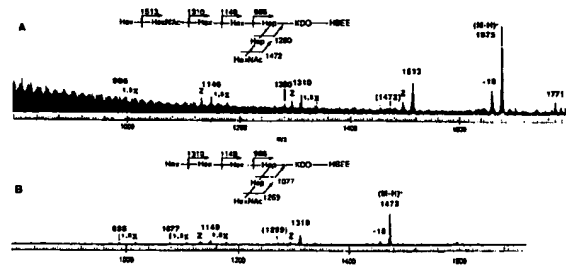


Figure 3. Negative-ion LSIMS spectra of HF-treated (a) 1291wt oligosaccharides-HBEE (m/z 1675) and (b) 1291b oligosaccharides-HBEE (m/z 1472). Please note that the original oligosaccharides (M-H)⁻ ions identified for these two oligosaccharides were at m/z 1678 and 1475, respectively. The difference in mass shown in these two spectra correspond to the loss of acetate (-42 Da) and PEA (-123 Da), and the addition of HBEE moiety at the reducing terminal KDO (+162 Da).

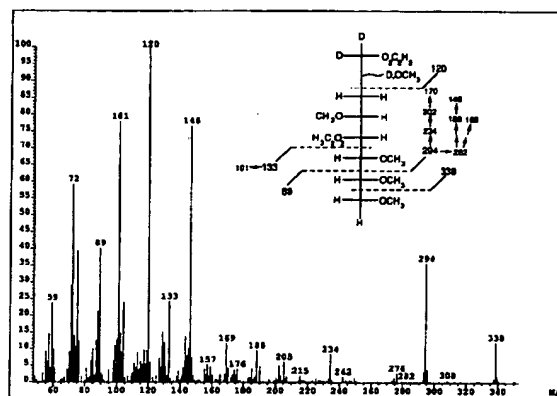


Figure 5. EI spectrum of 1,5-O-acetyl-2,4,6,7,8-O-methyl-3-deoxyoctitol corresponding to the reducing terminal KDO linked through the C-5 position.

Conservation and Accessibility of an Inner Core Lipopolysaccharide Epitope of *Neisseria meningitidis*

JOYCE S. PLESTED,^{1,2*} KATHERINE MAKEPEACE,¹ MICHAEL P. JENNINGS,³ MARGARET ANNE J. GIDNEY,⁴
 SUZANNE LACELLE,⁴ J.-R. BRISSON,⁴ ANDREW D. COX,⁴ ADELE MARTIN,⁴ A. GRAHAM BIRD,²
 CHRISTOPH M. TANG,¹ FIONA M. MACKINNON,¹ JAMES C. RICHARDS,⁴
 AND E. RICHARD MOXON¹

*Molecular Infectious Disease Group, Oxford University Department of Paediatrics, John Radcliffe Hospital, Oxford OX3 9DU,¹
 and Department of Clinical Immunology, Churchill Hospital, Headington, Oxford OX3 7LJ,² United Kingdom;
 Department of Microbiology, University of Queensland, St. Lucia, Brisbane, QLD 4072, Australia³; and
 the Institute for Biological Sciences, National Research Council, Ottawa, Canada K1A 0R6⁴*

Received 29 March 1999/Returned for modification 17 May 1999/Accepted 23 June 1999

We investigated the conservation and antibody accessibility of inner core epitopes of *Neisseria meningitidis* lipopolysaccharide (LPS) because of their potential as vaccine candidates. An immunoglobulin G3 murine monoclonal antibody (MAb), designated MAb B5, was obtained by immunizing mice with a *galE* mutant of *N. meningitidis* H44/76 (B.15.P1.7,16 immunotype L3). We have shown that MAb B5 can bind to the core LPS of wild-type encapsulated MC58 (B.15.P1.7,16 immunotype L3) organisms in vitro and ex vivo. An inner core structure recognized by MAb B5 is conserved and accessible in 26 of 34 (76%) of group B and 78 of 112 (70%) of groups A, C, W, X, Y, and Z strains. *N. meningitidis* strains which possess this epitope are immunotypes in which phosphoethanolamine (PEtn) is linked to the 3-position of the β -chain heptose (HepII) of the inner core. In contrast, *N. meningitidis* strains lacking reactivity with MAb B5 have an alternative core structure in which PEtn is linked to an exocyclic position (i.e., position 6 or 7) of HepII (immunotypes L2, L4, and L6) or is absent (immunotype L5). We conclude that MAb B5 defines one or more of the major inner core glycoforms of *N. meningitidis* LPS. These findings support the possibility that immunogens capable of eliciting functional antibodies specific to inner core structures could be the basis of a vaccine against invasive infections caused by *N. meningitidis*.

Septicemia and meningitis caused by *Neisseria meningitidis* remain a global health problem, especially in young children. *N. meningitidis* is usually a commensal of the nasopharynx, the only major natural reservoir of this organism. The virulence factors that potentiate the capacity of *N. meningitidis* to cause invasive disease include capsular polysaccharides, pili (fimbriae) or outer membrane proteins and lipopolysaccharides (LPS) (12, 23, 39, 45, 48, 63, 68). Existing licensed vaccines against capsular serogroups A, C, W, and X are available (15, 20, 51) but generally lack satisfactory immunogenicity in very young children and do not induce long-lasting protective immunity (8, 33, 42, 43, 49). Nonetheless, their utility has been significant in affording protection to selected populations such as the military, travellers, and those at exceptional risk in outbreaks or epidemics (10). The problems are to identify vaccines that are highly effective in infants and to give long-term protection against group B strains. Group B strains have accounted for a substantial, often a majority of invasive *N. meningitidis* infections in many countries in Europe and the United States (11). Prevention of group B invasive disease represents a particularly difficult challenge in vaccine development since the capsular polysaccharide is very poorly immunogenic and even conjugates have shown disappointing immunogenicity (24). Further, there are concerns about the safety of vaccines whose rationale is to induce antibodies to the group B polysaccharide, a homopolymer of α -linked 2-8 neuraminic

acid. The identical polysialic acid is a posttranslational modification of a glycoprotein present on human cells, especially neurons, and is referred to as neural cell adhesion molecule (14). Both theoretical and experimental evidence have been used to argue that the induction of antibodies might result in autoimmune, pathological damage to host tissues. Alternative approaches for developing vaccine candidates against group B *N. meningitidis* are being actively explored. These include: outer membrane porins (47, 50, 75, 76), transferrin-binding proteins (2), and LPS (19, 25, 27, 38, 69).

The structure of *N. meningitidis* LPS has been studied in considerable detail by Jennings and coworkers with additional contributions by others (4, 18, 44, 59, 64). The structures of major glycoforms for several immunotypes (L1 to L9) have been published: L1 and L6 (13, 73), L3 (41), L5 (37), L2 (16), L4 and L7 (32), and L9 (26) (Fig. 1). It is known that, in addition to this interstrain variation, individual *N. meningitidis* strains exhibit extensive phase variation of outer core LPS structures (reviewed in references 3 and 66). The molecular mechanism of this intrastrain variation involves hypermutable loci within the reading frames of several glycosyl transferases (17, 28). Similar mechanisms of phenotypic variation have been reported for other phase-variable surface components of pathogenic *Neisseria* spp., including Opc (52), Opa (61), and PilC proteins (31). This high-frequency, reversible molecular switching of LPS is mediated by homopolymeric tracts of cytosines or guanines through slippage-like mechanisms that result in frameshifts (17, 28, 60). Despite the extensive antigenic variation of LPS, the inner core of the LPS is relatively highly conserved. Furthermore, key biosynthetic genes for each step have been identified (reviewed in reference 48), and this allows

* Corresponding author. Mailing address: Department of Clinical Immunology, Churchill Hospital, Oxford OX3 7LJ, United Kingdom. Phone: (01865)-226002. Fax: (01865)-225990. E-mail: Joyce.Plested@paediatrics.ox.ac.uk.

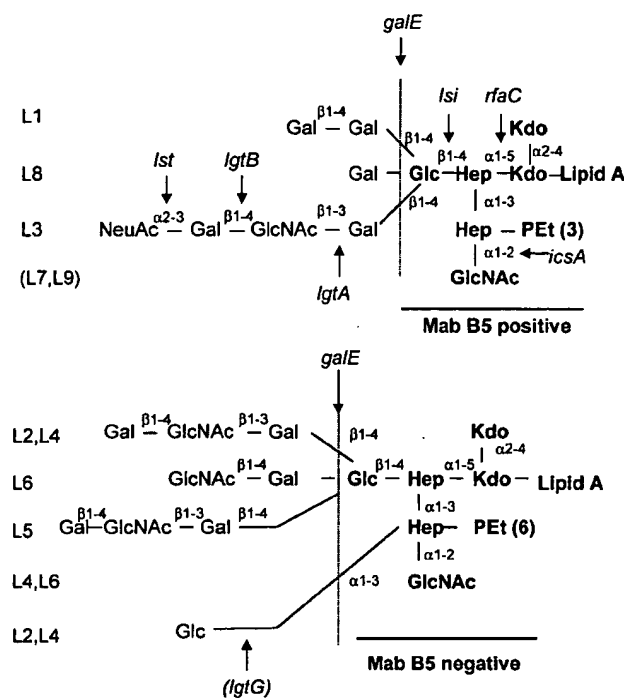


FIG. 1. Representation of the structure of meningococcal LPS oligosaccharides of immunotypes L1 to L9. Immunotypes are indicated to the extreme left. The vertical line marks the junction between the inner core structures to the right and outer core structures to the left. The epitope recognized by MAb B5 is indicated in boldface (Mab B5 positive). Arabic numerals indicate the linkage between sugars or amino sugars. Alpha and beta indicate the carbon 1 linkage at the nonreducing end of the sugar. Genes for incorporating each of the key sugars or amino sugars into the LPS oligosaccharide in the biosynthetic pathway are indicated with arrows indicating where in the pathway the gene product is required. Abbreviations: Kdo, 2-keto-2-deoxyoctulosonic acid; Gal, galactose; GlcNAc, *N*-acetylglucosamine; Glu, glucose; Hep, heptose. Immunotype L5 has no PEtn on the second heptose. The gene that adds the glucose to the second heptose (*lgtG*) is phase variable.

the construction of a series of mutants from which LPS glycoforms of various sizes and complexities can be made available to facilitate the identification of conserved epitopes (29, 30, 64, 65). Our hypothesis is that one or more of these inner core epitopes may be conserved and accessible to antibodies and that a specific immune response to these epitopes could mediate protection. If so, LPS inner core oligosaccharides could be candidate vaccines.

Here we report that a monoclonal antibody (Mab), designated B5, has identified a cross-reacting epitope on the LPS of the majority of naturally occurring but genetically diverse strains of *N. meningitidis*. Critical to the epitope of strains recognized by the Mab B5 is a phosphoethanolamine (PEtn) on the 3-position of the β -chain heptose (HepII) (Fig. 1). In contrast, all *N. meningitidis* strains lacking reactivity with Mab B5 are immunotypes characterized by the absence of PEtn substitution or by PEtn substitution at an exocyclic position (i.e., position 6 or 7) of HepII (Fig. 1). Thus, a limited repertoire of inner core LPS variants is found among natural isolates of *N. meningitidis* strains, and these findings support the possibility that a vaccine might be developed containing a few glycoforms representative of all natural *N. meningitidis* strains.

MATERIALS AND METHODS

Bacterial strains. The *N. meningitidis* strains MC58 and H44/76 (both B:15:P1.7,16 immunotype L3) have been described previously (21, 71). Derivatives of MC58 and H44/76 with defined alterations in LPS were obtained by inactivating

the genes, *galE* (30), *lgtA* (29), *lgtB* (28), *rfaC* (62), and *icsA* and *icsB* (64) (Table 1). Other wild-type *N. meningitidis* strains used in the study were from three collections: (i) representatives of immunotypes L1 to L12 (46), a (ii) global collection of 34 representative *N. meningitidis* group B strains (56), and (iii) a global collection of 100 strains from 107 representative *N. meningitidis* strains of all major serogroups (A, B, C, W, X, Y, and Z) (35).

Capsule-deficient and *galE* mutants were constructed in six *N. meningitidis* group B strains obtained from the collection described earlier (56) (Table 1). Other, related *Neisseria* strains studied included 10 strains of *N. gonorrhoeae* and the commensal strains *N. lactamica* (eight strains), *N. polysaccharaea* (one strain), *N. mucosa* (one strain), *N. cinerea* (one strain), *N. elongata* (one strain), *N. sicca* (one strain), and *N. subflava* (one strain). Other gram-negative organisms included: *Haemophilus influenzae* type b (seven strains), *H. somnus* (one strain), nontypable *H. influenzae* (eight strains), *Escherichia coli* (one strain), and *Salmonella typhimurium* (one strain) and its isogenic LPS mutants (*rfaC*, *rfaP*, and *rfaI*) (Table 1).

Bacterial culture in vitro. All strains were grown overnight at 37°C on standard brain heart infusion (BHI) medium base (Oxoid) in an atmosphere of 5% CO₂.

Bacterial culture in vivo using the chick embryo model. To determine the accessibility of inner core epitopes of *N. meningitidis* grown in vivo, the chick embryo model was used (6, 7, 55). The method was modified by using an inoculum of 10⁴ or 10⁵ *N. meningitidis* organisms in a final volume of 0.1 ml to infect the chorio-allantoic fluid of 10-day-old Pure Sussex chick eggs (obtained from the Poultry Unit, Institute of Animal Health, Compton, Berkshire, United Kingdom). After overnight incubation (37°C), the allantoic fluid (ca. 3 to 5 ml) was removed from the eggs, and the bacteria were recovered after centrifugation at 350 \times g for 15 min. The organisms were washed in sterile phosphate-buffered saline (PBS) and stored in Greaves solution (5% bovine serum albumin [BSA], 5% sodium glutamate, 10% glycerol) at -70°C.

LPS extraction. LPS samples were obtained from an overnight growth of *N. meningitidis* plated on five BHI plates from which the organisms were scraped and suspended in 30 ml of 0.05% phenol in PBS and incubated at room temperature for 30 min. Alternatively, batch cultures were prepared in fermenters with bacteria from an overnight growth (six plates) in 50 ml of Bacto Todd-Hewitt broth (Difco) to inoculate 2.5 liters of the same medium. For insertion mutant strains, the medium contained 50 μ g of kanamycin per ml. After incubation at 37°C for 6 to 8 h, the culture was inoculated into 60 liters of Bacto Todd-Hewitt broth in a New Brunswick Scientific 1F-75 fermenter. After overnight growth (17 h at 37°C), the culture was killed by the addition of phenol (1%) and then chilled to 15°C; the bacteria were then harvested by centrifugation (13,000 \times g for 20 min) (72). In either case, the crude LPS was extracted from the bacterial pellet by using the standard hot phenol-water method (74) and purified from the aqueous phase by repeated ultracentrifugation (105,000 \times g, 4°C, two times for 5 h) (36).

Tricine gels. Equivalent amounts of whole-cell (WC) lysates of *N. meningitidis* strains or purified LPS were boiled in dissociation buffer and separated on standard tricine gels (30 mA for 18 h) (34). Gels were fixed and silver stained according to the manufacturer's instructions (Bio-Rad). To determine the presence of sialic acid, WC lysates were incubated with 2.5 μ l of neuraminidase at 37°C for 18 to 20 h (4 U/ml; Boehringer 1585886) and then with 5 μ l of proteinase K at 60°C for 2 to 3 h to remove proteins (Boehringer 1373196) prior to separation on tricine gels (16.5%).

Characterization of LPS from Mab B5-negative strains. LPS from wild-type and *galE*, *cap* mutant Mab B5-negative strains were *O*-deacylated with anhydrous hydrazine as described previously (5). *O*-Deacylated LPS were analyzed by electrospray mass spectrometry (ES-MS) in the negative ion mode on a VG Quattro (Fisons Instruments) or API 300 (Perkin-Elmer/Sciex) triple quadrupole mass spectrometer. Samples were dissolved in water which was diluted by 50% with acetonitrile-water-methanol-1% ammonia (4:4:1:1), and the mixture was enhanced by direct infusion at 4 μ l/min. Deacylated and dephosphorylated LPS (L8 odA HF) was prepared according to the following procedure. LPS (160 mg) was treated with anhydrous hydrazine (15 ml) with stirring at 37°C for 30 min. The reaction was cooled (0°C), cold acetone (-70°C, 50 ml) was added gradually to destroy excess hydrazine, and precipitated *O*-deacylated LPS (L8 odA) was obtained by centrifugation. L8 odA was washed twice with cold acetone and then redissolved in water and lyophilized. The structure of L8 odA was confirmed by negative ion ES-MS before dephosphorylation. L8 odA was dephosphorylated by treatment with 48% aqueous hydrogen fluoride (10 ml) at 0°C for 48 h. The product was dialyzed against water, and the *O*-deacylated, dephosphorylated LPS sample (L8 odA HF) was lyophilized (50 mg). Loss of phosphate was confirmed by ES-MS.

Molecular modelling. Molecular modelling of LPS epitopes was carried out as described previously (5). The starting geometry for all sugars was submitted to a complete refinement of bond lengths, valence, and torsion angles by using the molecular mechanics program MM3(92) (Quantum Chemistry Program Exchanger [QCPE], Indiana University, Bloomington, Ind.). All calculations were performed by using the minimized coordinates for the methyl glycoside. The phosphorus groups were generated from standard coordinates (Tripos Software; Alchemy) and minimum energy conformations found in crystal structures. Calculations were performed by the Metropolis Monte Carlo (MMC) method. All pendant groups were treated as invariant except for the phosphorus groups, which were allowed to rotate about the Cx-Ox and Ox-P bonds. The starting

TABLE 1. Bacterial strains

Strain	Relevant immunotype and/or genotype	Source and/or reference
<i>Neisseria meningitidis</i>		
MC58	L3	CSF isolate (71)
H44/76	L3	21
MC58	<i>galE</i>	30
MC58	<i>lsi1 (rfaF)</i>	29
MC58	<i>lgtA</i>	28
MC58	<i>lgtB</i>	28
H44/76	<i>rfaC</i>	62
H44/76	<i>icsA</i>	64
H44/76	<i>icsB</i>	64
126E, 35E, H44/76, 89I, M981, M992, 6155, 892257, M978, 120M, 7880, 7889, 3200	L1 to L12, respectively	46
BZ157	L2	56
BZ157	<i>galE</i>	This study
1000	NT	56
1000	<i>galE</i>	This study
NGE30	NT	56
NGE30	<i>galE</i>	This study
EG327	NT	56
EG327	<i>galE</i>	This study
NGH38	L2 and L5	56
NGH38	<i>galE</i>	This study
EG328	NT	56
EG328	<i>galE</i>	This study
3906, NGH15, BZ133, BZ83, EG329, SWZ107, BZ198, NGH41, NG4/88, 2970, BZ147, NGG40, NGH36, NG3/88, NGF26, NG6/88, NGH38, NGE28, BZ169, 528, DK353, BZ232, DK24, BZ159, BZ10, BZ163, B6116/77, L93/4286, NG3/88, NG6/88, NGF26, NGE31, DK24, 3906, EG328, EG327, 1000, B534, A22, 71/94, 860060, NGG40, NGE28, NGH41, 890326, 860800, NG4/88, E32, 44/76, 204/92, BZ8, SWZ107, NGH38, DK353, BZ232, E26, 400, BZ198, 91/40, NGH15, NGE30, 50/94, 88/03415, NGH36, BZ147, 297-0		35
<i>Neisseria lactamica</i> L12, L13, L17, L18, L19, L20, and L22; <i>N. polysaccharae</i> P4; <i>N. mucosa</i> M7; <i>N. cinerea</i> F1; <i>N. elongata</i> I8; <i>N. sicca</i> Q29; <i>N. subflava</i> U37		B. Spratt & N. Smith
<i>Neisseria gonorrhoeae</i>		
F62, MS11, FA19, FA1090, 179008, 150002, 15253		R. Goldstein
SN-4		S. Normavk
P9-2		M. Virji
<i>Haemophilus influenzae</i> type b		22
Eagan, 7004, Rd, 5B33, 3Fe, E3Fi, E1B1	<i>opx rfaF orfH</i>	
PLAK33	<i>lpxA</i>	58
<i>Haemophilus somnus</i> 738 L1		J. Richards
Nontypeable <i>Haemophilus influenzae</i> 54, 375, 477, 1003, 1008, 1042, 1147, 1231		J. Eskola
<i>Escherichia coli</i> DH5α		40
<i>Salmonella typhimurium</i> LT2	<i>rfaC rfaI rfaP</i>	53

angles for the oligosaccharide were taken from the minimum energy conformers calculated for each disaccharide unit present in the molecule. 24-Dimensional MMC calculations of the hexasaccharides with or without PEtn groups attached were carried out with 5,000 macro moves. The graphics were generated by using the Schakal software (Egbert Keller, Kristal-logographisches Institut der Universität, Freiburg, Germany).

Antibodies. (i) **Rabbit polyclonal antibody.** We used a rabbit polyclonal antibody specific for group B *N. meningitidis* capsular polysaccharide obtained by immunizing a rabbit six times subcutaneously with lysates of MC58 at 2-week intervals. The first and second immunizations contained Freund complete adjuvant and Freund incomplete adjuvant, respectively. Serum was obtained from bleed 6. To increase specificity for the group B capsular polysaccharide, rabbit polyclonal antibody (1 ml) was incubated overnight at 4°C with ethanol-fixed capsule-deficient MC58 (5×10^9 organisms/ml). This preadsorbed polyclonal antibody did not react with a capsule-deficient mutant of MC58 as determined by immunofluorescence microscopy.

(ii) **MAbs to inner core LPS.** Murine MAbs to H44/76 *galE* LPS were prepared by standard methods. Briefly, 6- to 8-week-old BALB/c mice were immunized three times intraperitoneally, followed by one intravenous injection with formalin-killed *galE* mutant whole cells. Hybridomas were prepared by the fusion of spleen cells with SP2/O-Ag 14 (57) as described earlier (9). Putative hybridomas secreting *galE*-specific antibodies were selected by enzyme-linked immunosorbent assay (ELISA) employing purified LPS from L3 and its *galE* mutant and L2. Immunoglobulin class, subclass, and light chain were determined by using an isotyping kit (Amersham Canada Ltd., Oakville, Ontario, Canada). Clones were expanded in BALB/c mice after treatment with pristane to generate ascitic fluid. Spent culture supernatant was collected after in vitro culture of hybridoma cell lines. Further testing of *galE* MAbs was carried out by screening against purified LPS from *N. meningitidis* L3 *lgtA*, *lgtB*, and *lgtE* mutant strains (Fig. 1), and *S. typhimurium* Ra and Re mutants. One of the MAbs, MAb B5 (immunoglobulin G3 [IgG3]), was selected for more detailed study.

(iii) **Immunotyping MABs.** To determine the immunotypes of *N. meningitidis* strains studied, especially L2 and L4 to L6, the following murine MABs were used in dot blots and whole-cell ELISA: MN42F12.32 (L2 and L5), MN4A8B2 (L3, L7, and L9), MN4C1B (L4, L6, and L9), MN40G11.7 (L6), and MN3A8C (L5) (54).

(iv) **Huvec assay.** Cultured human umbilical vein endothelial cells (Huvecs) were prepared as described previously (70) and were infected with strains of *N. meningitidis* for 3 h at 37°C. *N. meningitidis* strains were grown either in vitro or in vivo by using the chick embryo model (as described above). The accessibility of the inner core LPS epitopes of whole-cell *N. meningitidis* to specific MAB B5 was determined by using immunofluorescence and confocal microscopy. Gelatin-coated glass coverslips coated with Huvecs were infected with wild-type *N. meningitidis* as described previously (71), except that bacteria were fixed with 0.5% paraformaldehyde for 20 min instead of methanol. For accessibility studies, coverslips were washed with PBS, blocked in 3% BSA-PBS, and incubated with MAB B5 culture supernatant and/or preadsorbed polyclonal rabbit antiscapular antibody. Binding of antibody to wild-type *N. meningitidis* strains was detected by anti-mouse IgG rhodamine (tetramethyl rhodamine isocyanate [TRITC]; Dako) and anti-rabbit IgG fluorescein isothiocyanate (FITC; Sigma). Huvecs were stained with diaminophenylamine DAPI; (4',6-diamidino-2-phenylindole; 1 µg/ml; Sigma). Mounted coverslips were viewed for immunofluorescence by using appropriate filters (Zeiss microscope with Fluorograbber, Adobe Photoshop, or confocal microscope [Nikon]).

ELISA. (i) Purified LPS ELISA. A solid-phase indirect ELISA with purified LPS was used to determine the binding specificities of MABs. Nunc Maxisorp plates were coated overnight with 1.0 µg of purified LPS per well derived from wild-type and mutants. LPS (10 µg/ml) was diluted in 0.05 M carbonate buffer containing 0.02 M MgCl₂ (pH 9.8). Nonspecific binding sites were blocked for 1 h with 1% BSA-PBS (Sigma) and washed three times with PBS-Tween 20 (0.05% [vol/vol]; PBS-T). Plates were incubated for 1 h with MAB B5 culture supernatant and washed three times in PBS-T. Primary antibody was detected with anti-mouse IgG-alkaline phosphatase (Sigma and Cedarlane Laboratories, Ltd.) incubated for 1 h, washed three times in PBS-T, and detected with *p*-nitrophenyl phosphate alkaline phosphatase substrate system (Sigma and Kirkegaard & Perry Laboratories). The reaction was stopped after 1 h with 50 µl of 3 M NaOH, and the absorbance ($A_{405-410}$) was determined (Dynatech EIA plate reader).

(ii) **Inhibition ELISA.** For inhibition ELISA studies, MAB B5 was incubated with purified LPS samples prior to addition to L3 *galE* LPS-coated plates and then assayed as described above.

(iii) **WC ELISA.** WC ELISA was performed by using heat-inactivated lysates of *N. meningitidis* organisms as described previously (1). Nunc Maxisorp 96-well plates were coated with 100 µl of bacterial suspension (optical density [OD] of 0.1 at A_{620}) overnight at 37°C and blocked with 1% BSA-PBS; an identical protocol was followed as for LPS ELISA.

Dot blots. Bacterial suspensions prepared as described above (2 µl) were applied to a nitrocellulose filter (45 µm, pore size; Schleicher & Schuell) and allowed to air dry. The same procedure as described for WC ELISA was followed except that the detection substrate was 5-bromo-4-chloro-3-indolyl-phosphate-nitroblue tetrazolium (2 mg/ml; Sigma). The color reaction was stopped after 30 min by several washes with PBS, and the blots were air dried.

RESULTS

To investigate the potential of inner core LPS structures of *N. meningitidis* as vaccines, we have studied the reactivity of an isotype IgG3 murine MAB, designated B5, raised against *N. meningitidis* H44/76 immunotype L3 *galE* mutant. MAB B5 was one of seven MABs to the LPS inner core produced against *N. meningitidis* immunotype L3 *galE* by standard immunological methods (see Materials and Methods). Preliminary ELISA testing showed that B5 cross-reacted with LPS from the L3 parent strain and with *galE* (*lgtE*), *lgtA*, and *lgtB* mutants but did not cross-react with *S. typhimurium* Ra or Re LPS. In order to determine the specific inner core epitope recognized by MAB B5, various *N. meningitidis* strains of known structure were examined by ELISA for cross-reactivity (Fig. 2). The most significant finding of this analysis was that *N. meningitidis* immunotype L4 LPS was not recognized by MAB B5. The only structural difference between immunotypes L4 and L3 (which is recognized by MAB B5) is the position of attachment of the PETn group (Fig. 3). In immunotype L3 LPS the PETn is attached at the 3-position of HepII, whereas in immunotype L4 LPS the PETn is attached at the 6- or 7-position (Fig. 3). Additionally, LPS from immunotype L2 and its *galE* mutant (in which the PETn group is attached at the 6-position and a glucose residue is present at the 3-position of HepII) are not

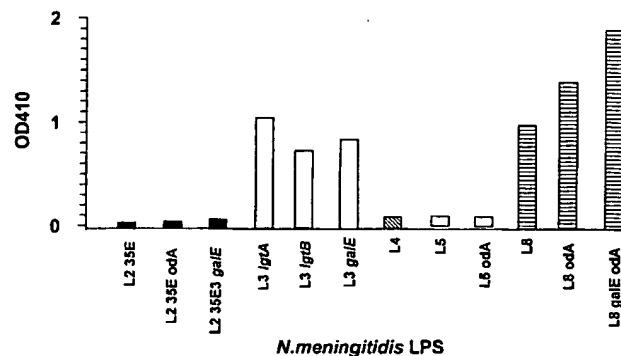


FIG. 2. Cross-reactivity of MAB B5 with selected immunotypes and mutants of *N. meningitidis* LPS and *O*-deacylated (odA) LPS as determined by solid-phase ELISA. LPS glycoforms of immunotypes L2 (35E) (solid bars), L3 (H44/76) (open bars), L4 (891) (hatched bars), L5 (M981) (open bars), L8 (M978) (horizontal-line-filled bars), wild-type, and respective mutants (*galE*, *lgtA*, or *lgtB*), in a native or *O*-deacylated form, were coated onto ELISA plates (see Materials and Methods), and the reactivity of MAB B5 was determined by standard ELISA (OD, A_{410}).

recognized by MAB B5. Immunotype L5, which has no PETn in the inner core, is not recognized by B5, whereas immunotype L8 and its *galE* mutant which have PETn at the 3-position of HepII are recognized. These results suggest that MAB B5 specifically recognises PETn when it is attached at the 3-position of HepII. In order to prove the essential inclusion of PETn in the epitope recognized by MAB B5, immunotype L8 odA LPS was dephosphorylated (48% HF, 4°C, 48 h) (Fig. 3). The absence of PETn after dephosphorylation was confirmed by ES-MS analysis. As indicated in Fig. 4, dephosphorylation of L8 odA LPS abolished reactivity to MAB B5. To further characterize the epitope recognized by MAB B5, several structurally defined genetic mutants of immunotype L3 were screened for cross-reactivity (Fig. 4). The highly truncated LPS of mutant strain *icsB* was only weakly recognized, while mutant strain *icsA* LPS was not recognized by MAB B5. These results suggest that the presence of glucose on the proximal heptose residue (HepI) is not absolutely necessary for binding by B5 but is required for optimal recognition (Fig. 1). Furthermore, MAB B5 does not bind LPS in which both the glucose on the β -chain and the *N*-acetylglucosamine residue on the β -chain are absent. This suggests that the presence of *N*-acetylglucosamine is required to present the PETn residue in the correct conformation for binding by MAB B5. Genetic modifications that produce severely truncated LPS glycoforms were also examined for reactivity with MAB B5. LPS from immunotype L3 *lgi* which has a trisaccharide of Hep-Kdo-Kdo attached to lipid A, as well as L3 PB4 which only contains the Kdo disaccharide and lipid A, were not recognized by MAB B5 (Fig. 4). Inhibition ELISA studies (data not shown) were in accord with this result, thus confirming the specificity of MAB B5 to the PETn molecule linked at the 3-position of HepII.

To demonstrate the ability of MAB B5 to recognize this inner core epitope in encapsulated strains, we devised an assay in which natural isolates of *N. meningitidis* were studied when they were grown on and became adherent to tissue-cultured cells (i.e., Huvecs). Initially, this methodology was developed by using the fully encapsulated strain MC58. The advantages of using the Huvec assay were that it provided a monolayer of endothelial cells to which the bacteria could adhere and that it provided a biologically relevant environment. Previous attempts with *N. meningitidis* directly adherent to gelatin- or

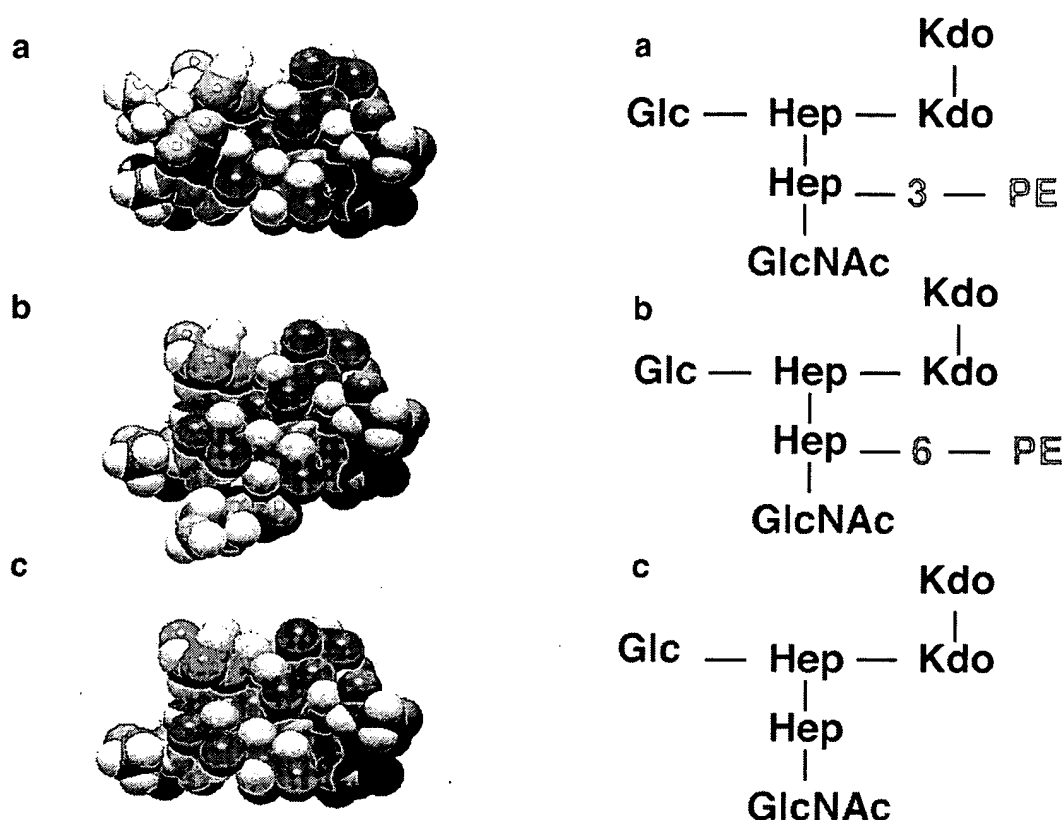


FIG. 3. Space-filling three-dimensional molecular models of the calculated (MMC) lowest-energy states of the core oligosaccharide from *galE* mutants of L3 (a), L4 (b), and L8-dephosphorylated (c). The Kdo moiety indicated in gray is substituted at the O-5 position by the heptose disaccharide inner core unit (red); HepI provides the point via a glucose residue (dark green) for extension to give α -chain epitopes, while HepII is substituted by an *N*-acetylglucosamine residue (lighter green) at O-2. PEtn (brown) is shown in O-3 position in the L3 immunotype and O-6 in the L4 immunotype.

matrigel-coated coverslips resulted in low numbers of adherent bacteria after repeated washings and high levels of nonspecific background staining.

Primary antibodies, MAb B5, and a polyclonal anticapsular antibody were detected by use of anti-mouse TRITC and anti-

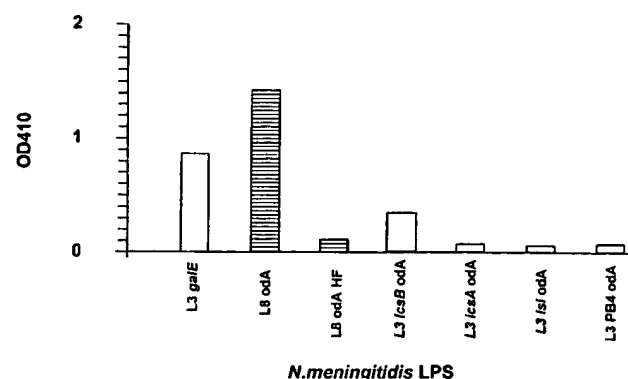


FIG. 4. Cross-reactivity of MAb B5 with genetically modified L3 LPS and chemically modified L8 LPS from *N. meningitidis*, as determined by solid-phase ELISA. LPS glycoforms of immunotype L8 (M978) (horizontal-line-filled bars) chemically modified by *O* deacylation and HF treatment and immunotype L3 (H44/76) (open bars) *galE*, *icsB*, *icsA*, *lsi*, and PB4 mutants (*O* deacylated) were coated onto ELISA plates (see Materials and Methods), and the reactivity of MAb B5 was determined by standard ELISA (OD, A_{410}).

rabbit FITC, respectively. This demonstrated that an inner core LPS epitope of the fully encapsulated strain (MC58) was accessible to MAb B5 (Fig. 5a and b). Confocal microscopy showed that MAb B5 and anticapsular antibodies colocalized and that the result was consistent irrespective of the sequence in which the antibodies were added. We also investigated, in addition to this in vitro demonstration of accessibility of MAb B5 to inner core LPS, organisms grown in vivo by using the chick embryo model. Strain MC58 (10^4 organisms/ml) was inoculated into chorioallantoic fluid of 10-day-old chick embryos and harvested the next day to provide ex vivo organisms. The results observed by confocal microscopy were identical to those observed in vitro, that is, MAb B5 and anticapsular antibodies colocalized (Fig. 5c and d). This demonstrated that the inner core LPS epitopes were also accessible in vivo on whole-encapsulated wild-type *N. meningitidis*.

The observation of double staining of the inner core LPS epitope in the presence of capsule is key to the concept of this approach, and therefore a number of controls were used to confirm the validity of this finding. (i) The first control involved double staining an MAb B5-negative strain (e.g., immunotype L4 strain) with MAb B5 and anti-capsular antibody. This resulted in no reactivity of MAb B5 by using a rhodamine filter but positive reactivity with anticapsular antibody, ruling out a band-passing effect during the recording of the pictures. (ii) The second control involved single staining of encapsulated MAb B5-positive strains with either MAb B5 alone or anticapsular antibody alone, followed by staining with rhodamine or

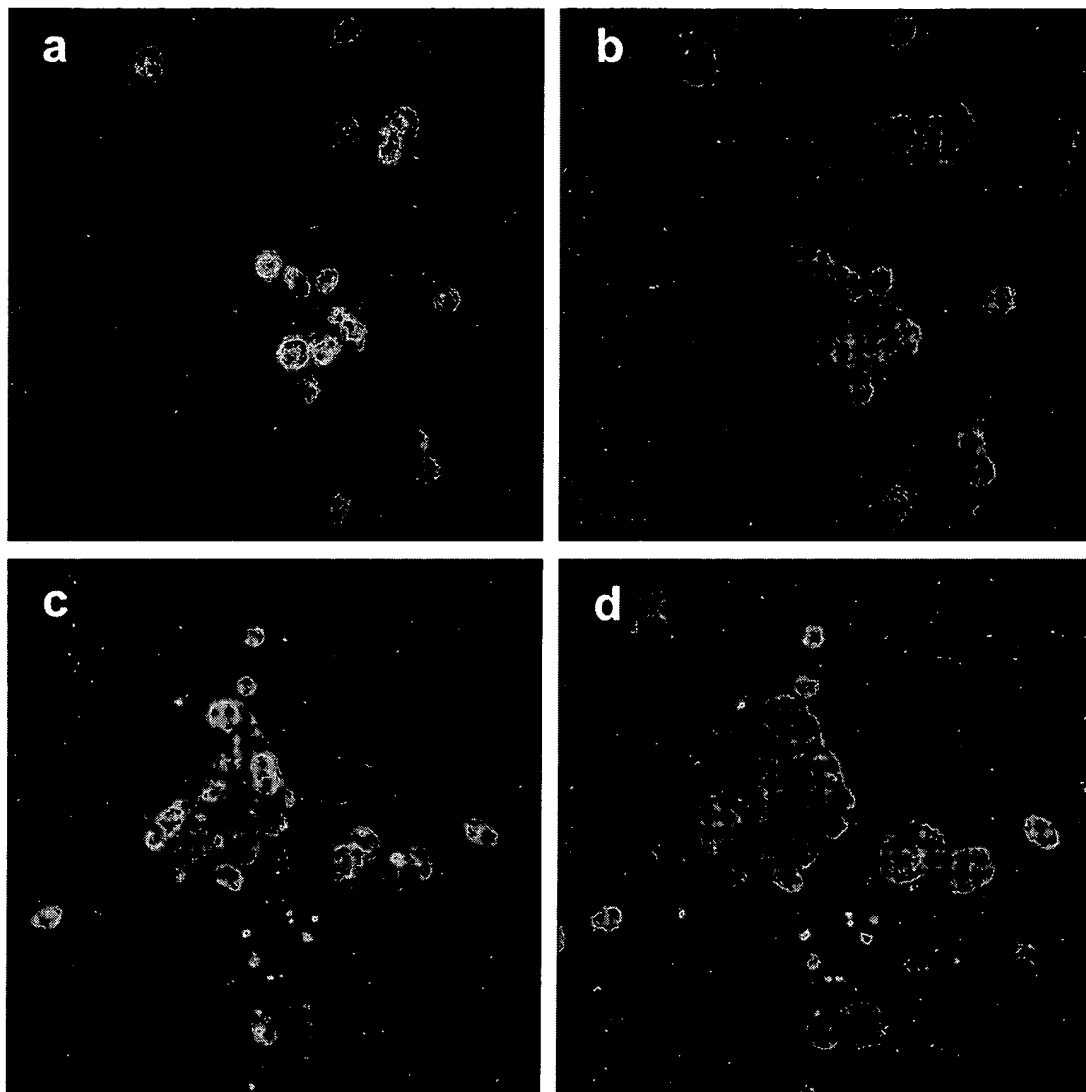


FIG. 5. (a and b) Confocal immunofluorescence microscopy of in vitro-grown *N. meningitidis* MC58 adherent to Huvecs. (a) Fluorescein tagging with rabbit polyclonal antibody specific for group B *N. meningitidis* capsule. (b) rhodamine tagging of MAb B5 specific for *galE* LPS. (c and d) Confocal immunofluorescence microscopy of in vivo-grown MC58 organisms stained as described for panels a and b. (c) Anticapsular antibody (green). (d) MAb B5 (red). Magnification, $\times 2,400$ (all four panels).

FITC, respectively. When the results were viewed at the appropriate wavelength, there was no cross-reactivity seen during immunofluorescent staining, nor any band-passing effect. (iii) The third control involved double-staining an MAb B5-positive or -negative strain with MAb B5 and anticapsular antibody. This resulted in no capsular staining but either MAb B5-positive or -negative reactivity when viewed on the rhodamine filter. This result excluded cross-reactivity during staining or band-passing effect resulting in artifactual inner core staining.

To survey the extent of MAb B5 reactivity with other *N. meningitidis* strains, three collections of strains were investigated: (i) 12 strains representative of LPS immunotypes L1 to L12; (ii) 34 group B strains selected to represent genetically diverse isolates from many different countries obtained between the years 1940 and 1988 (56); and (iii) a global collection of 107 genetically diverse strains representing all capsular serogroups, also obtained from different countries from 1940 to 1994 (35).

Of the 12 immunotypes, MAb B5 recognized the LPS of strains in which the inner core oligosaccharide has a PETn linked to the 3-position of HepII (Table 2 and Fig. 1). Thus, immunotypes L2, L4, and L6 did not react with MAb B5, whereas immunotypes L1, L3, and L7 to L12 were recognized by MAb B5. This confirmed that the presence of PETn in the 3-position of the HepII is necessary to confer MAb B5 reactivity (Fig. 3).

To investigate further the MAb B5 reactivity with other group B strains, a collection of genetically diverse strains was studied (56). MAb B5 reactivity was detected in 26 of 34 (76%) of group B *N. meningitidis* strains tested. This included representative ET-5, ET-37, A4, and Lineage-3 strains. This represents the most complete available collection of hyperinvasive lineages of *N. meningitidis* group B strains.

We obtained capsule-deficient and *galE* mutants from six of eight of the MAb B5-negative group B strains (transformations were unsuccessful in the other two strains). These strains were

TABLE 2. Reactivity of MAb B5 with representative *N. meningitidis* strains of immunotypes L1 to L12 as determined by WC ELISA, dot blots of lysates, immunofluorescence, and confocal microscopy

Strain	Serogroup: serotype	Immunotype	WC ELISA (OD, A ₄₀₅) ^a	Dot blot ^b	Immunofluorescence ^c
126E	C:3:P1.5,2	L1	+1.8	+++	+
35E	C:20:P1.1	L2	<0.4	—	—
H44/76	B:15:P1.7,16	L3	+1.3	+++	++
89I	C:nt:P1.16	L4	<0.4	—	—
M981	B:4:P1.—	L5	<0.4	±	—
M992	B:5:P1.7,1	L6	<0.4	±	—
6155	B:nt:P1.7,1	L7	+0.8	++	+
M978	B:8:P1.7,1	L8	+1.9	+++	++
892257	B:4:P1.4	L8	+1.9	+++	++
120M	A:4:P1.10	L9	+1.8	+++	+
7880	A:4:P1.6	L10	+2.2	+++	+
7889	A:4:P1.9	L11	+2.0	+++	++
3200	A:4:P1.9	L12	+2.1	+++	++

^a +, positive reactivity (OD > 0.4); —, negative reactivity (OD < 0.4).^b +++, strongly positive; ++, positive; ±, weakly positive; —, negative.^c +++, strongly positive; +, positive; —, negative.

also negative with MAb B5 as determined by dot blot, WC ELISA, or immunofluorescence, with the exception of a BZ157 *galE* capsule-deficient mutant, which had low-level reactivity as seen both by immunofluorescence and by dot blot. The MAb B5 strains were characterized by using a battery of immunotyping MAbs. We determined the immunotype of the eight MAb B5-negative strains by using combinations of the appropriate MAbs (see Materials and Methods) and dot blots of WC lysates (obtained from P. van der Ley) (Table 3). In addition, structural fingerprinting of the inner core region of MAb B5-negative strains was performed by ES-MS on *O*-deacylated LPS from five of the respective capsule-deficient *galE* mutants (1000, NGE30, EG327, BZ157, and NGH38) (Table 4). Strains 1000, NGE30, and EG327 were nontypeable as determined by the use of MAbs, and LPS from these strains lacked PETn on HepII of the inner core. BZ157, which corresponded to immunotype L2 by MAbs, contained PETn in the inner core and, by analogy, to L2 at the 6/7-position of HepII (Table 3). NGH38 was immunotype L2 and L5 and was analogous to L2 as determined by structural analysis. Those strains that were nontypeable failed to react with MAbs that recognize L3,7,9, L6, L2,5, and L4,6,9. However, 15 of 17 MAb B5-negative *N. meningitidis* strains (all serogroups) were positive for L2,5, and all MAb B5-positive strains were positive for L3,7,9. No reaction with any immunotyping MAbs was ob-

served with 8 of 32 MAb B5-negative strains and 24 of 68 of MAb B5-positive strains.

To determine if the degree of sialylation of the LPS was a factor in the ability of MAb B5 to recognize its inner core epitope, MAb B5-negative strains were examined by LPS gels. MAb B5 reactivity was unaffected by varying the state of sialylation through exposure to neuraminidase as described in Materials and Methods (Fig. 6). Furthermore, strain MC58, with which the MAb B5 reacted strongly, was found to be highly sialylated (Fig. 6), and this finding was confirmed by ES-MS of purified *O*-deacylated LPS (data not shown). Therefore, our data did not support a contribution of sialylation to the lack of MAb B5 reactivity.

With respect to the other *Neisseria* species, MAb B5 also recognized the inner core LPS of five strains of *N. gonorrhoeae* (F62, MS11, FA19, 179008, and 150002) (two were negative) and (at least) two strains of *N. lactamica* (L19 and L22). However, MAb B5 did not react with one strain each of *N. polysaccharaea* (M7), *N. mucosa* (F1), *N. cinerea* (I8), *N. elongata* (Q29), *N. sicca* (Q39), and *N. subflava* (U37). Also, MAb B5 did not react with *E. coli* (DH5 alpha) or *S. typhimurium* (LT2) or its isogenic LPS mutants (*rfaC*, *rfaI*, and *rfaP*).

Finally, we investigated the reactivity of MAb B5 with 100 strains that included representatives of serogroups A, B, C, W, X, Y, and Z (35). Of these strains, 70% were MAb B5 positive. Clustering according to genetic relatedness was evident. For example, none of the MAb B5-negative strains were in the ET5 complex. Among group A strains, MAb B5-positive and -negative strains also fell into distinct clusters. For example, lineages I to III and lineage A4 were positive, and lineage IV to VI was negative. This collection, together with the one described earlier (56), represents the most complete set available for known hyperinvasive lineages in all major serogroups of *N. meningitidis* strains.

DISCUSSION

The prerequisites for any candidate *N. meningitidis* group B vaccine would be that it contain a highly conserved epitope(s) that is found in all group B strains and is accessible to antibodies in the presence of capsule. Our approach has combined genetics, structural analysis, and immunobiology to define candidate epitopes in inner core LPS of *N. meningitidis* group B. This study used murine MAb B5, isotype IgG3, which was

TABLE 3. Correlation between reactivity with MAb B5, immunotyping, and location of PETn on HepII of the inner core

Strain	MAb B5	Immunotype ^a	Position of PETn on HepII	
			O-3	O-6
MC58	+	L3 and L7	+	—
1000	—	NT	—	—
NGE30	—	NT	—	—
EG327	—	NT	—	—
BZ157 ^b	—	L2 and L5	—	+
BZ157 ^c	+	L3 and L7	+	—
NGH38	—	L2 and L5	—	+

^a NT, nontypeable. MN4A8B2 (L3, 7, 9), MN42F12.32 (L2,5), MN4C1B (L4,6,9), and MN40G11.7 (L6).^b BZ157, MAb B5-negative variant.^c BZ157, MAb B5-positive variant.

TABLE 4. Negative-ion ES-MS data and proposed compositions of *O*-deacylated LPS from *galE* capsule-deficient mutant *N. meningitidis* MAb B5-negative strains^a

Strain	Observed ions (<i>m/z</i>)		Molecular mass (Da)			Proposed composition
	(<i>M</i> -2H) ²⁻	(<i>M</i> -H) ⁻	Observed	Calculated	Lipid A ^b	
1000	1,213.0	2,427.6	2,427.7	2,427.2	1,075	2Glc, GlcNAc, 2Hep, 2 Kdo, Lipid A
	1,252.9	2,507.8	2,507.8	2,507.2	1,155	2Glc, GlcNAc, 2Hep, 2 Kdo, Lipid A
	1,314.5	2,630.9	2,630.9	2,630.3	1,278	2Glc, GlcNAc, 2Hep, 2 Kdo, Lipid A
NGH38	1,293.8	2,589.5	2,589.3	2,589.3	952	3Glc, GlcNAc, 2Hep, PEtn, 2Kdo, Lipid A
EG327	1,151.2	2,304.4	2,304.4	2,304.1	952	2Glc, GlcNAc, 2Hep, 2 Kdo, Lipid A
NGE30	1,132.1			2,265.1	1,075	Glc, GlcNAc, 2Hep, 2 Kdo, Lipid A
	1,396.1	2,793.4	2,793.7	2,792.5	1,075	3Glc, 2GlcNAc, 2Hep, 2 Kdo, Lipid A
	1,436.0	2,873.7	2,873.9	2,872.5	1,155	3Glc, 2GlcNAc, 2Hep, 2 Kdo, Lipid A
	1,498.0	2,997.2	2,997.1	2,995.6	1,278	3Glc, 2GlcNAc, 2Hep, 2 Kdo, Lipid A
BZ157	1,274.6	2,551.4		2,550.3	1,075	2Glc, GlcNAc, 2Hep, PEtn, 2Kdo, Lipid A
	1,314.8	2,631.1	2,631.2	2,630.3	1,155	2Glc, GlcNAc, 2Hep, PEtn, 2Kdo, Lipid A
	1,376.4	2,754.4	2,754.5	2,753.4	1,278	2Glc, GlcNAc, 2Hep, PEtn, 2Kdo, Lipid A
	1,457.5	2,916.6	2,916.6	2,915.6	1,278	3Glc, GlcNAc, 2Hep, PEtn, 2Kdo, Lipid A

^a Average mass units were used for calculation of molecular weight based on proposed composition as follows: Glc, 162.15; Hep, 192.17; GlcNAc, 203.19; Kdo, 220.18; PEtn, 123.05. Hep, heptose; Kdo, 3-deoxy-D-manno-octulosonic acid; Glc, glucose; GlcNAc, N-acetylglucosamine; PEtn, phosphoethanolamine.

^b As determined by MS-MS analyses.

raised to a genetically defined immunotype L3 *galE* mutant in order to specifically target inner core LPS epitopes. The epitope(s) recognized by MAb B5 was defined by cross-reactivity studies with purified LPS glycoforms of known structure. MAb B5 recognized all LPS glycoforms in which the PEtn is at the 3-position of HepII (immunotypes L1, L3, L7, L8, and L9) and failed to react with immunotypes where PEtn is at the 6- or 7-position (L2, L4, and L6) or absent from HepII (L5) (Fig. 1). MAb B5 reacted with 70% of the *N. meningitidis* strains tested from the two most complete sets of *N. meningitidis* strains available worldwide (35, 56). Of these strains, 76% of the *N. meningitidis* group B strains tested were positive with MAb B5, and 70% of a collection that included all *N. menin-*

gitidis serogroups tested were positive with MAb B5. Therefore, it may be envisaged that a vaccine containing a limited number of glycoforms, representing all the possible PEtn positions (none, 3, and 6/7) on HepII of the inner core, would cover 100% of *N. meningitidis* group B strains.

The LPS structures of MAb B5-negative strains were confirmed by structural analysis. Two structural variants were recognized: one variant without PEtn in the inner core LPS (e.g., NGE30, EG327, and 1000) and the other with PEtn group on HepII (e.g., BZ157 and NGH38) at the 6- or 7-position instead of the 3-position.

With a view to developing inner core LPS epitopes as vaccine candidates, it is significant that there were no effects of the capsule on MAb B5 accessibility, as shown by colocalization of the anticapsular antibody and MAb B5 in wild-type organisms (MC58) grown in vitro and in vivo and visualized by confocal microscopy (Fig. 5). Nor did the presence or absence of sialic acid have an effect, since both MAb B5-positive and -negative strains had high sialylation states, as shown by tricine gels (Fig. 6) and confirmed by ES-MS (data not shown).

There was no evidence of phase variation in MAb B5-positive or -negative strains in this study, except for one strain (BZ157) which had a very low level of MAb B5-positive strains in parent and *galE* mutant (0.06%) (data not shown). Structural analysis of LPS extracted from these two variants is currently under investigation.

Three-dimensional space-filling models of the inner core LPS of L3 and L4 immunotypes show that the position of the PEtn, either the 3- or the 6-position, respectively (Fig. 3, shown in brown), alters the accessibility and conformation of PEtn in the inner core epitope. The most striking example of the importance of PEtn for MAb B5 reactivity was observed when PEtn was removed from the immunotype L8 (MAb B5 positive) by treatment with hydrogen fluoride, which totally abolished MAb B5 reactivity.

Previous studies with oligosaccharide conjugates in mice and rabbits have demonstrated that PEtn is important in immunogenicity and in the functional activity of polyclonal antibodies (67). These studies identified two sets of polyclonal antibodies

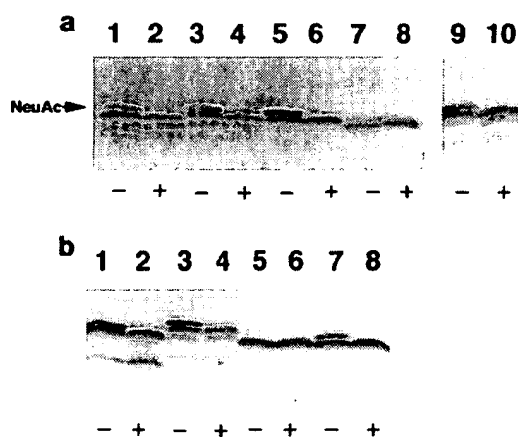


FIG. 6. Silver-stained tricine gels of LPS preparations (10 μ g/lane) from *N. meningitidis* group B strains which were not reactive with MAb B5. These LPS preparations were either not treated (-) or treated with neuraminidase (+) to show the presence of sialic acid. (a) MAb B5-negative strains: lanes 1 and 2, NGE30; lanes 3 and 4, BZ157; lanes 5 and 6, EG327; lanes 7 and 8, 1000; lanes 9 and 10, 3906. (b) MAb B5-negative strains: lanes 1 and 2, EG327; lanes 3 and 4, NGH38; lanes 5 and 6, NGH15; and MAb B5-positive strain: lanes 7 and 8, MC58. The presence of sialic acid is indicated (NeuAc). This band was seen in untreated (-) and removed in treated (+) neuraminidase preparations.

One set resulting from L1 and L3,7,9 oligosaccharides had PEtn in the 3-position of HepII, were immunogenic, and had opsonophagocytic (OP) activity and chemiluminescence in oxidative burst reaction but had no serum bactericidal activity. The other set of antibodies resulting from L2 conjugates (6- or 7-position or without PEtn at HepII) were poorly immunogenic and had greatly reduced OP activity and chemiluminescence (67). Future studies will look at the safety and immunogenicity of inner core LPS conjugates (PEtn at the 3-position of HepII and alternative glycoforms) and the functional ability of these polyclonal antibodies in opsonic and serum bactericidal assays, initially in mice and rabbits. Preliminary studies with MAb B5 in an OP assay with *N. meningitidis* MC58 and donor human polymorphonuclear cells suggests MAb B5 is opsonic in the presence of complement and that the uptake of *N. meningitidis* bacteria correlates with an oxidative burst reaction within the neutrophil (data not shown). MAb B5 does not appear to have any significant serum bactericidal activity with *N. meningitidis* MC58; however, this is not unexpected in view of its isotype (IgG3). The functionality of MAb B5 is currently under further investigation.

In conclusion, MAb B5 recognizes a conserved inner core epitope in which the PEtn is at the 3-position of HepII. This epitope was present in 76% of *N. meningitidis* group B strains and in 70% of all *N. meningitidis* serogroups and was accessible in the presence of capsule. A limited number of alternative glycoforms have been identified that are not recognized by MAb B5 where the PEtn is either absent or at an exocyclic position of HepII. Therefore, a vaccine containing a limited number of glycoforms might give 100% coverage of all *N. meningitidis* group B strains.

ACKNOWLEDGMENTS

This work was supported by Programme grants from the Medical Research Council (E.R.M.) and Wellcome Trust (E.R.M. and K.M.). Funding was also provided by the Oxford Regional Health Authority Research and Development Programme (J.P. and G.B.), the National Meningitis Trust (E.R.M. and J.P.), and Chiron vaccines (E.R.M. and J.R.). M.P.J. was supported by a grant from the NHMRC (96/1084).

We thank D. W. Griffith for large-scale production of bacterial cells, P. Thibault and D. Krajcarski for recording ES-MS, and J. Eskola for providing NTHi strains obtained as part of the Finnish Otitis Media Cohort Study.

REFERENCES

- Abdillahi, H., and J. T. Poolman. 1988. Typing of group-B *Neisseria meningitidis* with monoclonal antibodies in the whole-cell ELISA. *J. Med. Microbiol.* 26:177-180.
- Al'Aldeen, A. A., and K. A. Cartwright. 1996. *Neisseria meningitidis*: vaccines and vaccine candidates. *J. Infect.* 33:153-157.
- Andersen, S. R., J. Kolberg, E. A. Hoiby, E. Namork, D. A. Caugant, L. O. Froholm, E. Jantzen, and G. Bjune. 1997. Lipopolysaccharide heterogeneity and escape mechanisms of *Neisseria meningitidis*: possible consequences for vaccine development. *Microb. Pathog.* 23:139-155.
- Apicella, M. A., J. M. Griffiths, and H. Schneider. 1994. Isolation and characterization of lipopolysaccharides, lipooligosaccharides, and lipid A. *Meth. Enzymol.* 235:242-252.
- Brisson, J. R., S. Uhrinova, R. J. Woods, M. van der Zwan, H. C. Jarrell, L. C. Paoletti, D. L. Kasper, and H. Jennings. 1997. NMR and molecular dynamics of the conformational epitope of the type III group B *Streptococcus* capsular polysaccharide and derivatives. *Biochemistry* 36:3278-3292.
- Buddingh, G. J., and A. Polk. 1937. Meningococcal infection of the chick embryo. *Science* 86:20-21.
- Buddingh, G. J., and A. Polk. 1939. Experimental meningococcal infection of the chick embryo. *J. Exp. Med.* 70:485-498.
- Cadoz, M. 1998. Potential and limitations of polysaccharide vaccines in infancy. *Vaccine* 16:1391-1395.
- Carlin, N. I., M. A. Gidney, A. A. Lindberg, and D. R. Bundle. 1986. Characterization of *Shigella flexneri*-specific murine monoclonal antibodies by chemically defined glycoconjugates. *J. Immunol.* 137:2361-2366.
- Centers for Disease Control. 1990. Availability of meningococcal vaccine in single-dose vials for travellers and high-risk persons. *Morbidity and Mortality Weekly Rep.* 39:763.
- Centers for Disease Control. 1997. Communicable disease weekly report, vol. 7, no. 14. Centers for Disease Control, Atlanta, Ga.
- DeVoe, I. W. 1982. The meningococcus and mechanisms of pathogenicity. *Microbiol. Rev.* 46:162-190.
- Di Fabio, J. L., F. Michon, J. R. Brisson, and H. J. Jennings. 1990. Structure of L1 and L6 core oligosaccharide epitopes of *Neisseria meningitidis*. *Can. J. Chem.* 68:1029-1034.
- Finne, J., M. Leinonen, and P. H. Makela. 1983. Antigenic similarities between brain components and bacteria causing meningitis. Implications for vaccine development and pathogenesis. *Lancet* ii:355-357.
- Frasch, C. E. 1989. Vaccines for prevention of meningococcal disease. *Clin. Microbiol. Rev.* 2(Suppl.):S134-S138.
- Gamian, A., M. Beurret, F. Michon, J. R. Brisson, and H. J. Jennings. 1992. Structure of the L2 lipopolysaccharide core oligosaccharides of *Neisseria meningitidis*. *J. Biol. Chem.* 267:922-925.
- Gotschlich, E. C. 1994. Genetic locus for the biosynthesis of the variable portion of *Neisseria gonorrhoeae* lipooligosaccharide. *J. Exp. Med.* 180:2181-2190.
- Griffiths, J. M., J. P. O'Brien, R. Yamensaki, G. D. Williams, P. A. Rice, and H. Schneider. 1987. Physical heterogeneity of neisserial lipopolysaccharides reflects oligosaccharides that differ in apparent molecular weight, chemical composition, and antigenic expression. *Infect. Immun.* 55:1792-1800.
- Gu, X. X., and C. M. Tsai. 1993. Preparation, characterization, and immunogenicity of meningococcal lipooligosaccharide-derived oligosaccharide-protein conjugates. *Infect. Immun.* 61:1873-1880.
- Herbert, M. A., P. T. Heath, and R. T. Mayon-White. 1995. Meningococcal vaccines for the United Kingdom. *Commun. Dis. Rep. CDR Rev.* 5:R130-R135.
- Holten, E. 1979. Serotypes of *Neisseria meningitidis* isolated from patients in Norway during the first six months of 1978. *J. Clin. Microbiol.* 9:186-188.
- Hood, D. W., M. E. Deadman, T. Allen, H. Masoud, A. Martin, J. R. Brisson, R. Fleischman, J. C. Venter, J. C. Richards, and E. R. Moxon. 1996. Use of the complete genome sequence information of *Haemophilus influenzae* Rd to investigate lipopolysaccharide biosynthesis. *Mol. Microbiol.* 22:951-965.
- Jennings, H. J. 1989. The capsular polysaccharide of group B *Neisseria meningitidis* as a vehicle for vaccine development. *Contrib. Microbiol. Immunol.* 10:151-165.
- Jennings, H. J., and H. C. Lugowski. 1981. Immunochemistry of groups A, B, and C meningococcal polysaccharide-tetanus toxoid conjugates. *J. Immunol.* 127:1011-1018.
- Jennings, H. J., C. Lugowski, and F. E. Ashton. 1984. Conjugation of meningococcal lipopolysaccharide R-type oligosaccharides to tetanus toxoid as route to a potential vaccine against group B *Neisseria meningitidis*. *Infect. Immun.* 43:407-412.
- Jennings, H. J., K. J. Johnson, and L. Kenne. 1983. The structure of an R-type oligosaccharide core obtained from some lipopolysaccharides of *Neisseria meningitidis*. *Carbohydr. Res.* 121:233-241.
- Jennings, H. J., M. Beurret, A. Gamian, and F. Michon. 1987. Structure and immunochemistry of meningococcal lipopolysaccharides. *Antonie van Leeuwenhoek* 53:519-522.
- Jennings, M. P., D. W. Hood, I. R. Peak, M. Virji, and E. R. Moxon. 1995. Molecular analysis of a locus for the biosynthesis and phase-variable expression of the lacto-N-neotetraose terminal lipopolysaccharide structure in *Neisseria meningitidis*. *Mol. Microbiol.* 18:729-740.
- Jennings, M. P., M. Bisceric, K. L. Dunn, M. Virji, A. Martin, K. E. Wilks, J. C. Richards, and E. R. Moxon. 1995. Cloning and molecular analysis of the *lsl* (*rfaF*) gene of *Neisseria meningitidis* which encodes a heptosyl-2-transferase involved in LPS biosynthesis: evaluation of surface exposed carbohydrates in LPS mediated toxicity for human endothelial cells. *Microb. Pathog.* 19:391-407.
- Jennings, M. P., P. van der Ley, K. E. Wilks, D. J. Maskell, J. T. Poolman, and E. R. Moxon. 1993. Cloning and molecular analysis of the *galE* gene of *Neisseria meningitidis* and its role in lipopolysaccharide biosynthesis. *Mol. Microbiol.* 10:361-369.
- Jonsson, A. B., G. Nyberg, and S. Normark. 1991. Phase variation of gonococcal pili by frameshift mutation in pilC, a novel gene for pilus assembly. *EMBO J.* 10:477-488.
- Kogan, G., D. Uhrin, J. R. Brisson, and H. J. Jennings. 1997. Structural basis of the *Neisseria meningitidis* immunotypes, including the L4 and L7 immunotypes. *Carbohydr. Res.* 298:191-199.
- Lepow, M. L., J. Beeler, M. Randolph, J. S. Samuelson, and W. A. Hankins. 1986. Reactogenicity and immunogenicity of a quadrivalent combined meningococcal polysaccharide vaccine in children. *J. Infect. Dis.* 154:1033-1036.
- Lesse, A. J., A. A. Campagnari, W. E. Bittner, and M. A. Apicella. 1990. Increased resolution of lipopolysaccharides and lipooligosaccharides utilizing tricine-sodium dodecyl sulfate-polyacrylamide gel electrophoresis. *J. Immunol. Methods* 126:109-117.
- Maiden, M. C. J., J. A. Bygraves, E. Feil, G. Morelli, J. E. Russell, R. Urwin, Q. Zhang, J. Zhou, K. Zurth, D. A. Caugant, I. M. Feavers, M. Achtman, and B. G. Spratt. 1998. Multilocus sequence typing: a portable approach to the identification of clones within populations of pathogenic microorganisms. *Proc. Natl. Acad. Sci. USA* 95:3140-3145.

36. Masoud, H., E. R. Moxon, A. Martin, D. Krajcarski, and J. C. Richards. 1997. Structure of the variable and conserved lipopolysaccharide oligosaccharide epitopes expressed by *Haemophilus influenzae* serotype b Eagan. *Biochemistry* 36:2091–2103.
37. Michon, F., M. Beurret, A. Gamian, J. R. Brisson, and H. J. Jennings. 1990. Structure of the L5 lipopolysaccharide core oligosaccharide of *Neisseria meningitidis*. *J. Biol. Chem.* 265:7243–7247.
38. Moxon, E. R., D. Hood, and J. C. Richards. 1998. Bacterial lipopolysaccharides: candidate vaccines to prevent *Neisseria meningitidis* and *Haemophilus influenzae* infections. *Adv. Exp. Med. Biol.* 435:237–243.
39. Nassif, X., M. Marceau, C. Pujol, B. Pron, J. L. Beretti, and M. K. Taha. 1997. Type-4 pili and meningococcal adhesiveness. *Gene* 192:149–153.
40. Neidhardt, F. C. 1996. Derivations and genotypes of some mutant derivatives of *Escherichia coli* K-12, p. 2460–2488. In F. C. Neidhardt, R. Curtiss III, J. L. Ingraham, E. C. C. Lin, K. Low, Jr., B. Magasanik, W. S. Reznikoff, M. Riley, M. Schaechter, and H. E. Umbarger (ed.), *Escherichia coli* and *Salmonella*, 2nd ed. ASM Press, Washington, D.C.
41. Pavliak, V., J. R. Brisson, F. Michon, D. Uhrin, and H. J. Jennings. 1993. Structure of the sialylated L3 lipopolysaccharide of *Neisseria meningitidis*. *J. Biol. Chem.* 268:14146–14152.
42. Peltola, H., A. Safary, H. Kayhty, V. Karanko, and F. E. Andre. 1985. Evaluation of two tetravalent (ACYW135) meningococcal vaccines in infants and small children: a clinical study comparing immunogenicity of O-acetyl-negative and O-acetyl-positive group C polysaccharides. *Pediatrics* 76:91–96.
43. Peltola, H., H. Makela, H. Kayhty, H. Jousimies, E. Herva, K. Hallstrom, A. Sivenon, O. V. Renkonen, O. Petay, V. Karanko, P. Ahvonen, and S. Sarna. 1977. Clinical efficacy of meningococcus group A capsular polysaccharide vaccine in children three months to five years of age. *N. Engl. J. Med.* 297:686–691.
44. Poolman, J. T. 1990. Polysaccharides and membrane vaccines, p. 57–86. In A. Mizrahi (ed.), *Bacterial vaccines*. Wiley-Liss, New York, N.Y.
45. Poolman, J. T. 1996. Bacterial outer membrane protein vaccines. The meningococcal example. *Adv. Exp. Med. Biol.* 397:73–77.
46. Poolman, J. T., C. T. P. Hopman, and H. C. Zanen. 1982. Problems in the definition of meningococcal serotypes. *FEMS Microbiol. Lett.* 13:339–348.
47. Poolman, J. T., P. van der Ley, and J. P. M. Tommassen. 1995. Surface structures and secreted products of meningococci, p. 21–34. K. Cartwright (ed.), *Meningococcal disease*. John Wiley & Sons, Inc., New York, N.Y.
48. Preston, A., R. E. Mandrell, B. W. Gibson, and M. A. Apicella. 1996. The lipooligosaccharides of pathogenic gram-negative bacteria. *Crit. Rev. Microbiol.* 22:139–180.
49. Reingold, A. L., C. V. Broome, G. W. Hightower, G. A. Ajello, C. Bolaw, E. E. Adambaum, C. Jones, H. Phillips, H. Tiendrebego, and A. Yada. 1985. Age-specific differences in duration of clinical protection after vaccination with polysaccharide A vaccine. *Lancet* ii:114–118.
50. Rosenqvist, E., E. A. Hoiby, E. Wedge, K. Bryn, J. Kolberg, A. Klem, E. Ronnild, G. Bjune, and H. Nøkleby. 1995. Human antibody responses to meningococcal outer membrane antigens after three doses of the Norwegian group B meningococcal vaccine. *Infect. Immun.* 63:4642–4652.
51. Rosenstein, N., O. Levine, J. P. Taylor, D. Evans, B. D. Plikaytis, J. D. Wenger, and B. A. Perkins. 1998. Efficacy of meningococcal vaccine and barriers to vaccination. *JAMA* 279:435–439.
52. Sakari, J., N. Pandit, E. R. Moxon, and M. Achtman. 1994. Variable expression of the Opc outer membrane protein in *Neisseria meningitidis* is caused by size variation of a promoter containing poly-cytidine. *Mol. Microbiol.* 13:207–217.
53. Schnaitman, C. A., and F. D. Klena. 1993. Genetics of lipopolysaccharide biosynthesis in enteric bacteria. *Microbiol. Rev.* 57:655–682.
54. Scholten, R. J., B. Kuipers, H. A. Valkenburg, J. Dankert, W. D. Zollinger, and J. T. Poolman. 1994. Lipo-oligosaccharide immunotyping of *Neisseria meningitidis* by a whole-cell ELISA with monoclonal antibodies. *J. Med. Microbiol.* 41:236–243.
55. Schroten, H., M. Deadman, and E. R. Moxon. 1995. Development of chick embryo models for analysis of bacterial virulence factors. *Pediatr. Grenzgeb.* 34:319–324.
56. Seiler, A., R. Reinhardt, J. Sakari, D. A. Caugant, and M. Achtman. 1996. Allelic polymorphisms and site-specific recombination in the opc locus of *Neisseria meningitidis*. *Mol. Microbiol.* 19:841–856.
57. Shulman, M., C. D. Wilde, and G. Kohler. 1978. A better cell line for making hybridomas secreting specific antibodies. *Nature* 276:269–270.
58. Steeghs, L., R. den Hartog, A. den Boer, B. Zomer, P. Roholl, and P. van der Ley. 1998. Meningitis bacterium is viable without endotoxin. *Nature* 392:449–450.
59. Stephens, D. S., C. F. McAllister, D. Zhou, F. K. Lee, and M. A. Apicella. 1994. Tn916-generated, lipooligosaccharide mutants of *Neisseria meningitidis* and *Neisseria gonorrhoeae*. *Infect. Immun.* 62:2947–2952.
60. Stern, A., and T. F. Meyer. 1987. Common mechanism controlling phase and antigenic variation in pathogenic neisseriae. *Mol. Microbiol.* 1:5–12.
61. Stern, A., M. Brown, P. Nickel, and T. F. Meyer. 1986. Opacity genes in *Neisseria gonorrhoeae*: control of phase and antigenic variation. *Cell* 47:61–71.
62. Stojilkovic, I., V. Hwa, J. Larson, L. Lin, M. So, and X. Nassif. 1997. Cloning and characterization of the *Neisseria meningitidis* rfaC gene encoding alpha-1,5-heptosyltransferase I. *FEMS Microbiol. Lett.* 151:41–49.
63. Tonjum, T., and M. Koomey. 1997. The pilus colonization factor of pathogenic neisserial species: organelle biosynthesis and structure/function relationships—a review. *Gene* 192:155–163.
64. van der Ley, P., M. Kramer, A. Martin, J. C. Richards, and J. T. Poolman. 1997. Analysis of the icsBA locus required for biosynthesis of the inner core region from *Neisseria meningitidis* lipopolysaccharide. *FEMS Microbiol. Lett.* 146:247–253.
65. van der Ley, P., M. Kramer, L. Steeghs, B. Kuipers, S. R. Andersen, M. P. Jennings, E. R. Moxon, and J. T. Poolman. 1996. Identification of a locus involved in meningococcal lipopolysaccharide biosynthesis by deletion mutagenesis. *Mol. Microbiol.* 19:1117–1125.
66. van Putten, J. P., and B. D. Robertson. 1995. Molecular mechanisms and implications for infection of lipopolysaccharide variation in *Neisseria*. *Mol. Microbiol.* 16:847–853.
67. Verheul, A. F., A. K. Braat, J. M. Leenhouts, P. Hoogerhout, J. T. Poolman, H. Snippe, and J. Verhoef. 1991. Preparation, characterization, and immunogenicity of meningococcal immunotype L2 and L3,7,9 phosphoethanolamine group-containing oligosaccharide-protein conjugates. *Infect. Immun.* 59:843–851.
68. Verheul, A. F., H. Snippe, and J. T. Poolman. 1993. Meningococcal lipopolysaccharides: virulence factor and potential vaccine component. *Microbiol. Rev.* 57:34–49.
69. Verheul, A. F., J. A. Van Gaans, E. J. Wiertz, H. Snippe, J. Verhoef, and J. T. Poolman. 1993. Meningococcal lipopolysaccharide (LPS)-derived oligosaccharide-protein conjugates evoke outer membrane protein- but not LPS-specific bactericidal antibodies in mice: influence of adjuvants. *Infect. Immun.* 61:187–196.
70. Virji, M., H. Kayhty, D. J. P. Ferguson, C. Alexandrescu, J. E. Heckels, and E. R. Moxon. 1991. Interactions of *Haemophilus influenzae* with cultured human endothelial cells. *Microb. Pathog.* 10:231–245.
71. Virji, M., H. Kayhty, D. J. P. Ferguson, J. E. Heckels, and E. R. Moxon. 1991. The role of pili in the interactions of pathogenic *Neisseria* with cultured human endothelial cells. *Mol. Microbiol.* 5:1831–1841.
72. Wakarchuk, W., A. Martin, M. P. Jennings, E. R. Moxon, and J. C. Richards. 1996. Functional relationships of the genetic locus encoding the glycosyltransferase enzymes involved in expression of the lacto-N-neotetraose terminal lipopolysaccharide structure in *Neisseria meningitidis*. *J. Biol. Chem.* 271:19166–19173.
73. Wakarchuk, W. W., M. Gilbert, A. Martin, Y. Wu, J. R. Brisson, P. Thibault, and J. C. Richards. 1998. Structure of an alpha-2,6-sialylated lipooligosaccharide from *Neisseria meningitidis* immunotype L1. *Eur. J. Biochem.* 254:626–633.
74. Westphal, O., and J. K. Jann. 1965. Bacterial lipopolysaccharides extraction with water-phenol and further applications of the procedure. *Methods Carbohydr. Chem.* 5:83–91.
75. Wetzler, L. M. 1994. Immunopotentiating ability of neisserial major outer membrane proteins. Use as an adjuvant for poorly immunogenic substances and potential use in vaccines. *Ann. N. Y. Acad. Sci.* 730:367–370.
76. Zollinger, W. D., E. E. Moran, S. J. Devi, and C. E. Frasch. 1997. Bactericidal antibody responses of juvenile rhesus monkeys immunized with group B *Neisseria meningitidis* capsular polysaccharide-protein conjugate vaccines. *Infect. Immun.* 65:1053–1060.

**This Page is Inserted by IFW Indexing and Scanning
Operations and is not part of the Official Record**

BEST AVAILABLE IMAGES

Defective images within this document are accurate representations of the original documents submitted by the applicant.

Defects in the images include but are not limited to the items checked:

- ☐ BLACK BORDERS
- ☒ IMAGE CUT OFF AT TOP, BOTTOM OR SIDES
- ☐ FADED TEXT OR DRAWING
- ☐ BLURRED OR ILLEGIBLE TEXT OR DRAWING
- ☐ SKEWED/SLANTED IMAGES
- ☒ COLOR OR BLACK AND WHITE PHOTOGRAPHS
- ☐ GRAY SCALE DOCUMENTS
- ☒ LINES OR MARKS ON ORIGINAL DOCUMENT
- ☐ REFERENCE(S) OR EXHIBIT(S) SUBMITTED ARE POOR QUALITY
- ☐ OTHER: _____

IMAGES ARE BEST AVAILABLE COPY.

As rescanning these documents will not correct the image problems checked, please do not report these problems to the IFW Image Problem Mailbox.